



**Task 13** Reliability and Performance of Photovoltaic Systems

PVPS

# Photovoltaics and Energy Security in the Greater Arctic Region 2026



## What is IEA PVPS TCP?

The International Energy Agency (IEA), founded in 1974, is an autonomous body within the framework of the Organization for Economic Cooperation and Development (OECD). The Technology Collaboration Programme (TCP) was created with a belief that the future of energy security and sustainability starts with global collaboration. The programme is made up of 6.000 experts across government, academia, and industry dedicated to advancing common research and the application of specific energy technologies.

The IEA Photovoltaic Power Systems Programme (IEA PVPS) is one of the TCP's within the IEA and was established in 1993. The mission of the programme is to “enhance the international collaborative efforts which facilitate the role of photovoltaic solar energy as a cornerstone in the transition to sustainable energy systems.” In order to achieve this, the Programme's participants have undertaken a variety of joint research projects in PV power systems applications. The overall programme is headed by an Executive Committee, comprised of one delegate from each country or organisation member, which designates distinct ‘Tasks,’ that may be research projects or activity areas.

The 28 IEA PVPS participating countries are Australia, Austria, Belgium, Canada, China, Denmark, Finland, France, Germany, India, Israel, Italy, Japan, Korea, Lithuania, Malaysia, Morocco, the Netherlands, Norway, Portugal, South Africa, Spain, Sweden, Switzerland, Thailand, Türkiye, the United Kingdom and the United States of America. The European Commission, Solar Power Europe and the Solar Energy Research Institute of Singapore are also members.

Visit us at: [www.iea-pvps.org](http://www.iea-pvps.org)

## What is IEA PVPS Task 13?

Within the framework of IEA PVPS, Task 13 aims to provide support to market actors working to improve the operation, the reliability and the quality of PV components and systems. Operational data from PV systems in different climate zones compiled within the project will help provide the basis for estimates of the current situation regarding PV reliability and performance.

The general setting of Task 13 provides a common platform to summarize and report on technical aspects affecting the quality, performance, reliability and lifetime of PV systems in a wide variety of environments and applications. By working together across national boundaries, we can all take advantage of research and experience from each member country and combine and integrate this knowledge into valuable summaries of best practices and methods for ensuring PV systems perform at their optimum and continue to provide competitive return on investment.

Task 13 has so far managed to create the right framework for the calculations of various parameters that can give an indication of the quality of PV components and systems. The framework is now there and can be used by the industry who has expressed appreciation towards the results included in the high-quality reports.

The IEA PVPS countries participating in Task 13 are Australia, Austria, Belgium, Canada, Chile, China, Denmark, Finland, France, Germany, Israel, Italy, Japan, the Netherlands, Norway, Spain, Sweden, Switzerland, Thailand, and the United States of America, and the Solar Energy Research Institute of Singapore.

### DISCLAIMER

The IEA PVPS TCP is organised under the auspices of the International Energy Agency (IEA) but is functionally and legally autonomous. Views, findings and publications of the IEA PVPS TCP do not necessarily represent the views or policies of the IEA Secretariat or its individual member countries.

### COPYRIGHT STATEMENT

This content may be freely used, copied and redistributed, provided appropriate credit is given (please refer to the ‘Suggested Citation’). The exception is that some licensed images may not be copied, as specified in the individual image captions.

### SUGGESTED CITATION

Stein, J.S., Whitney, E. (2026). Maugeri, G., Stein, J.S., Jahn, U. (Eds.), *Photovoltaics and Energy Security in the Greater Arctic Region* (Report No. T13-40:2026). IEA PVPS Task 13. <https://iea-pvps.org/key-topics/t13-security-greater-arctic-region-2026/> DOI: 10.69766/JXHM9635

### COVER PICTURE

100 kW vertical bifacial PV pilot plant near Luleå, Sweden constructed by the Sunna Group.



INTERNATIONAL ENERGY AGENCY  
PHOTOVOLTAIC POWER SYSTEMS PROGRAMME

# Photovoltaics and Energy Security in the Greater Arctic Region

## **IEA PVPS Task 13 Reliability and Performance of Photovoltaic Systems**

Report IEA-PVPS T13-40:2026  
February 2026

ISBN: 978-1-7642902-9-6  
DOI: 10.69766/JXHM9635



## AUTHORS

---

### Main Author(s)

Joshua S. Stein, Sandia National Laboratories, USA  
Erin Whitney, University of Alaska Fairbanks, USA  
Erin Tonita, University of Ottawa, Canada  
Alexander Granlund, RISE Research Institutes of Sweden, Sweden  
Mattias Lindh, RISE Research Institute of Sweden, Sweden  
André Augusto, Sustainable Energy Research Centre, Dalarna University, Sweden  
Mari Ogaard, Institute for Energy Technology, Norway  
Adam R. Jensen, Technical University of Denmark, Denmark  
Silvia Ma Lu, Mälardalen University, Sweden  
Christopher Pike, University of Alaska Fairbanks, USA  
Sami Jouttijärvi, University of Turku, Finland  
Michelle Wilber, University of Alaska Fairbanks, USA  
Henry Toal, University of Alaska Fairbanks, USA  
Mattia Manni, Norwegian University of Science and Technology, Norway  
Silvana Ovaitt, National Laboratory of the Rockies, USA  
Anna Malou Peterson, RISE Research Institute of Sweden, Sweden

### Editors

Giosuè Maugeri, RSE, Italy  
Joshua S. Stein, Sandia National Laboratories, USA  
Ulrike Jahn, Fraunhofer Center for Silicon Photovoltaics CSP, Germany



## TABLE OF CONTENTS

---

Acknowledgements .....	6
List of Abbreviations .....	7
Executive Summary.....	8
1 Introduction .....	12
2 Unique Environmental Characteristics of the Arctic: Irradiance, Temperature, and Snow .....	14
2.1 Irradiance.....	14
2.2 Ambient Temperature .....	16
2.3 Snow and Albedo Effects.....	18
3 Data Challenges and Opportunities .....	22
4 Design and Modeling Considerations for High-Latitude Irradiance and Albedo Conditions .....	27
4.1 Design Considerations.....	27
4.2 Modeling Considerations .....	32
5 Performance and Design of Solar PV in Extreme Cold Temperatures ...	34
5.1 Temperature-dependence of Different Solar Cell Technologies ....	34
5.2 Foundations and Frozen Ground .....	36
5.3 Degradation Mechanisms and Performance Loss Rates.....	40
6 Design and Modeling Considerations for Snow and Ice Accumulations.	42
6.1 Snow Accumulations .....	42
6.2 Shading Losses .....	43
6.3 Accumulation of Soiling .....	44
6.4 Reliability .....	45
6.5 Mitigation and Adaptation .....	46
7 Integration .....	49
8 Arctic Country Summaries and Projections .....	54
8.1 Electricity Sources in High-Latitude Regions .....	55
8.2 Regional Summaries .....	56
8.3 Photovoltaic Installation Status .....	62
9 Conclusions.....	65
References .....	66



## ACKNOWLEDGEMENTS

---

This paper received valuable contributions from several IEA-PVPS Task 13 members and other international experts. Many thanks to: Gabi Friesen and Ulrike Jahn for their helpful comments and suggestions.

- Sandia National Laboratories is a multimission laboratory managed and operated by National Technology & Engineering Solutions of Sandia, LLC, a wholly owned subsidiary of Honeywell International Inc., for the U.S. Department of Energy's National Nuclear Security Administration under contract DE-NA0003525. This paper describes objective technical results and analysis. Any subjective views or opinions that might be expressed in the paper do not necessarily represent the views of the U.S. Department of Energy or the United States Government.
- This report is supported by the German Federal Ministry for Economic Affairs and Climate Action (BMWK) under contract no. 03EE1120A.
- Adam R. Jensen was supported the Danish Energy Agency's EUDP programme under grant no. 134223-496801.
- Evaluation of the first agrivoltaic system facility in Sweden to compare commercially available agrivoltaic technologies - MATRIX" (grant number P2022-00809) from the Swedish Energy Agency. This applies to Table 2, Figures 20-22.
- A part of this work was authored in part by the National Laboratory of the Rockies for the U.S. Department of Energy (DOE), operated under Contract No. DE-AC36-08GO28308. Funding provided by U.S. DOE Office of Critical Minerals and Energy Innovation (CMEI) Solar Energy Technologies Office (SETO), Agreement 52789. The views expressed in the article do not necessarily represent the views of the DOE or the U.S. Government.
- Office of Naval Research Award: N00014-19-1-2235 - Alaska Regional Collaboration for Technology Innovation and Commercialization



## LIST OF ABBREVIATIONS

---

AA	average albedo
AM	air mass
BHI	beam horizontal irradiance
BMWK	German Federal Ministry for Economic Affairs and Climate Action
BRDF	bidirectional reflectance function
BSA	black-sky albedo
CHP	combined heat and power
CIGS	copper indium gallium selenide
DHI	diffuse horizontal irradiance
DNI	direct normal irradiance
ECMWF	European Centre for Medium-Range Weather Forecasts
EV	electric vehicle
EVA	ethylene-vinyl acetate
GHI	global horizontal irradiance
IEA	International Energy Agency
ITC	investment tax credit
LCF	load coverage factor
NOCT	nominal operating cell temperature
NSRDB	National Solar Radiation Database
O&M	operations and maintenance
OECD	Organization for Economic Cooperation and Development
PERC	passivated emitter and rear contact
PLR	performance loss rate
POA	plane of array
PTC	production tax credit
PV	photovoltaic
RENEWFM	Renewable Energy Financing Mechanism
RH	relative humidity
RISE	representative identification of spectra and environments
SD	snow depth
SH	specific humidity
SEPA	Smart Electric Power Alliance
STC	standard test conditions
TA	air temperature
TCP	Technology Collaboration Programme
TMY	typical meteorological year
UV	ultraviolet
VRE	variable renewable energy
WS	wind speed
WSA	white-sky albedo



## EXECUTIVE SUMMARY

---

The greater Arctic region (>60°N latitude) has been largely overlooked as a promising location for photovoltaic (PV) installations, with lower latitude and warmer regions receiving more attention. While few large PV installations currently exist in the Arctic, a closer examination of the region's geography, climate, PV technology characteristics, and energy needs reveals that PV systems can significantly contribute to energy security in high-latitude areas. This report examines both the opportunities and significant challenges for such a vision.

### Unique Environmental Characteristics of the Arctic Region

The Arctic environment presents distinct challenges and opportunities for PV systems due to its unique irradiance, temperature, and snow-related characteristics:

- **Solar Resource:** Solar insolation decreases with latitudes above 35°N due to lower solar elevation during winter months and pronounced seasonal variations. Above the Arctic Circle, the sun remains below the horizon during the winter solstice, resulting in dramatic differences in day length, solar elevation, and azimuth ranges. Diffuse fraction increases with latitude, shifting the spectral content of sunlight toward longer wavelengths, which affects PV efficiency and output power.
- **Temperature:** Ambient temperatures decrease with higher latitude, exhibiting significant seasonal fluctuations compared to lower latitudes. These variations correlate positively with solar irradiance, as colder conditions are often associated with lower irradiance levels.
- **Snow and Albedo:** Snow accumulation can obstruct sunlight and exert mechanical stress on PV components, but it also enhances ground reflectivity through increased albedo. High-latitude regions experience extensive snow cover, often exceeding 200 days annually, with significant snow depth. Permafrost and frost heave, prevalent above 50°N, pose additional challenges for PV installations.

These environmental factors highlight the need for improved datasets and tailored PV system designs to optimize performance in Arctic and high-latitude locations.

### Data Challenges and Modeling for PV Performance

Accurate predictions of PV performance are critical for planning installations and optimizing energy dispatch in high-latitude regions. However, reliable input data—such as solar irradiance, albedo, and meteorological parameters—are often scarce:

- **Data Sources:** Ground-based measurements using research-grade solar radiometers provide the highest quality data but are limited in high-latitude areas due to operational challenges such as snow buildup, calibration drift, and accessibility issues. Alternative sources, including satellite data, reanalysis models, and land surface assimilation models, often suffer from reduced accuracy in high-latitude regions.



- **Site Adaptation Techniques:** These methods can improve the accuracy of satellite or model-derived data by correcting systematic biases using high-quality ground measurements. Despite the challenges, high-quality observations are essential for validating models and improving dataset accuracy.
- **Database Resources:** Public and commercial databases provide solar radiation, albedo, and weather data relevant to high-latitude PV studies, but they vary in spatial and temporal resolution, data sources, and quality control procedures.

The development of rigorous maintenance protocols, specialized quality control measures, and high-quality datasets is essential to support PV deployment in challenging high-latitude environments.

### Design and Modeling Adaptations for High-Latitude PV Systems

PV systems deployed in high-latitude regions require specific design adaptations to address unique climatic conditions.

- **System Design:** Fixed-tilt systems are preferred for their simplicity and reliability in freeze-thaw cycles, while tracking systems are less recommended due to operational challenges in cold temperature environments. Ground-mounted fixed-tilt systems often feature larger row spacing to minimize shading losses and higher mounting heights to prevent snow accumulation.
- **Bifacial Technologies:** Bifacial PV systems are particularly advantageous in high-latitude regions, as they leverage increased diffuse light fraction and seasonal snow albedo to enhance energy yield. Vertically oriented bifacial systems, often oriented east-west, reduce snow coverage, align better with daily electricity demand, and improve building integration.
- **Modeling Challenges:** Modeling PV systems in high-latitude regions is essential for financial planning and system design but faces increased uncertainty due to limited data availability, high albedo variability, and challenges in validating models for vertical and façade systems. Snow loss models, localized sky coefficients, and high-quality ground-station data can improve accuracy and reliability.
- **Economic Modeling:** Economic modeling for PV systems in high-latitude regions is complicated by higher shipping, installation, and maintenance costs in remote northern communities. Despite these challenges, PV modeling remains a critical tool for optimizing system performance.

### Performance and Degradation in Extreme Cold Temperatures

PV systems deployed in extreme cold temperatures face unique challenges and opportunities:

- **Temperature Effects:** Solar cell performance improves at lower temperatures due to the widening of the semiconductor bandgap, which increases voltage and overall power output. However, temperature coefficients vary across technologies, necessitating adjustments to PV performance modeling practices.
- **Ground Conditions:** Foundations in cold climates are prone to frost heaving, which can damage PV racking systems. Detailed geotechnical surveys tailored



to PV installations are essential to mitigate these risks. In permafrost regions, solar arrays can act as snow fences, leading to snow drifts that insulate the ground and potentially cause permafrost warming and structural instability.

- **Degradation Mechanisms:** Snow load, freeze-thaw cycles, and extreme cold temperatures are primary stressors for PV systems in high-latitude regions. These conditions can lead to cell cracking, moisture ingress, delamination, and material corrosion. However, observed PV systems in colder climates tend to degrade more slowly than those in warmer regions, with a median degradation rate of -0.37% per year (sample size = 16) for systems above 59°N, compared to -0.75% per year for systems across the continental USA.

Proper design adaptations, such as using durable materials, optimizing racking systems, and integrating snow loss models, are critical for ensuring the long-term viability and efficiency of PV systems in high-latitude environments.

### Snow and Ice Management for PV Systems

Snow and ice accumulation significantly impact the design, performance, and reliability of PV systems in cold climates:

- **Snow Behavior:** Snow behavior varies based on temperature, moisture content, and particle size, influencing how it adheres to PV modules and forms cohesive snowpacks or loose drifts. Snow shedding is more effective with higher module tilt angles and sufficient clearance beneath arrays, but snow accumulation beneath modules can obstruct shedding and prolong snow cover. Snow drifting is influenced by the PV array design and then impacts reflected light and also ground temperatures.
- **Energy Losses:** Snow-covered modules experience shading losses that severely limit energy output. Snow loss models simulate the adherence and shedding of snow from the module surface and provide empirical and threshold-based approaches to estimate energy impacts. Site-specific calibration or machine learning techniques can improve accuracy.
- **Mechanical Stress:** Heavy snow loads exert mechanical stress on PV modules, potentially leading to deflection, cracked glass, damaged cells, or frame separation. Standards like IEC 61215-2 and IEC 62938 address uniform and non-uniform snow loads, but real-world conditions amplify risks in Arctic environments.
- **Mitigation Strategies:** Passive solutions include hydrophobic or ice-phobic coatings, steeper tilt angles, and snow fences, while active strategies such as mechanical snow removal, surface heating, and chemical treatments can be costly or environmentally harmful. A combination of tailored design, advanced modeling, and innovative mitigation techniques is necessary to address these challenges.

### Integration of PV Systems into Arctic Power Systems

The integration of PV systems into Arctic power systems presents unique challenges and opportunities:



- **Geographic and Political Contexts:** In Nordic countries, national power grids extend into many high-latitude areas, enabling large-scale utility PV installations. In North America, isolated microgrids dominate sparsely populated Arctic regions, requiring tailored approaches to PV integration.
- **Economic Viability:** Utility-scale PV plants are becoming economically viable even in high-latitude locations, but they face challenges such as the "cannibalization effect," where overproduction during peak hours reduces electricity prices and profitability. Land use concerns make dual-use installations, such as agrivoltaics or PV carports, more acceptable to the public.
- **Residential and Rooftop Systems:** These systems offer advantages in self-consumption, avoiding transfer costs and electricity taxes, and reducing grid interaction. Financial incentives and market policies, such as net metering, significantly influence the design and operational strategies of PV systems.
- **Strategies for Integration:** Hybrid PV and wind power plants, energy communities, load shifting, virtual power plants, and energy storage can enhance PV generation and support integration into Arctic power systems. Policies such as investment tax credits, feed-in tariffs, and aggregated net metering incentivize PV adoption, while policies supporting the disposal and recycling of used PV modules encourage sustainable practices.

Integrating PV systems into Arctic power systems requires innovative strategies, supportive policies, and tailored designs to address the unique environmental, economic, and operational conditions of high-latitude regions. Despite the challenges, PV technologies have the potential to play a significant role in the future energy landscape of the Arctic.

### Key Takeaways

- High-latitude solar resource has high seasonality, low sun elevations and a wide range in solar azimuth angles. Fixed arrays experience more time with the sun behind the array than at lower latitudes.
- Bifacial modules & vertical arrays see significant performance advantages by capturing more light (direct, diffuse, and reflected) and by effectively shedding snow.
- Lower temperatures lead to higher PV efficiency and likely lower module degradation rates.
- Foundations must be adapted to ground freezing and frost heaves.
- Array design should account for snow drifting
- Many Arctic nations are actively installing PV systems and developing region-specific solutions.



## 1 INTRODUCTION

---

Solar photovoltaics (PV) present critical local energy security opportunities in the greater Arctic region due to the area's unique environmental and social characteristics. We define the greater Arctic region as the part of the world at latitude greater than 60 °N, encompassing not only the region above the Arctic Circle at 66 °N but also regions that are commonly associated with the Arctic in terms of climate, flora and fauna, and human populations, such as alpine environments at lower latitudes.

In 2005, approximately 17.2 million people lived above 60°N [1], an area that comprises ~13.4% of the Earth's surface area.<sup>1</sup> While the population density is small, the region's resources and inhabitants impact the world economy through the supply of natural resources including fisheries, minerals, and fossil fuels. Where land use may be constrained in other parts of the world, the Arctic possesses vast tracts of land. Adding a cultural and artistic dimension, the region's diverse Indigenous cultures enrich the global creative sector, contributing to international arts and culture through distinct storytelling, art, and performance.

Despite significant natural resources, certain Arctic communities (e.g., Alaska) rely primarily on imported fossil fuels for their energy needs and experience unique logistical and infrastructural challenges for transitioning to local energy sources. Additionally, fossil fuel supplies to many Arctic communities are subject to costly transportation challenges and global price fluctuations, which reduce the security of these communities and challenge the sovereignty goals of Indigenous communities in the region. Electricity costs in isolated Arctic communities can be much higher and less stable compared to grid-connected regions due to volatility in fuel prices and challenging logistics of fuel deliveries by water or air, which may not be possible in the winter.

The unique characteristics of Arctic regions provide both advantages and challenges to the development of solar PV. Long summer days provide PV systems significant radiation for energy harvesting, but dark winters mean these systems are mostly dormant for several months each year. High-latitude regions are characterized by low sun elevations and a much wider range in solar azimuths than observed at lower latitudes. This means that, in the summer, the sun will be behind a south-facing fixed-tilt PV array for many hours of the day. Temperatures, while increasing due to climate change, are still much lower on average than in lower latitude regions but periods of extreme high temperatures have become more common. The efficiency of crystalline silicon PV cells linearly increases as temperature decreases, so PV systems in the Arctic can operate at higher efficiencies. Also, because most PV module degradation processes are enhanced at higher temperatures, modules may have a longer lifespan in colder climates. However, data on degradation in the greater Arctic region remains scarce. Snow usually remains on the ground into the late spring, meaning that there is additional ground-reflected sunlight during this time. Therefore, bifacial PV module technology is of great interest for Arctic systems since the technology can take

---

<sup>1</sup> Spherical surface area between 60° N and 90° N:  $2\pi r^2(\sin(90^\circ) - \sin(60^\circ))$



advantage of light hitting the rear side of a module as well as light from enhanced ground reflections.

The challenges of using solar PV as an energy source in the Arctic are varied. Extreme weather, including heavy snow loads, high winds, low temperatures, and large temperature changes affect equipment reliability through increased risk of equipment failure from mechanical loading and material property changes (e.g., glass transition temperature of common encapsulants). The seasonal mismatch between solar production in the Summer and heating loads in the Winter are also challenging. The cost of doing business in some parts of the Arctic is also significantly higher than in most lower latitude areas. The remoteness of many Arctic communities means that shipping logistics and materials costs are high, and there is often limited availability of skilled labor, spare parts, machinery, and other necessary installation equipment. Furthermore, many Arctic communities are isolated microgrids, particularly in North America. To use intermittent solar energy, these microgrid systems require significant energy storage and power controllers to be reliable. These requirements incur additional costs, making it more difficult for PV systems to be economically feasible.

Hence, despite the technical challenges described above, the cost of solar PV installations is often lower than prevailing energy sources in many of these regions. Consequently, developers are considering and pursuing larger installations and greater levels of penetration, which necessitate accurate solar irradiance data to fulfill investor due diligence requirements and accurately gauge project risks and returns. However, accurate irradiance data at appropriate resolution for the Arctic is a particular challenge for high-latitude solar installation development. Furthermore, as the cost of solar installations continues to drop worldwide, solar PV technology is migrating into not just high-latitude regions but also upper mid-latitude regions which also experience snow and cold temperatures, thus necessitating research into these parameters and their effects on solar PV performance, operation, and maintenance.

Arctic communities have unique needs for which innovative applications of PV and renewable energy technologies can be applied. Reliance on a unique mix of transportation options including small off-road/snow transportation, watercraft, and private aircraft also present different challenges for decarbonization.

This report puts these and other factors into perspective as Arctic communities and investors participate and engage in the transition away from fossil fuel-based technologies to renewable energy sources. As with any challenge, solutions come in many forms including new technologies, applications, and practices.



## 2 UNIQUE ENVIRONMENTAL CHARACTERISTICS OF THE ARCTIC: IRRADIANCE, TEMPERATURE, AND SNOW

### 2.1 Irradiance

Annual solar insolation for global horizontal irradiance (GHI), direct normal irradiance (DNI), and diffuse horizontal irradiance (DHI) components are presented in Figure 1 for >3000 locations using hourly typical meteorological year (TMY) files from the National Solar Radiation Database (NSRDB) v3.2.2 [2]. Above 60°N, TMY files come from PVGIS 5.2. A few example locations are indicated in the subplots by labeled black stars.

On an annual basis, the total amount of terrestrial solar irradiation decreases as a function of latitude for latitudes greater than 35 degrees. This is largely driven by the lower solar elevation during winter months because of the tilt of the Earth’s axis relative to its orbit around the Sun. Figure 2 demonstrates the cumulative monthly GHI in three locations of differing latitudes (19°N, 45°N, and 65°N). Seasonal variations are greater at high latitudes, with the Sun remaining below the horizon at the winter solstice for latitudes at and above the Arctic Circle (66.56°N).

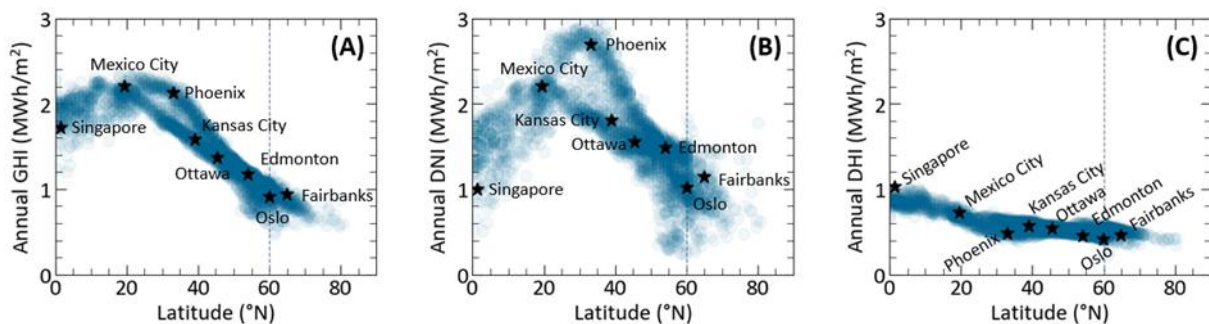


Figure 1: Annual (A) GHI, (B) DNI, and (C) DHI as a function of latitude for ~3000 locations, with some labeled example locations. The dashed line highlights a latitude of 60°N.

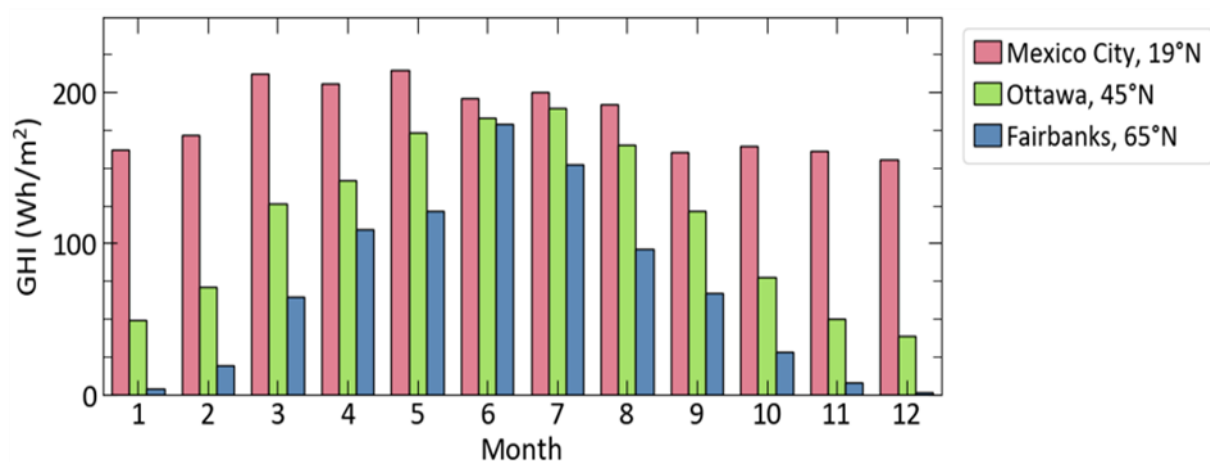
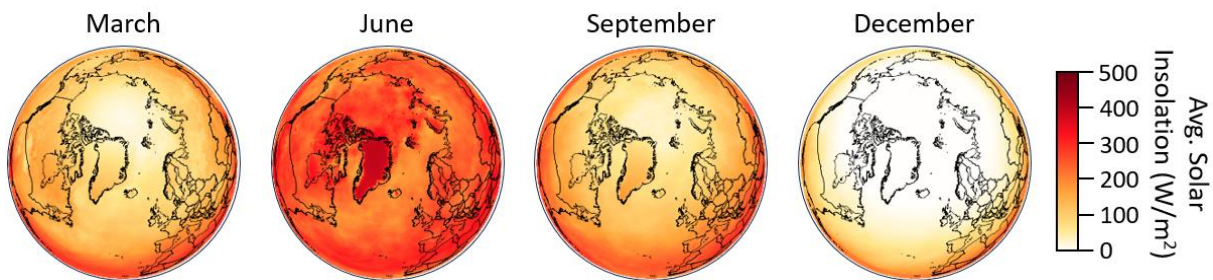


Figure 2: Monthly GHI for three example locations with different latitudes.

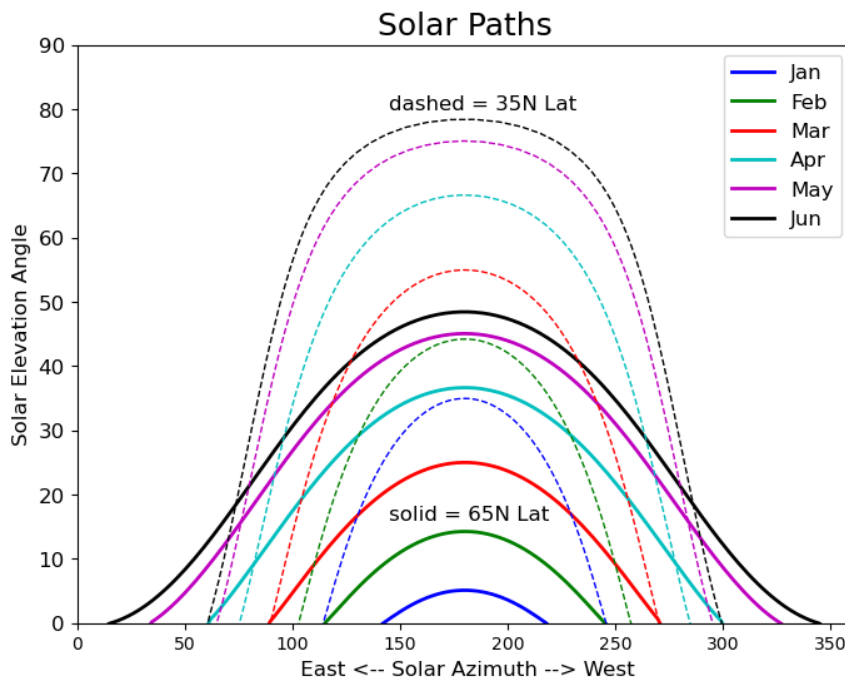


The seasonal effects of the solar resource are also illustrated in Figure 3 with monthly average GHI plotted for March, June, September, and December of 2023 based on data from the NASA Earth Observations website [3]. The plot shows the effect length of daylight has on irradiation patterns. Near the summer solstice (June), high-latitude regions receive large amounts of solar radiation. In contrast, near the winter solstice (December) high-latitude regions receive little to no solar radiation.



**Figure 3: Average monthly solar irradiation maps of the northern hemisphere.**

The relative position of the sun in the sky over time follows a significantly different pattern in high latitudes than at lower latitudes (Figure 4). Above 60°N, there is a dramatic difference in day length at the solstices, low solar elevations, and very large solar azimuth ranges.



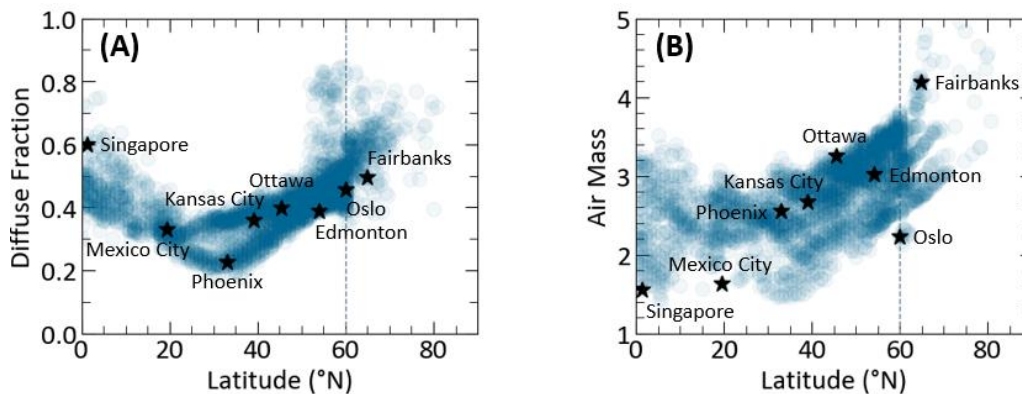
**Figure 4: Sun path diagrams showing the relative position of the Sun on six representative days throughout the year for two locations (dashed: 35° N, and solid: 65° N).**

Figure 5A shows the annual average diffuse fraction as a function of latitude for several locations. Diffuse fraction is calculated as the ratio between DHI and GHI, and tends to increase as a function of latitude, though a wide range of diffuse fractions is



observed for locations at similar latitudes  $>50^{\circ}\text{N}$ . Increasing diffuse fraction is an indicator of frequent cloudy conditions, higher air mass, and/or higher humidity.

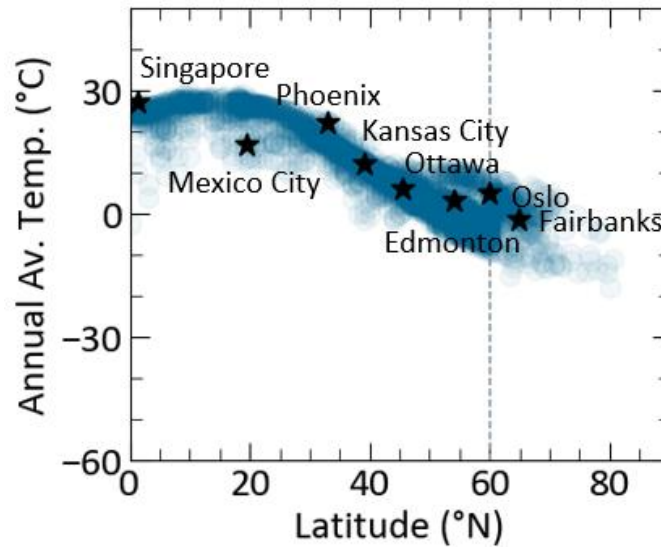
Not only does the total amount of annual and seasonal solar irradiation change as a function of latitude corresponding to differences in solar path, the spectral contents of the sunlight change as well. Figure 5B shows the GHI-weighted annual average relative air mass (AM) for these same locations. GHI-weighted AM was calculated using pvlib-python's *get\_relative\_airmass* function (with default kastinyoung1989 model) for all hours in a year in each location [4]. A larger portion of annual solar irradiation tends to occur with higher AM in high latitudes, a consequence of lower solar elevation angles. The compounding effects of clouds and high AM can shift the spectral contents of solar radiation, resulting in varied spectral mismatch, photovoltaic conversion efficiency, and output power.



**Figure 5: Latitude trends for annual GHI-weighted (A) diffuse fraction and (B) air mass.**

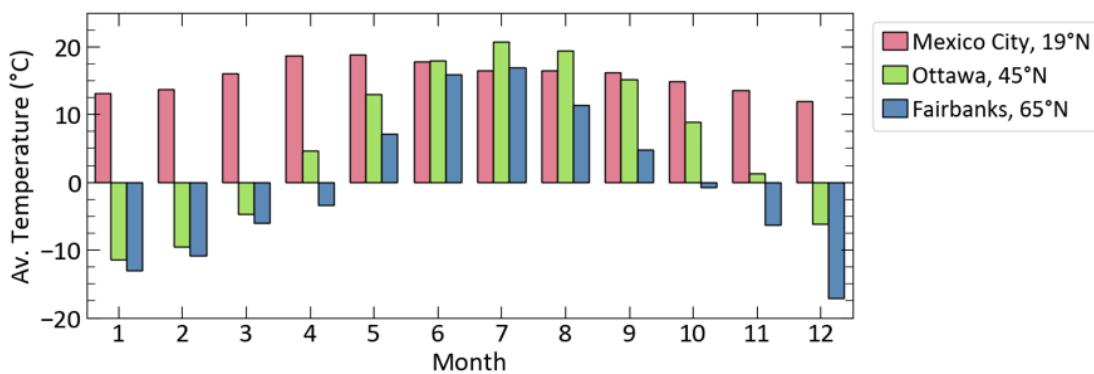
## 2.2 Ambient Temperature

Ambient surface temperature on the Earth generally decreases as one moves away from the Equator toward the Poles, especially north of the Tropic of Cancer ( $23^{\circ} 26'$  N). Figure 6 shows the annual average ambient temperature for  $>3000$  locations using MERRA-2 reanalysis data obtained through the NSRDB [5].



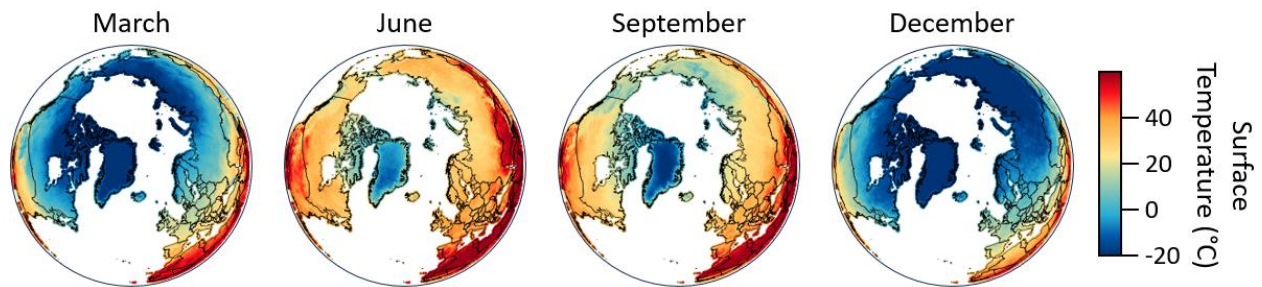
**Figure 6: Annual average ambient temperature as a function of latitude.**

Surface temperatures are consistently lower compared to those at lower latitudes, regardless of the season. Figure 7 presents the TMY average ambient temperature for three locations at different latitudes. In Figure 7, the monthly average temperature in Mexico City (19°C) varies by <10°C throughout the year, whereas higher latitude locations like Ottawa (45°N) and Fairbanks (65°N) experience much more pronounced seasonal fluctuations. In lower latitude regions, temperatures tend to remain closer to the annual average.



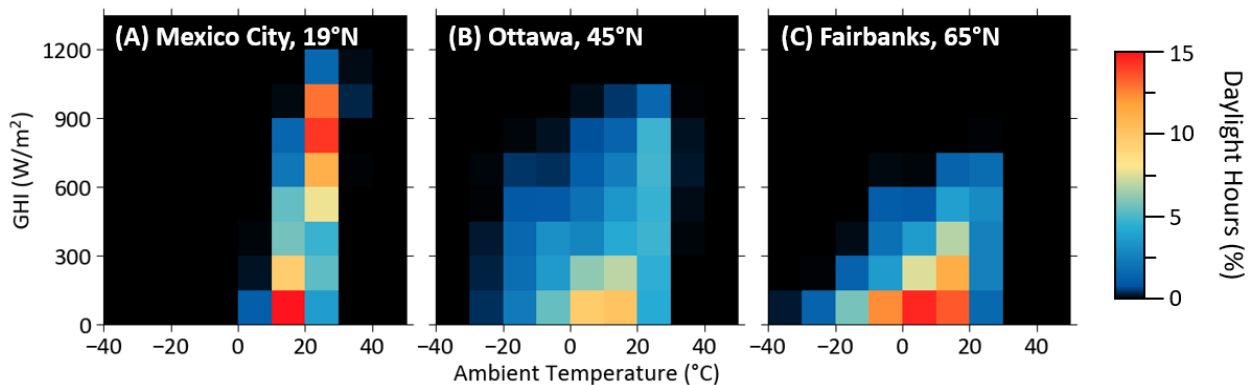
**Figure 7: Monthly average ambient temperature for three example locations.**

Figure 8 illustrates the seasonal variations in ambient surface temperature across the Northern Hemisphere, with monthly average temperatures for March, June, September, and December of 2023 [3]. High-latitude regions reach their warmest average temperatures around the summer solstice (June), when sunlight is most abundant, in contrast to the colder temperatures during the winter solstice in December. The seasonal disparity between the equinox months of March and September is also evident, with March exhibiting significantly lower temperatures than September, a result of Earth’s seasonal lag due to the high latent heat of water.



**Figure 8: Average monthly surface temperature map of the northern hemisphere.**

As there is a positive correlation between ambient temperature and solar irradiance, Figure 9 shows the distribution of GHI and ambient temperature for all daylight ( $GHI > 10 \text{ W/m}^2$ ) hours in TMY files for Mexico City, Ottawa, and Fairbanks. Though winter temperatures reach below  $-30^\circ\text{C}$  in Fairbanks, Alaska, these conditions are associated with  $GHI < 150 \text{ W/m}^2$ . In Mexico City, ambient daylight temperatures largely fall between  $10\text{-}30^\circ\text{C}$  with GHI often between  $450\text{-}1050 \text{ W/m}^2$ .



**Figure 9: Distribution of GHI and ambient temperature for three example locations from TMY data.**

### 2.3 Snow and Albedo Effects

Snowfall tends to occur primarily in the northern half of the Northern Hemisphere, Antarctica, and in high-altitude mountainous regions with sufficiently cool temperatures and humidity. In the context of high-latitude solar PV installations, snow accumulation can block solar irradiance from reaching PV arrays and exert mechanical stress on installation components (modules, mounting structure, foundations, etc.). However, snow can also provide a reflective ground surface that enhances the reflection of sunlight, quantified by its albedo. Albedo is the ratio of reflected irradiance relative to the incident irradiance and can be used as a measure for quantifying the presence of snow.

The annual average albedo and percentage of the year with snow cover for TMY locations are shown in Figure 10. Snow coverage is calculated by assuming any timestamp with an albedo  $> 0.5$  is indicative of snow on the ground. All hours of the year are considered in this calculation, including timestamps with high albedo and no sunlight. This



figure gives an approximate idea of how the annual average albedo tends to increase with latitude, driven by periods of snow accumulation during the year. However, the albedo data provided in TMY files are limited in many cases, particularly for high-latitude locations where data availability is low- and high-quality ground-station or satellite measurements of albedo are sparse. In many cases, albedo is simply assumed to always be a fixed value (commonly 0.2,) leading to a series of locations with average albedos at 0 and 0.2 in Figure 10A. This results in the calculated percent of the year with snow coverage in Figure 10B to be 0% for many high-latitude locations. In many cases, a simple binary between fresh snow (albedo=0.85) and non-snow (albedo=0.2) ground cover is also assumed in the datasets [6]. This can lead to an over-estimation of ground albedo [7], as the albedo of snow tends to decay as snowpacks age [8]. The initial albedo of fresh snow may also be different due to variations in temperature, humidity, grain size, and impurity concentration[8]. This figure highlights the need for ongoing development of appropriate meteorological datasets for PV systems in high-latitude locations.

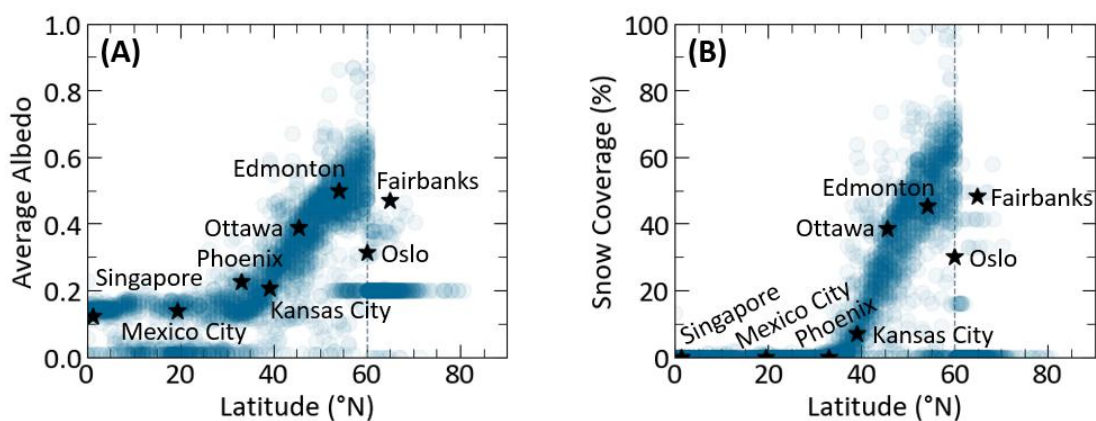


Figure 10: (A) Average annual albedo as a function of latitude and (B) percentage of the year with snow coverage for select sites in the NSRDB database.

Figure 11 shows the monthly average map of surface albedo for the northern hemisphere, with data retrieved from NASA Earth Observations. Close to the North Pole, snow is present on the ground continuously throughout the year, but at more moderate latitudes, albedo tends to significantly fluctuate seasonally.

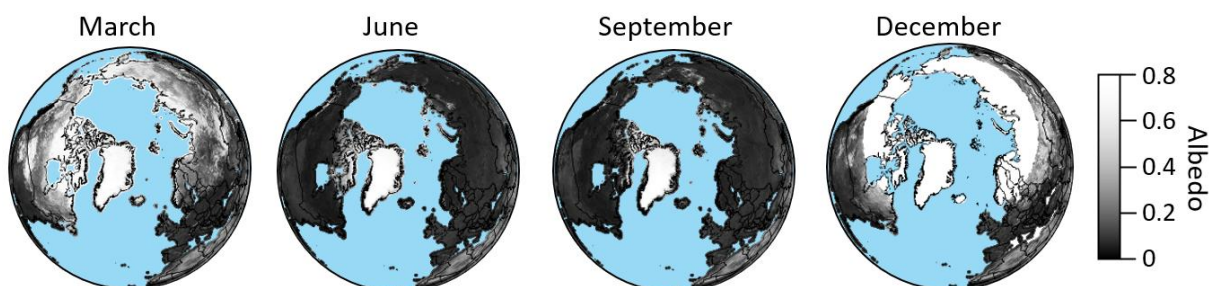
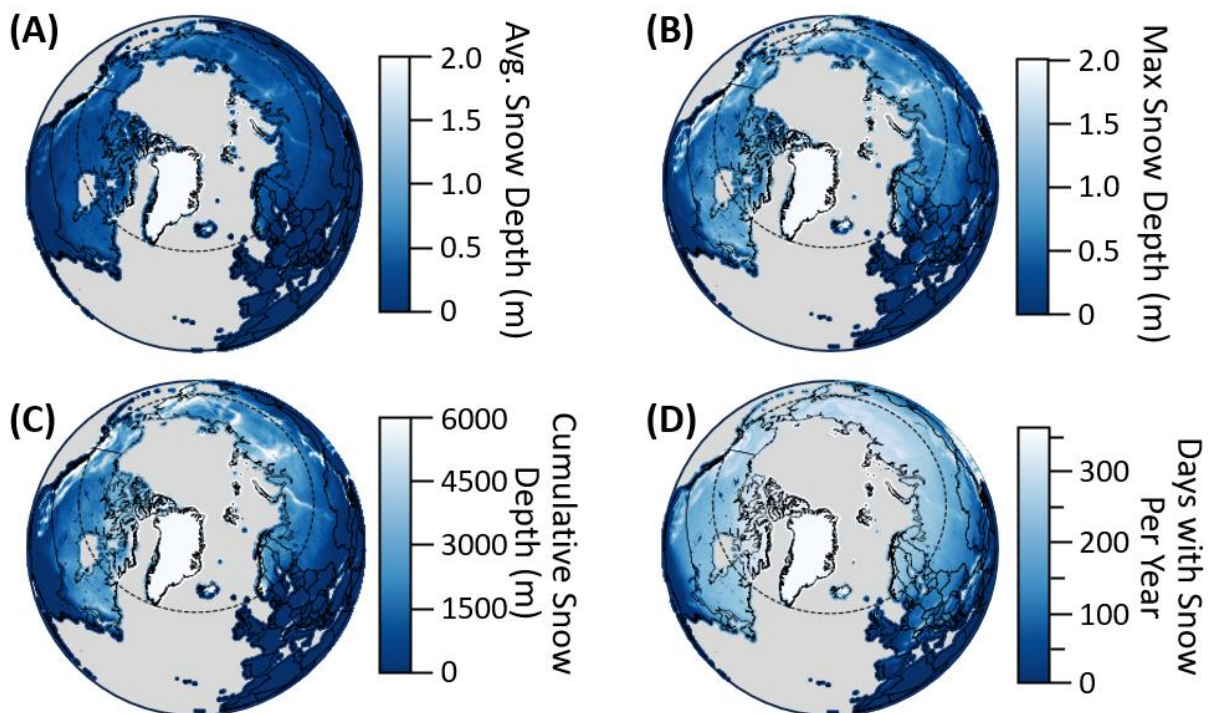


Figure 11: Average monthly albedo map of the northern hemisphere.



Figure 12 shows the total number of days with a snow cover and the average snow depth in 2023. Data were retrieved from the European Centre for Medium-Range Weather Forecasts (ECMWF) ERA5-Land reanalysis dataset [9]. Snow on the ground occurs for more than 200 days annually in high-latitude countries. Average snow depth is plotted in Figure 12B considering an upper limit for the color map of 2 m. The average values are calculated considering all the days of the year (i.e., it includes days with snow depth equal to zero). Figure 12 highlights that regions located below 60°N, such as southern Canada and Russia, present similar snow characteristics compared to Arctic regions.



**Figure 12:** (A) Average annual snow depth, (B) maximum measured snow depth, (C) cumulative snow depth, and (D) the number of days with snow depth greater than zero in 2023.

Finally, Figure 13 depicts the regions of the northern hemisphere with permafrost from the NASA National Snow and Ice Data Center [10], where the ground soil has remained frozen for at least two continuous years and in most cases has been frozen for hundreds to thousands of years [11].

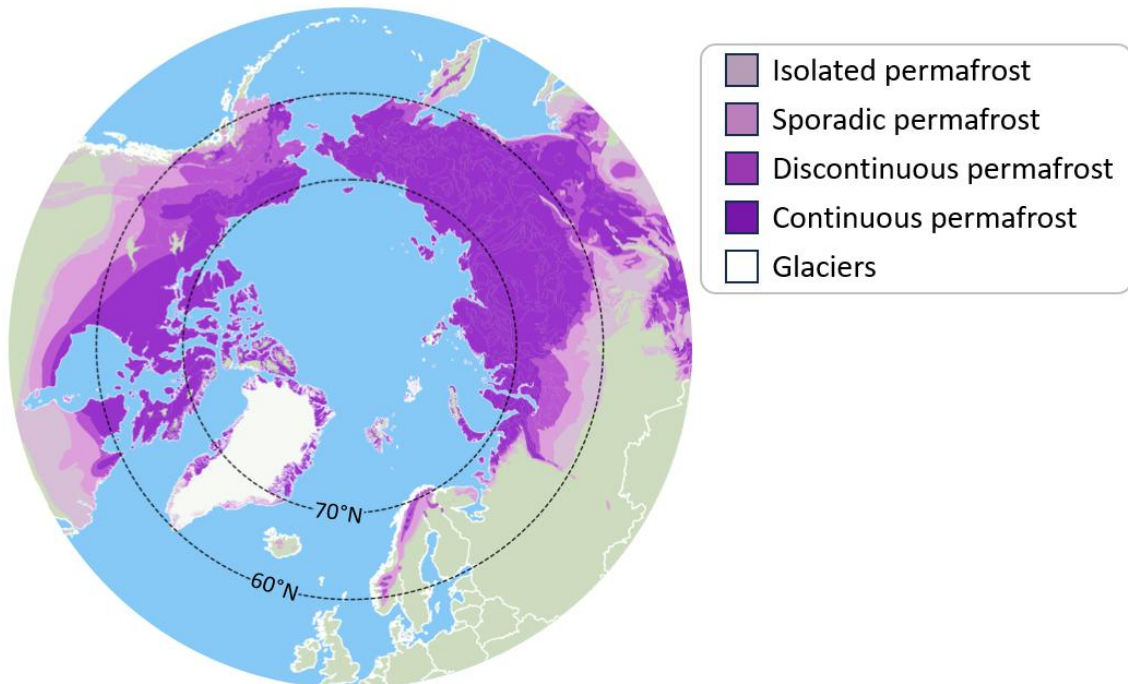


Figure 13: Distribution of permafrost >50°N, with data from the NASA National Snow and Ice Data Center [10].



### 3 DATA CHALLENGES AND OPPORTUNITIES

---

With the global expansion of PV systems and increasing interest in high-latitude regions, accurate predictions of PV performance are critical for the planning of future PV installations, as well as forecasting and optimizing energy dispatch. Most prediction tools and software used by the PV industry rely on precise input data, such as solar irradiance and site-specific climatic conditions, to simulate power output. These input variables (besides system design configuration and dimensions) can be categorized into incoming solar irradiance, reflected irradiance (albedo), and meteorological parameters. The highest quality data for a specific site is typically obtained through ground-based measurements using research-grade, class-A solar radiometers with high temporal resolution. However, such ground observations are very scarce [12]. As a result, the community has turned to alternative data sources, such as satellite data, reanalysis models, and land surface assimilation models, which are able to provide global coverage [13,14].

These alternatives, however, vary in their spatial and temporal resolution, often performing worse in high-latitude regions. Geostationary satellites are positioned over the equator and exhibit significant errors at latitudes beyond  $\pm 65^\circ$  due to the view angle. Polar orbiting satellites, while offering global coverage, have lower temporal resolution due to their longer revisit times compared to the image acquisition frequency of geostationary satellites. Moreover, while polar orbiting satellites can estimate solar irradiance in high latitudes, their accuracy decreases due to large solar zenith angles, leading to poorer cloud detection and parallax issues [15]. Similarly, satellite sensors in the visible spectrum struggle to differentiate between snow and cloud cover. Infrared sensors can distinguish between clouds and snow, but typically are of lower spatial resolution [16]. Reanalysis datasets, which combine historical observational data with numerical weather models, provide long-term global coverage but tend to be less accurate than satellite-based estimates, particularly in high-latitude regions [17,18].

One strategy to improve satellite- or model-derived data is through site adaptation techniques, which use high-quality ground measurements to correct systematic biases in satellite or reanalysis datasets [19]. However, ground observations, though accurate in reflecting site conditions, can be affected by issues such as missing data, faulty readings, misaligned instruments, soiling due to lack of cleaning, and calibration drift. In such cases, modeled data or interpolation from nearby and well-maintained stations are used to fill in gaps. Maintaining high-quality measurement equipment is costly, with additional challenges in high-latitude environments due to harsher conditions [20]. Common issues include rime, frost, and snow buildup on radiometer domes (Figure 14), malfunctions of movable parts (e.g., shadow balls and trackers), calibration temperature compensation [21], and operational problems due to limited or challenging access [20]. To ensure success of high-latitude ground measurement stations, adequate heated ventilation instruments, rigorous maintenance and calibration protocols,



data homogenization, and specialized quality control measures are required. Despite these challenges, high-quality observations remain essential for improving accuracy of datasets and validating models.



**Figure 14: Photo of sensors with snow buildup and without snow buildup (built-in heating option). Photo credit Sven Ruin, TERO AB.**

To support solar PV deployment in high-latitude regions, Table 1 provides a compilation of public and commercial databases offering full or partial coverage of these areas. These databases contain input data relevant to solar PV studies, including solar radiation parameters (e.g., global horizontal irradiance, diffuse horizontal irradiance, direct normal irradiance), weather-related variables (e.g., air temperature, wind speed, snow depth, surface air pressure, precipitation, relative humidity), and surface albedo. The table also details each database's spatial and temporal coverage, along with its spatial and temporal resolution. Furthermore, it specifies whether the data is derived from satellites, reanalysis models, physical models, or ground-based observations from specific stations. When using data from different databases, it is important to be aware of potential differences in quality control procedures, data treatment, averaging methods, and the resolution of the datasets. Figure 15 illustrates high-quality solar irradiance measurement stations north of 60°N measuring global and diffuse solar radiation components monitored.

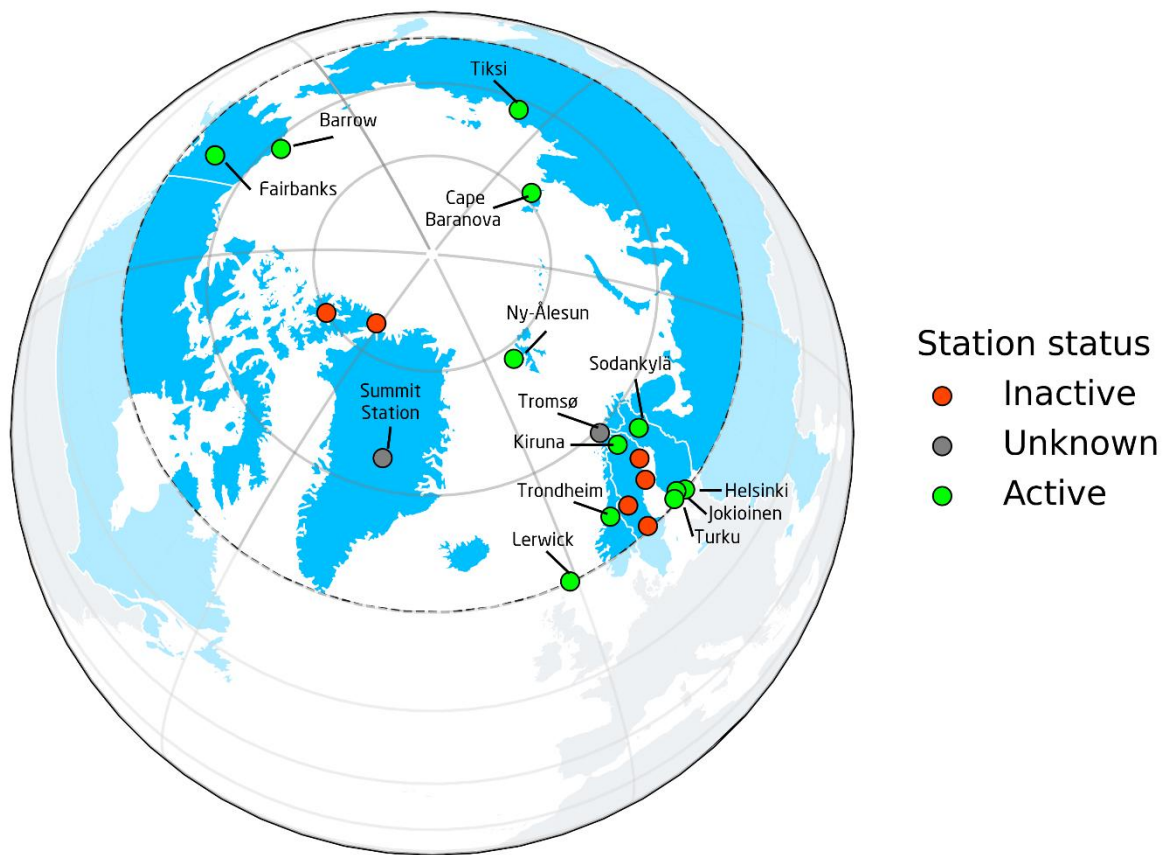


**Figure 15: Solar radiation monitoring stations located above 60 deg. N, from [22]. Only stations measuring diffuse or direct and global horizontal irradiance are included.**



**Table 1: Public domain and commercial solar radiation, albedo, and weather databases with partial or full high-latitude coverage.**

Database name	Type	Coverage (Latitude)	Spatial resolution	Highest Temporal resolution	Period	Surface Albedo Parameters*	Solar Irradiance Parameters*	Weather Parameters‡	Source
ASRv2 [23]	Reanalysis	24.54° to 90°	0.136°	3 h	2000-2016	AA	GHI	TA, WS, SD, P, Prec., RH	NCAR [23]
BSRN	Measurement	-90° to 80°	Individual stations	1 – 3 min	Variable	-	GHI, DHI, BHI	TA, RH, P	PANGAEA [24]
CAMS-RAD	Satellite	-66° to 66°	~4 km	1 min	2004- now	-	GHI, DHI, BHI, DNI	-	ECMWF/SoDa [25]
CERES SYN1deg	Satellite	Global	1°	1 h	2000-2 months ago	AA	GHI, DHI	-	NASA LaRC [26]
CLARA-A2.1	Satellite	Global	0.25°	24 h	1982-2019	BSA	GHI	-	EUMETSAT CMSAF [27]
ECCC	Measurement	Canada	Individual stations	1 h	1953-now	-	-	TA, WS, P, Prec., RH	Environment and Climate Change Canada [28],
ERA5	Reanalysis	Global	0.28125°	1 h	1940-now	AA	GHI, BHI	TA, WS, SD, P, Prec.	ECMWF [29]
FMI	Measurement	Finland	Individual stations	1 min	1959-now	-	GHI, DHI, DNI	TA, WS, SD, P, Prec., RH	FMI [30]
ICOS	Measurement	Europe	Individual stations	30 min	Variable	-	GHI, DHI	TA, WS, SD, P, RH, Prec.	ICOS [31]
LMT	Measurement	Norway	Individual stations	1 h	Variable	-	GHI	TA, WS, RH, Prec.	NIBIO, [32]
MCD18A1 MCD18C1	Satellite	Global	1 km 0.05°	3 h	2000-now	-	GHI, DHI, BHI,	-	USGS NASA [33,34]
MCD43GF MCD43A3 MCD43C3 MCD43D*	Satellite	Global	1 km 500 m 0.05° 1 km	24 h	2000-2017 2000-now 2000-now 2000-now	BRDF, BSA, WSA BSA, WSA BSA, WSA BRDF, BSA, WSA	-	-	USGS NASA [35–38]
MERRA-2	Reanalysis	Global	0.5° x 0.625°	1 h	1980-1 month ago	AA	GHI	TA, WS, P, Prec., SH	NASA [39]
Mete-onorm	Measurement + Satellite + Reanalysis above 62°	-62° to 62°	Stations	1 h	2008-1 month ago	-	GHI, DHI, DNI	TA, WS, RH, Prec.	Commercial product [40]
NSRDB	Model	-60° to 60°	2 km (4 km)	5 min (30 min)	1998-2022	-	GHI, DHI, DNI	-	NREL [2]



<b>POWER</b>	Com- bined	Global	1°	1 h	1984-7 days ago	AA	GHI, DNI, DHI	TA, WS, SD, P, Prec., RH	NASA LaRC [41]
<b>SARAH-2</b>	Satellite	-65° to 65°	0.05°	30 min	1983- 2015	-	GHI, DNI	-	EUMET SAT CMSAF [42]
<b>Seklima</b>	Meas- urement	Norway	Individ- ual sta- tions	24 h	Variable	-	-	TA, WS, SD, P, Prec., RH	MET Norway [43]
<b>SMHI Open Data</b>	Meas- urement	Sweden	Individ- ual sta- tions	1 h	Variable	-	GHI	TA, WS, SD, P, Prec, RH	SMHI [44]
<b>Solar- Anywhere</b>	Satellite	-60° to 60°	0.5 km	5 min	1998 now	-	GHI, DNI, DHI	TA, WS, RH	Com- mercial product [45]
<b>Solar- Anywhere High Lati- tude</b>	Satellite	-80° to 80°	30-100 km	1 h	TMY	AA	GHI, DNI, DHI	TA, WS	Com- mercial product [46]
<b>Solargis</b>	Satellite	-60° to 60/65°	2 or 4 km	10 min	1994/ 1999 now	AA	GHI, DNI, DHI	TA, WS, RH, Prec.	Com- mercial product [47]
<b>Solcast</b>	Satellite	-60° to 60/70°	1/2 km	5 min	2007 to 7 days ago	AA	GHI, DNI, DHI	TA, WS, RH, Prec.	Com- mercial pro- duct.[48 ]
<b>STRANG</b>	Model	Nordic countries	2.5 km	1 h	1999-now	-	GHI, DHI, BHI, DNI	-	SMHI [49]

\*AA = average albedo; BRDF = bidirectional reflectance function; BSA = black-sky albedo; WSA = white-sky albedo; Refl = reflectance; GHI = global horizontal irradiance; DHI = diffuse horizontal irradiance; BHI = beam horizontal irradiance; DNI = direct normal irradiance; TA = air temperature; WS = wind speed; SD = snow depth; P = pressure; Prec = precipi-  
tation; RH = relative humidity; SH = specific humidity.

‡ Many variations exist from MCD43D01 to MCD43D68.



## 4 DESIGN AND MODELING CONSIDERATIONS FOR HIGH-LATITUDE IRRADIANCE AND ALBEDO CONDITIONS

### 4.1 Design Considerations

Given the climatic conditions outlined in Section 2, PV systems may undergo adaptations to be better suited for high-latitude deployment [50]. Figure 16 shows eight example PV sites located near and above 60°N. Much like more southern climates, a wide range of PV technologies have been deployed in high latitudes to address differing energy priorities, including traditional equator-facing fixed-tilt systems, single-axis tracking systems, dual-axis tracking systems, roof-mounted systems, vertical and façade systems, and more. Due to their simplicity and increased reliability in areas with frequent freeze-thaw cycles, fixed-tilt systems are most common and recommended in high-latitude regions. Tracking systems are less common and may not be recommended due to reliability concerns when operating at very cold temperatures.

South-facing fixed-tilt  
Luleå, Sweden



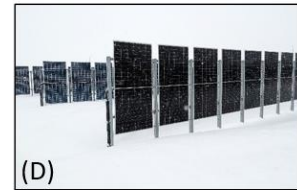
Single-axis tracker  
Lillestrøm, Norway



Dual-axis tracker  
Fairbanks, USA



E-W vertical  
Luleå, Sweden



Rooftop  
Fairbanks, USA



Building integrated  
Iqaluit, Canada



Artistic  
Piteå, Sweden



Fairbanks, USA

**Figure 16: Example high-latitude deployments. Photos (A), (D), and (G) by Erin Tonita; Photo (C) from [51]; Photo (F) from [52]**

For ground-mounted, fixed-tilt PV systems, high-latitude deployments generally require larger row spacing and higher mounting height compared to their mid- or low-latitude counterparts. Mounting height is typically reported as distance from the lower edge of the lowest module to the ground or mounting surface (e.g., roof). Increased row spacing is required to reduce inter-row shading losses caused by low solar elevation angles [53], while increased ground mounting height may also be required to allow snowfall to shed from the array without blocking shedding from accumulations on the ground. Further design considerations, such as the use of snow fences around ground-mounted PV arrays, may also be required to reduce snow drifts – discussed further in Section 6.

Bifacial gain increases with latitude due to long-lasting and seasonal snowfall in northern latitudes, increased diffuse light, and low solar elevation angles [54]. As a result,



bifacial technologies are recommended in high-latitude regions to make use of this natural enhancement.

Vertically oriented bifacial PV systems (typically oriented E-W) are able to capture light effectively in high-latitude regions where solar elevation angles are low and solar azimuths have a large range [55]. Vertical PV systems also better match daily electricity demand, improve building self-consumption when integrated into facades, and substantially reduce energy yield loss from snow accumulation [56–59]. Figure 17 shows examples of rooftop designs that incorporate vertically mounted PV in Norway [60], but most vertical systems are ground mounted.



**Figure 17: Vertical rooftop arrays in Norway. Photo credit: Over Easy Solar.**

A comparison of performance between latitude tilt, single-axis tracking and vertical PV is shown in Figure 18. It shows the cumulative plane-of-array insolation received on south-facing fixed-tilt, horizontal single-axis tracking, and E-W vertical PV modules in three different locations considering both monofacial and bifacial modules, modeled using TMY data in the System Advisor Model [61]. E-W vertical bifacial PV systems achieve similar annual insolation to south-facing fixed tilt systems in Fairbanks, Alaska at 65°N. Figure 19 compares normalized cumulative PV power generation for two latitude-tilt systems in Charlotte, North Carolina (USA) (monofacial and bifacial) and three systems in Fairbanks, Alaska (USA) (latitude-tilt monofacial and bifacial and vertical E-W bifacial). Simulations use TMY data from PVGIS and the Sandia Photovoltaic Array Performance Model implemented in pvlib-python and have the same number and type of modules and inverter. The results show the advantage of bifacial gain and lower operating temperatures in a cold temperature location that receives lots of snow (Fairbanks). This advantage is enough to bring the yield of the bifacial fixed-tilt system in Fairbanks to about 90% of a similar system in Charlotte.

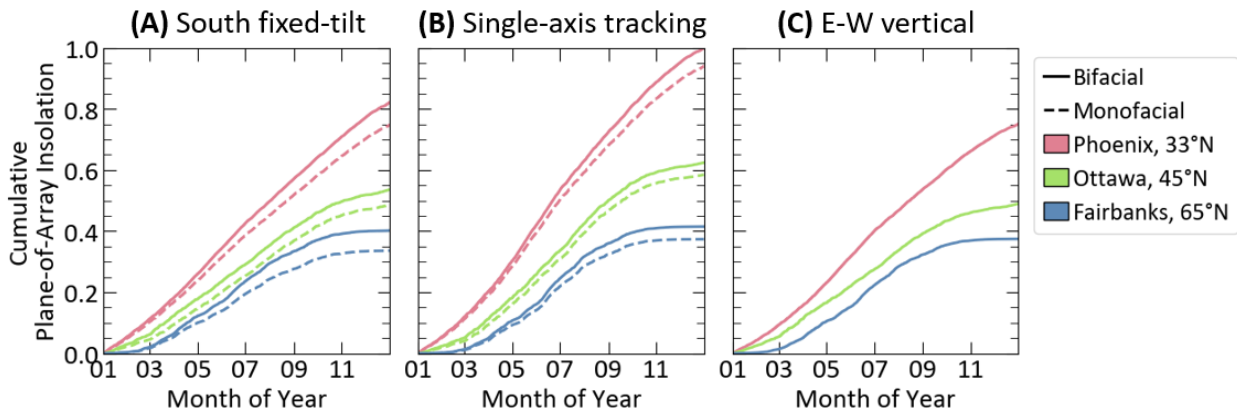


**Figure 18:** Cumulative annual plane of array (POA) insolation using TMY data in three different locations for (A) south-facing fixed-tilt PV, (B) single-axis tracking PV, and (C) E-W vertical PV. The cumulative POA insolation is normalized to the maximum POA in Phoenix under single-axis tracking.

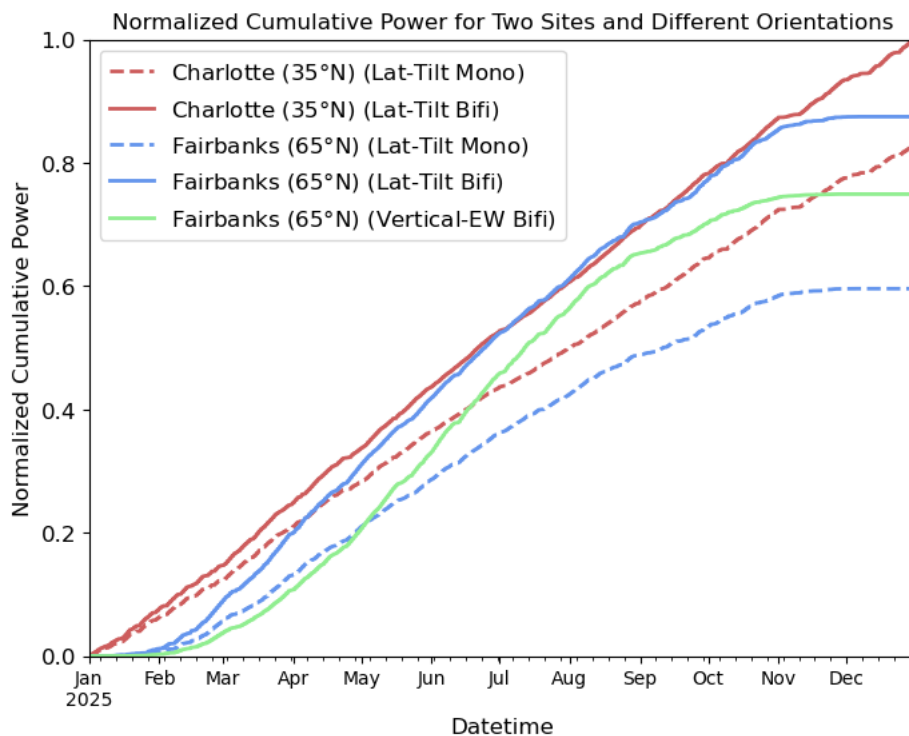


**Figure 19:** Normalized cumulative AC power simulated for latitude-tilt PV systems (monofacial and bifacial) in Charlotte, North Carolina, and Fairbanks, Alaska, and a bifacial vertical PV system in Fairbanks.

A field example from Sweden shows a comparison of two consecutive years of energy production between vertically-mounted agrivoltaic system (VAPV) and a ground-



mounted south-facing fixed-tilt (SFFT) system installed in Kärrobo Prästgård, Sweden, at 59.55°N (Figure 20, Table 2), both equipped with bifacial PV modules, reveals some interesting trends (Figure 21). In July and August of 2022, the VAPV system outperformed the SFFT system in terms of monthly specific yield. However, this trend reversed in 2023, when heavy rainfall characterized July and August.

The performance of the vertically mounted system in June 2022 was negatively impacted by inverter shut offs, as well as in October and November of 2022, and in April and July of 2023, which affected its overall production capability. Despite these issues, there were 105 days in 2022 when the normalized production of the vertically mounted system exceeded that of the SFFT system. In 2023, this occurred on 115 days. One notable advantage of the vertically mounted PV modules is their reduced snow coverage during snowy periods. In December 2023 (Figure 22), for example, the vertically mounted system outperformed the SFFT system on 28 days, with an average production of 6.1 kWh/kWp/month compared to the SFFT's 1.32 kWh/kWp/month. Additionally, on 14 days, the SFFT system recorded zero production due to snow coverage. In addition, a vertical E-W systems produces more power at the beginning and end of the day when the value of electricity is greater.



**Figure 20.** Picture of the VAPV and SFFT bifacial systems at Kärrobo Prästgård, Sweden, during a snowy day in 2022. Photo credit: Sven Ruin, TEROC AB.



**Table 2. Design characteristics and annual specific yields of the VAPV and SFFT bifacial systems at Kärro Prästgård, Sweden.**

Latitude: 59.55 °N Longitude: 16.76 °E	Vertical Agrivoltaic (VAPV)	South-facing fixed tilt (SFFT)
Installed capacity (kWp)	22.8	11.8
Number of rows	3	2
Row length (m)	18	10
Pitch (m)	10	9
Tilt angle (°)	90	30
Annual specific yield 2022 (kWh/kWp/y)	912.2	1117.3
Annual specific yield 2023 (kWh/kWp/y)	929.2	1154.3

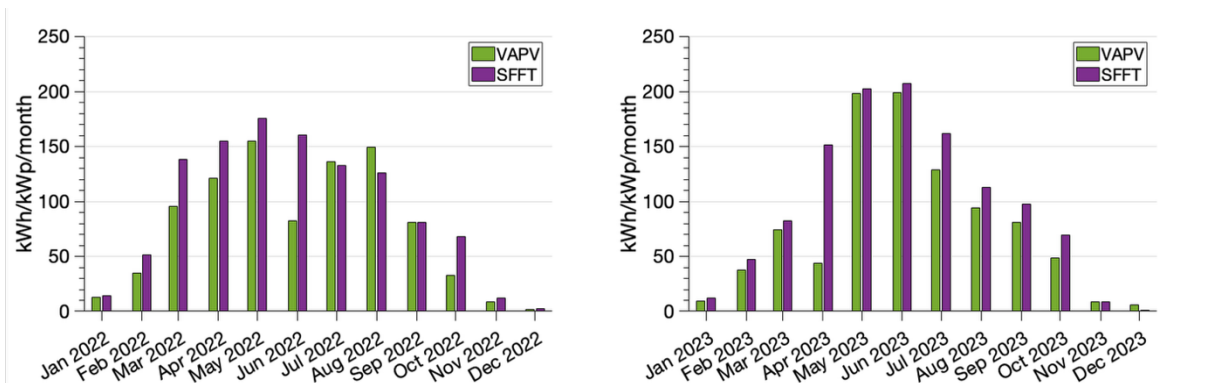


**Figure 21. Monthly specific yields of the VAPV and SFFT bifacial systems at Kärro Prästgård, Sweden in 2022 (left) and 2023 (right).**

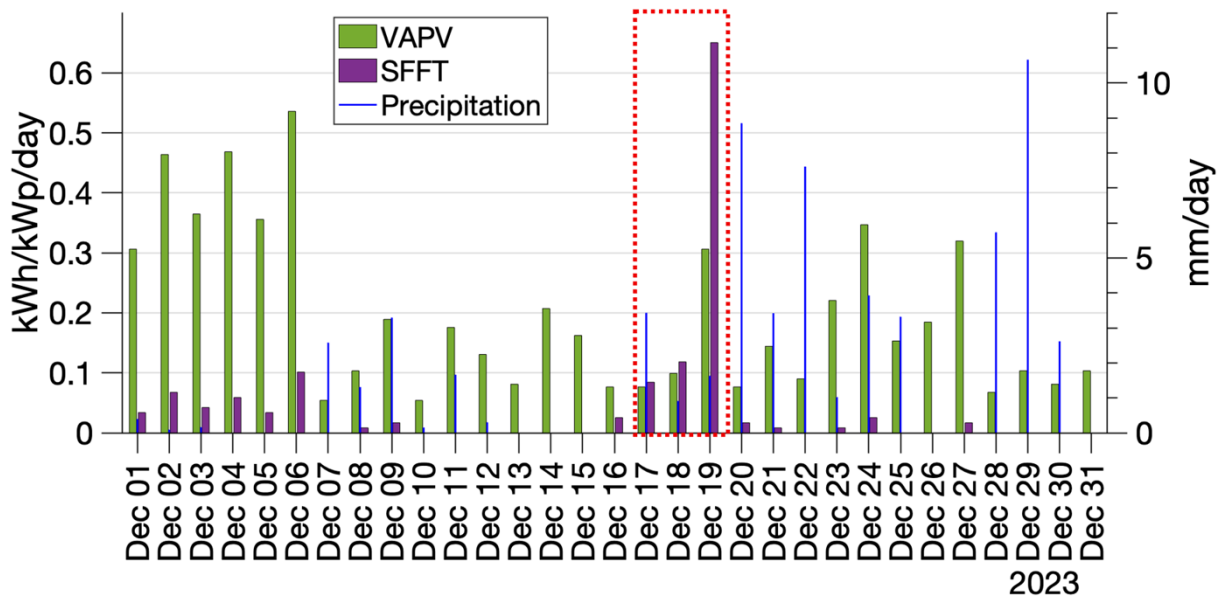


Figure 22. Daily average energy production of bifacial systems at Kärrbo Prästgård, Sweden, during Dec 2023. Daily precipitation is overlaid, occurring as snow, except for the days within the red dashed box, which experienced rainfall.

## 4.2 Modeling Considerations

Modeling PV systems in high-latitude locations is critical for financial planning, system monitoring, and deployment design. However, high-latitude conditions lead to increased uncertainty in PV models. There are multiple causes for this increased uncertainty, including lower data availability and quality above 60°N (see Section 3), increased modeling uncertainty associated with cloudy conditions and high albedo [62,63], and limited studies which validate PV models in high-latitude locations [62,64–66]. Model uncertainty has also been shown to be larger for façade and vertical PV systems [62,67,68].

Beyond irradiance and energy yield modeling, economic PV modeling can also be challenging. Low and mid-latitude cost assumptions often do not apply in high-latitude locations where shipping, installation, and maintenance costs can be vastly different. For example, for many communities in Northern Canada, new equipment such as PV modules and racking can only be brought into communities on a barge or airplane, leading to significant increases in shipping costs. In some communities, with an absence of permanent road infrastructure, the most cost-effective route for transporting PV array components is a winter ice road. At least 50 remote First Nations depend on approximately 6000 km of winter ice roads in Canada for their supplies. The length of the winter season when these roads are accessible is narrowing due to the warming climate.

Despite the challenges associated with PV system modeling in high latitudes, modeling of system performance remains a crucial tool for design decisions and provides useful insights on predicted performance. PV models can be adapted for high-latitude environments by integrating snow loss models (described in Section 6), locally optimizing



sky model coefficients, and using high-quality ground-station data. In high-latitude, snow-prone climates, vertical bifacial arrays could be the attractive design option, since it is the solution less susceptible to snow burial and thus able to maintain energy production during periods of significant snowfall.



## 5 PERFORMANCE AND DESIGN OF SOLAR PV IN EXTREME COLD TEMPERATURES

### 5.1 Temperature-dependence of Different Solar Cell Technologies

Temperature coefficients represent the relative change in a physical property per degree of temperature change. Modules with lower temperature coefficients exhibit less sensitivity to temperature fluctuations, which is desirable for maintaining consistent performance. Among the current-voltage (I-V) parameters, the open-circuit voltage is the most temperature-sensitive, as the semiconductor bandgap is highly temperature-dependent [69]. Solar cells generally perform better at lower temperatures because the semiconductor's bandgap widens, resulting in higher voltages. Although current decreases slightly as the bandgap widens, this reduction occurs at a much slower rate than the increase in voltage, leading to an overall increase in power as temperature decreases [69], see Figure 23.

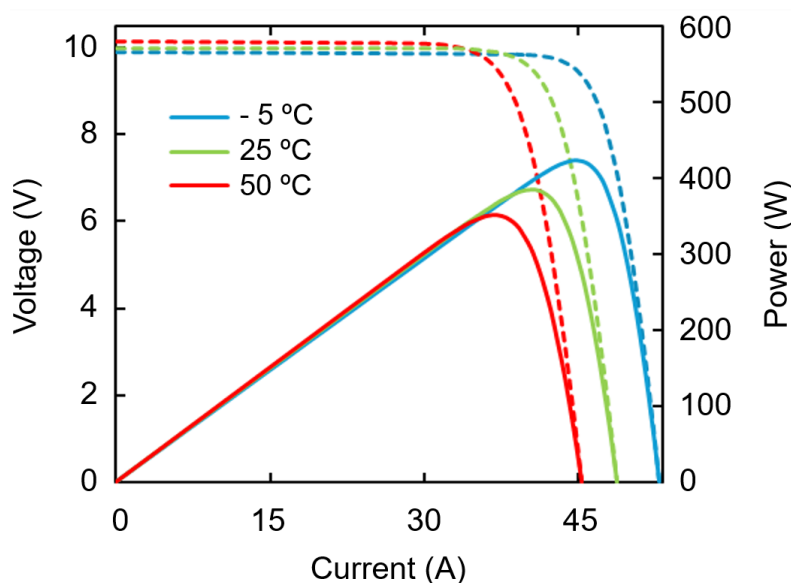


**Figure 23: Simulation of I-V (dashed lines) and power curves (solid lines) for a commercial monocrystalline silicon module operating with three different solar cell temperatures at 1000 W/m<sup>2</sup>. At -5°C, the maximum power of the module is higher than at 25°C and 50°C (ivcorrection version 0.0.7, Lawrence Berkeley National Laboratory) [70].**

Depending on the cell structure and technology, silicon solar cells typically have power temperature coefficients ranging from -0.25%/°C to -0.35%/°C [71,72]. Solar cells with superior surface passivation (e.g., Tunnel Oxide Passivated Contact - TOPCon and Polycrystalline Silicon on Oxide - POLO) solar cells tend to have lower temperature coefficients compared to Passivated Emitter and Rear Contact (PERC) solar cells, which were the industry standard until recently. Cadmium Telluride (CdTe) solar cells, widely used in the USA, have temperature coefficients similar to silicon solar cells [73]. Copper indium gallium selenide (CIGS) solar cells have an important market in the



Nordic countries, and temperature coefficients are in the same range as silicon-based solar cells [74].

Solar modules are rated at 25°C under an irradiance of 1000 W/m<sup>2</sup>, referred to as standard test conditions (STC). However, in real-world deployments, solar modules typically operate at higher temperatures and under lower irradiance levels. To accurately estimate the power output of a module, it is crucial to determine its expected operating temperature. The Nominal Module Operating Temperature (NMOT) mean equilibrium cell temperature of a module mounted on an open rack with a tilt angle of 37±5° and operating at its maximum power point under ambient air temperature of 20 °C, irradiance of 800 W/m<sup>2</sup> and wind speed of 1 m/s. Typical NMOT values for silicon solar modules range between 40°C and 60°C, depending on the module structure.

However, the conditions under which temperature coefficients and NMOT are measured differ significantly from those in high-latitude and Arctic regions, where modules often operate at low temperature and irradiance levels (<0°C and <800 W/m<sup>2</sup>). For example, Figure 24A shows the distribution of module temperature recorded on a south-facing 60° tilted system in Fairbanks, Alaska, from June 2019 to January 2024. The average module temperature while the sun is above the horizon is 12°C and the median is 15°C. The distribution of module temperature and plane-of-array irradiance is provided in Figure 24B for this same module.

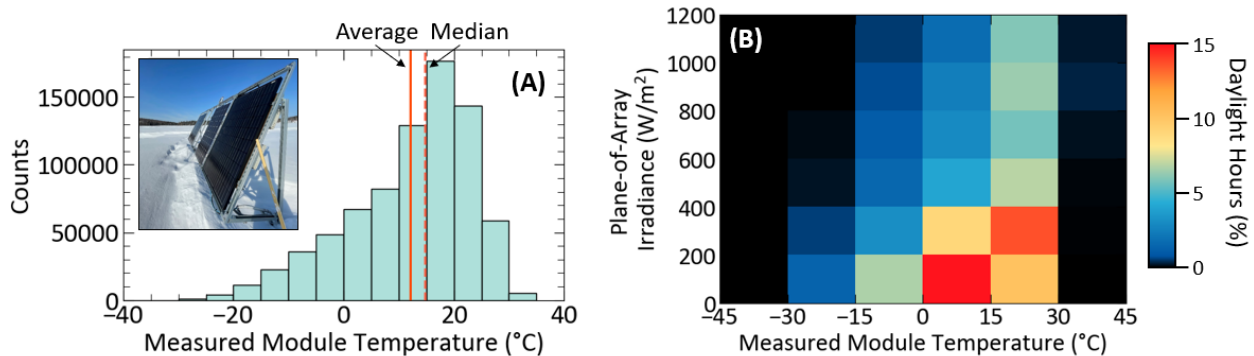


**Figure 24:** (A) Distribution of module temperature for a south-facing fixed-tilt (60°) module located in Fairbanks, Alaska (photo inset) from June of 2019 to January of 2024. (B) The distribution of measured module operating conditions over this same period. The color map shows the percentage of total daylight hours where the PV module operated within a specific bin of module temperature and plane-of-array irradiance. The most common operating condition for a module in Fairbanks (15% of daylight hours) is with a plane-of-array irradiance between 0-200 W/m<sup>2</sup> and a temperature between 0°C and 15°C.

While it is generally assumed that the behavior of temperature coefficients is linear, a recent study shows that certain silicon heterojunction technologies exhibit nonlinear behaviors in open-circuit voltage at cell temperatures below -10°C [75], suggesting that PV performance modeling practices may need to be adjusted for certain technologies [50].



## 5.2 Foundations and Frozen Ground

As the ground freezes in winter, water solidifies and expands into ice and subsequently causes the ground to lift or shift, known as frost heaving. This is different from permafrost which is defined as ground that remains completely frozen for more than two years (Figure 13). Frost heaving can be a recurring problem in cold climate regions. Literature about frost heaving implications for PV racking is limited. For system design, installers and contractors should use procedures meant for regular construction or road work, which might not be directly applicable for PV racking. One phenomenon that is widely observed by system owners and operators but not widely documented in publications is that PV racking can cause the ground to freeze deeper than surrounding areas. PV racking tends to cause the ground directly underneath the array to accumulate less snow than the surrounding area due to PV modules blocking snowfall, snow shedding at the lower edge of the rows and wind scour effects, resulting in a reduction of snow insulation locally [76]. Metal ground anchors and driven piles provide thermal conduits for heat loss from the ground [77]. The combinations of these effects result in the ground freezing deeper. Two examples of problematic frost heaving are presented in Table 3, one being in Luleå, Sweden, as can be seen in Figure 16A, and the other in Fairbanks, Alaska (Figure 25).

**Table 3: Two examples of PV systems that experienced system damage from frost heaving.**

Site	Luleå, Sweden, 66°N	Fairbanks, Alaska, United States, 65°N
Ground type	Clay, old lakebed	Silt, gravel, cobbles
Pre-planning	Geotechnical survey performed by external consultant with a methodology from construction and road work.	Geotechnical survey from a substation that was adjacent to the array was used.
PV specifications	699 kWp total, bifacial Trina Solar TSM-300DEG5C, ground mounted rows with 2-landscape orientation.	563 kW Ground Mounted fixed tilt, south facing 45 degree tilt angle. CSUN320-72P with APSystem YC-1000 micro inverters
Piling type	Two types of C-profiles. First piling had perforations that the asset owners believe made the racking extra sensitive to frost heave, since the ground might grip the piling better. Second piling was sturdier, deeper, and non-perforated.	Helical Piles



Piling depth	2–2.5 m initially, after change of piling and racking 3 m	2.5-3m initially (below frost line), repaired Section was reinstalled 5.5m deep
Snow removal from modules or ground	No	No
Snow accumulation beneath racking	Not much	No
When was the problem identified	First winter after installation	Problem began two years after installation.
Consequences	Noticeably uneven racking, tension in system, screws in some of the glass/glass module clamps came undone, a few modules came loose	Some piles jacked out of the ground and others sank causing racking to twist and resulted in several modules breaking. Problematic section was about 10% of the array.
How was the problem dealt with	The entire racking and clamping system was changed to deeper, sturdier, and non-perforated piling. Frost heave is still noticeable. The installers have since used infrared cameras to search for hotspots without finding any defects, and they measure how much the racking moves each winter.	The pilings in the problematic section were replaced. Replacement pilings were 5.5m helical piles with a PVC sleeve around the top ~2 m. To do this work a portion of the array had to be disassembled then re-assembled. Two years have passed since the array was repaired and no movement has occurred since then.
Cost	Covered by the O&M plan and warranty from the installer.	The utility owner paid out of pocket for the work. They indicated it was expensive, but the full cost is not publicly available.
Lessons learned	The geotechnical survey performed in the pre-planning was not done with a methodology for specifically PV racking. Interpreting the survey (for construction/road work) and applying it to PV was difficult for the asset owners, as none of the involved partners had previous experience with the conditions at the	After the array began to exhibit initial problems, the array owners consulted with a local engineering firm who were able to bring up old soil maps which showed that historically there was a thin slough which once ran through the portion of the array exhibiting problems. This slough had been filled in during the region's mining period about 100 years



	<p>site and how it might affect PV. The array owner would avoid clay and other soil prone to frost heave in future PV development and would like to see more expertise within geotechnical surveys for PV.</p>	<p>earlier. The geotechnical work that was used during the initial array design was from the adjacent substation but didn't show the historical slough. The array owner indicates that he would suggest spending money on detailed geotechnical work on the front end, because it is cheaper than fixing problems that occur later.</p>
--	--	---



**Figure 25: The 563-kW solar array owned by the Golden Valley Electric Association in Fairbanks, Alaska. The substation encircled by the orange dashes represents the area where the initial geotechnical survey was performed. In addition, a winter picture of the site is shown on the right.**

### Recent experience of deploying solar PV in permafrost areas

Alaska and Canada contain large areas of permafrost and as PV growth has increased in high-latitude regions, several new solar arrays have been built on permafrost rich ground. The Alaskan communities of Kotzebue, Noatak, and Shungnak all lie on permafrost rich soil and have recently installed solar arrays. Each of these arrays has relied on ground screws for foundation anchoring. These ground screws are generally at least 2.5 meters long and are driven into the ground with a rotary driver. Some of the ground screws installed in Kotzebue and Shungnak have experienced movement, which has caused undulations in parts of the arrays. To date, no modules have been damaged. To remedy this, the array owners have loosened set screws on the racking which allow the height of the array to be adjusted independent of the height of the ground screw. The long-term effects of the ground screw movement are unknown.

### Ground Temperatures and Snow Drifting



Since July of 2023, ground temperature data have been collected at the Kotzebue array in front of, under and behind the array to monitor if the solar array infrastructure is affecting the condition of the permafrost where it is installed. This is important because the frozen condition of the permafrost provides structural integrity to the array foundation. Typically, infrastructure built on permafrost soils is designed to keep the permafrost frozen. Graphs showing the location of the temperature monitoring and the first year of data are shown in Figure 26 and Figure 27 below.

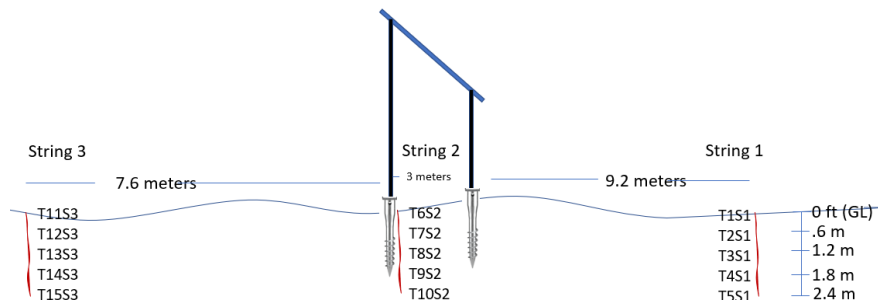


**Figure 26: The location of the ground temperature monitoring sensors is shown around an array in Kotzebue, Alaska.**

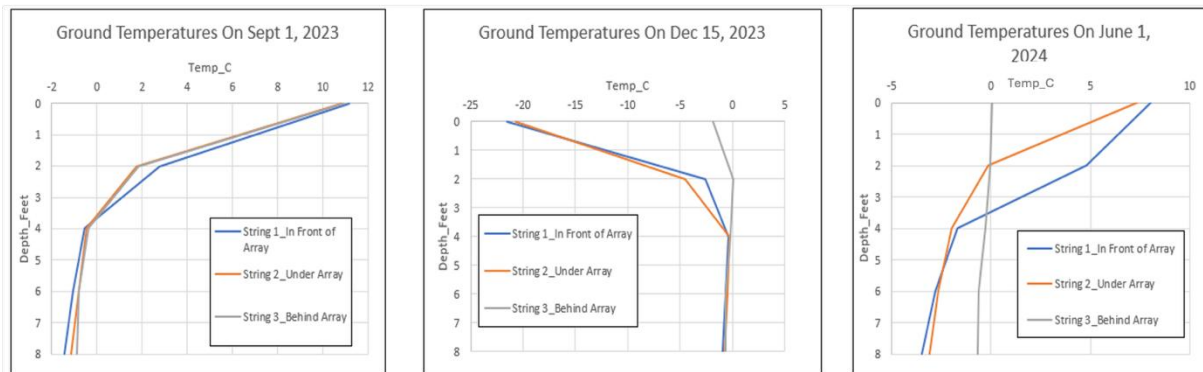


**Figure 27: Ground temperatures in September (2023), December (2023), and June (2024) at three locations around the solar array in Kotzebue, Alaska.**

The graphs in Figure 27 above show that in December, 2023 there is a large difference in shallow ground temperatures depending on position relative to the array, with lower ground temperatures during the winter months under and in front of the row and higher temperatures behind. It is believed that a snow drift that formed behind the array caused significant ground insulation and prevented the permafrost from getting as cold as it is under and in front of the array where very shallow snow depth provided minimal insulation of the ground to the cold wintertime temperatures. In June 2024 the shallow ground temperature next to the array foundation is warmer than the ground at the same depth in front of the array, which may reflect conductive heat transfer through the metal ground screws. As an example, Figure 28 shows a snowdrift from the same array, although at a slightly different location than where the temperature monitoring is taking place.



**Figure 28: A row of solar modules in Kotzebue, Alaska, with an approximately 3-meter-high snow drift behind the row.**

The solar array is functioning as a snow fence and, based on the data shown above, the long-term effect will likely be the warming of the permafrost and the formation of troughs in the locations where the snow drifts form behind the solar modules. The melting of the permafrost caused by the insulation of snow drifts near snow fences has been documented in other high-latitude locations in the literature [78,79].

### 5.3 Degradation Mechanisms and Performance Loss Rates

Modern PV modules are expected to last in the field for 25+ years before degrading to 80% of the initial efficiency. Outdoor environmental conditions such as ultraviolet radiation (UV), thermal cycling (diurnal and seasonal), and moisture exposure may stress PV modules and cause them to degrade faster than expected.

For PV systems located in high latitudes, the high temperatures and UV exposure associated with common module degradation mechanisms are suppressed. Instead, factors such as snow load, freeze-thaw cycle stresses, ground heave, and ambient temperatures as low as  $-40^{\circ}\text{C}$ , are suspected to be the primary drivers of PV system degradation in these regions. Snow load has been shown to lead to cell cracking in some cases, while moisture ingress from snow melt can cause delamination of module layers and material corrosion [80]. PV system components can also be impacted by the low ambient temperatures found in high-latitude regions. For example, some PV inverters are rated for operation between  $-25$  -  $+60^{\circ}\text{C}$ . Cell interconnection materials and bonds



have also been found to be susceptible to cracking during thermal cycling down to  $-40^{\circ}\text{C}$  [81], and glass transition of certain encapsulants can occur at temperatures below  $-15^{\circ}\text{C}$  [82]. Some encapsulants and backsheets become brittle at low temperatures.

In 2025, Tonita et al. reviewed existing literature on degradation rates in cold climates with continental (D-) and polar (E-) Koppen-Geiger climate code classification, where deployment latitudes spanned from  $44^{\circ}\text{N}$  to  $65^{\circ}\text{N}$  [83]. The degradation rate of a PV system quantifies its yearly decline in energy yield, caused by irreversible processes (ex. encapsulant yellowing and cell cracking). The most common reported degradation mechanisms were moisture ingress, with some instances of frame damage from freeze-thaw cycling and cell and glass damage that may be related to snow accumulation. The median degradation rate of the dataset, representing 27 unique PV systems, was found to be  $-0.33\%/year$ . PV systems have been found to degrade slower in colder climates than their warmer, historic counterparts. For instance, the median degradation rate of 1700 sites across the continental USA was reported to be  $-0.75\%/year$  in 2022 [84].

Figure 29 reproduces the work from [83], but instead limits the dataset to only high-latitude locations ( $>59^{\circ}\text{N}$ ). Due to the relatively high number of PV systems (6) deployed between  $59^{\circ}\text{N}$ – $60^{\circ}\text{N}$ , these systems are included in the analysis. Only 16 PV systems with reported degradation rates were identified by the authors above  $59^{\circ}\text{N}$ . The median degradation rate for high-latitude PV systems is  $-0.37\%/year$  (sample size = 16), with an average degradation rate of  $-0.62\%/year$ . These results support the finding that PV systems tend to degrade slower in cooler climates, though this finding is limited by the sparsity of long-term PV performance data  $>60^{\circ}\text{N}$ .

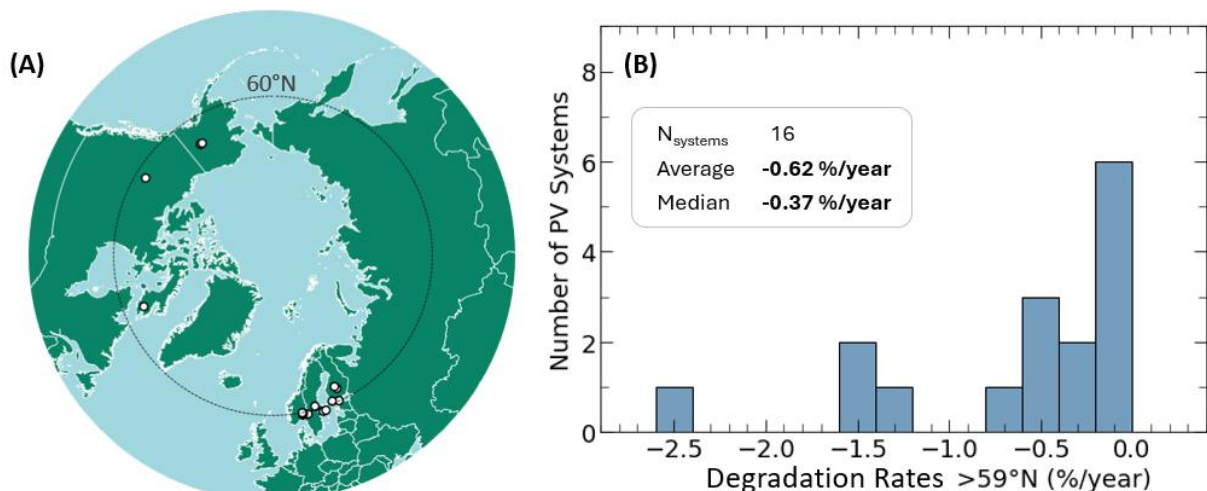


Figure 29: (A) Locations of reported degradation rates for PV systems  $>59^{\circ}\text{N}$ . (B) Histogram of reported degradation rates, with the average and median values inset.



## 6 DESIGN AND MODELING CONSIDERATIONS FOR SNOW AND ICE ACCUMULATIONS

Snow and ice accumulations impact the design and performance modeling of PV systems [85]. Previous reports provide some guidelines for optimizing PV system design and operation in cold climates [86,87]. An overview of design considerations is presented in Figure 30, with the following subsections describing these aspects in greater detail.

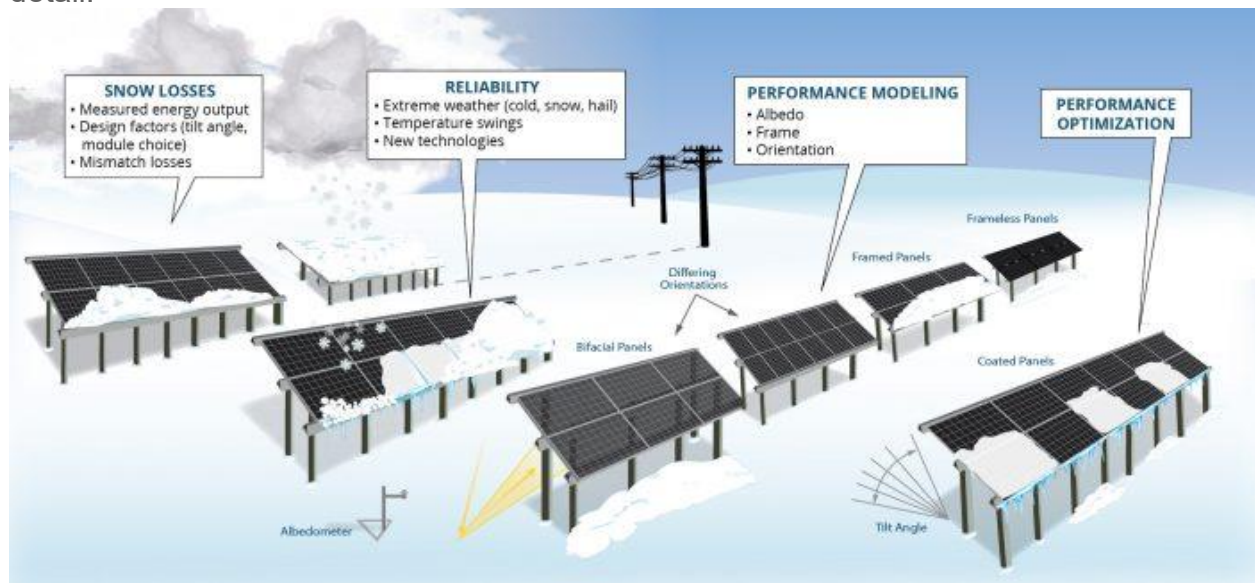


Figure 30: Snow impact on PV performance and design aspects to keep in mind. [Figure courtesy of L. Burnham, Sandia National Laboratories].

### 6.1 Snow Accumulations

Snow behaves differently based on its temperature, moisture saturation and particle size [88–90], which affects how it adheres to PV modules. Moist snow tends to form cohesive snowpacks whereas colder dry snow forms looser snowpacks or remains as individual particles [90]. These particles can be transported by wind and settle into snow drifts in aerodynamic wakes of obstacles such as PV arrays [87]. This can increase snow loads on the modules and extend snow coverage later in the Spring.

Just as wind can transport snow and build snow drifts, high velocity winds can also erode snowpacks and transport these features across the landscape [91], potentially reducing snow accumulation and coverage locally (scouring). Wind erosion is however a minor factor in natural snow cover reduction.

Snow shedding occurs when the gravitational force surpasses resistive forces from friction, adhesion and obstructions [89]. This could either be due to an increased mass of snow, a reduction in friction and adhesion, often caused by melted snow forming liquid water at the interface between the snowpack and PV module, or from removing obstacles directly beneath the modules, such as snow piles. Snow shedding is a quick



process but requires the modules to be tilted, where higher tilts perform better [92], and there must also be sufficient space beneath the PV modules for the snow to shed. When snow build directly beneath the modules reaches the lower edge of the module, snow shedding is hindered. In such cases natural snow cover reduction will be limited to phase change, either melting or sublimation. Phase change requires a lot of energy and can take a long time in cold climates, potentially leaving PV installations snow covered for many months.

## 6.2 Shading Losses

Snow on a module will severely limit how much light reaches the PV cells and their energy output. Such shading losses can prevent energy output throughout the snow-covered period. Since most PV modules have their cells interconnected in series, even partial snow coverage of the modules can cause significant losses. Modules typically separate series connected strings of PV cells with bypass diodes to limit the effect of partial shading and prevent damage, most commonly dividing each module into 3 or 6 substrings each protected with a bypass diode [93]. If the module's partial snow coverage affects all these substrings simultaneously, it could be equivalent to having the whole module covered. In a similar way, PV modules connected to string inverters are also connected in series. If there is non-uniform coverage of the PV array's module string this might lead to a string voltage below what is required for the inverter to operate and thus a suboptimal performance [93].

Because of their potential magnitude, snow losses should be included in PV system models used in energy yield assessments, forecasting etc. Because of the variation in snow losses between locations, from year to year, and between different system configurations, historical snow loss data may not always be sufficient to estimate expected losses. To accurately capture these variations, a dedicated snow loss model is essential. Several models have been developed to estimate snow losses [94].

The two most used snow loss models are those suggested by [95] and [96]. The model developed by Townsend et al. estimates monthly snow losses and is based on empirical correlations between energy loss and factors such as tilt angle, array size and height, ambient temperature, irradiance, humidity, and snowfall. The model developed by Marion et al. is a threshold-type model that estimates hourly snow loss. Snow accumulation, snow shedding, and the relation between snow cover and losses are modeled in dedicated steps. Due to the many factors impacting snow losses, and the fact that some of these factors will vary between different sites, snow loss modeling should be tested at many sites to demonstrate general applicability. The Townsend model was developed based on data from one system, while the Marion model was developed based on six systems. A study by Baldus-Jeursen et al. found that the Townsend model best predicted annual losses for a PV system in Quebec, Canada (45°N)[97]. For a specific site, improved results can be obtained by training the model on site data, either by using site-specific coefficients in the Marion and Townsend model [98] or by using a machine learning model [99]. Improved snow loss predictions have been achieved with the Marion model when snow depth [100] and/or the difference between framed and frameless modules [101] are taken into account in the modeling.



### 6.3 Accumulation of Soiling

Snow can form on dust particles in the atmosphere and also can trap particles as it falls. If the snow does not shed from the module and instead melts and sublimates in place, a winter's worth of soiling can be deposited onto the module surface, potentially causing extended soiling losses until cleaned. This has been observed but its impact has not been thoroughly studied in literature. An example can be seen in Figure 31 below.

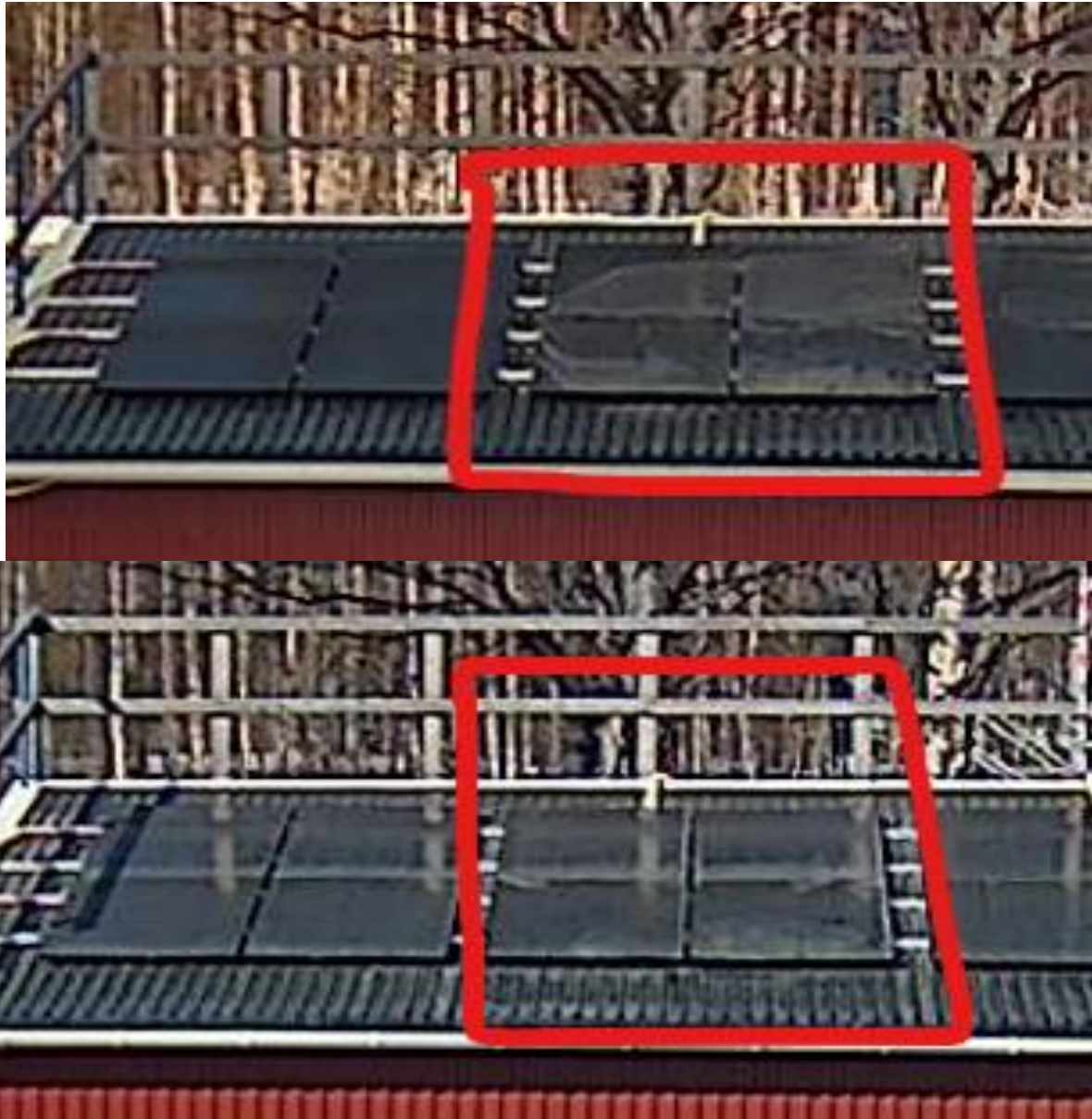


Figure 31: The module group marked in red has been unable to shed snow, likely due to an obstructive frame profile, resulting in melting snow leaving a deposit of soiling particles. The module group to the left has been able to shed snow. Piteå 65.3°N, Sweden, (upper) 2022-03-14 and (lower) 2022-04-18.



## 6.4 Reliability

Heavy snow loads can exert significant mechanical stress on PV modules, potentially causing deflection in the laminated structure. Under severe conditions, this deflection can result in cracked glass, damaged PV cells, or even snapped module frames [102]. Snow loads can also increase the risk of moisture ingress, which further degrades module performance over time [103].

There are two standards for snow load: IEC 61215-2 [104] and IEC 62938 [105]. IEC 61215-2 specifies a uniform mechanical test load of at least 2400 Pa for certification, assessing performance under horizontal loads, and recommends an increased load capacity of 5400 Pa for areas with heavy snow. However, real-world installations often involve inclined modules, leading to uneven snow distribution, with greater accumulation at the lower edge (see Figure 32) [106]. To address this, the IEC 62938 standard was introduced in 2020 to test modules under non-uniform snow loads, better simulating real-world conditions. The uneven accumulation of snow increases stress on the lower module frame [106–108], and repeated melting and freezing cycles can result in moisture ingress. Trapped moisture can freeze and expand, increasing the risk of frame separation. To reduce the likelihood of snow build-up at the edge of the modules, it is generally recommended to use frameless modules [109], however these are not very common and present additional challenges during installation.

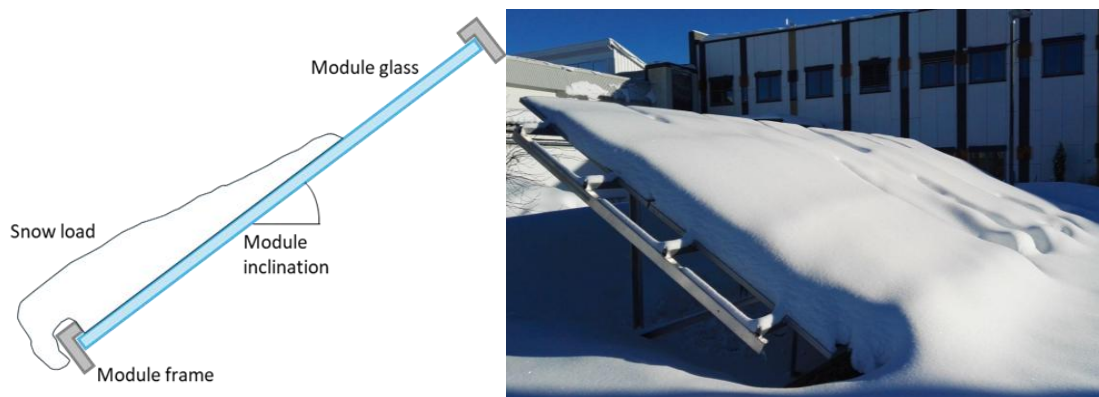


**Figure 32: (Left) Representation of uneven snow distribution in a framed module and (right) a practical example at Kjeller 60°N, Norway. The representation is inspired by Figure 6.1.5 of reference [5].**

In a study conducted in the southern and northern regions of Sweden over three winters [110], it was verified that rooftop PV mounted systems can either enhance or reduce the snow loads on roofs. When PV arrays are mounted parallel to the roof surface, reduced snow loads were observed due to the lower friction between the snowpack and the smooth glass surface compared to a roof without PV arrays. On the other hand, when PV modules are installed at an angle relative to the roof, an increased accumulation of snow under the modules was observed. As the angle increases, snow tends to build up beneath the modules, creating larger local loads that can exceed the roof's design load limits and potentially lead to damage to the cabling and mounting system. The same study also observed a similar effect, as shown in Figure 32, with



inhomogeneous loads on individual modules, where the lower part of the module experiences the highest load. These issues are compounded when snow sliding off the modules accumulates below them, obstructing further snow shedding and exacerbating the problem.

In standard snow load testing, PV modules are typically tested at 25°C. However, in very cold environments, such as those typical of the Arctic region, the risks are amplified, especially when temperatures drop below -20°C. Studies have shown that under such conditions, PV modules can fail at much lower loads than their ratings suggest [111–115]. A study by P. Romer et al. [111] highlighted that at these low temperatures, differences in material thermal expansion and wind loads exacerbate the effects. The study found that colder temperatures reduce the stress-buffering capability of the encapsulant, increase module stiffness, and create compressive stress due to thermal contraction. For the widely used encapsulant ethylene-vinyl acetate (EVA), it was reported [116] to undergo a glass transition beginning at approximately -15°C. This transition raises concerns about reliability in climates where temperatures remain below -15°C for extended periods, as the modules become more vulnerable to damage from mechanical loads, such as snow or wind. The study suggested additional testing beyond the scope of IEC 61215 to address these challenges. In contrast, other encapsulants (e.g., POE and PDMS) have glass transition temperatures starting at -40°C and lower [117].

## 6.5 Mitigation and Adaptation

Active and passive solutions for mitigating snow deposition and ice accretion have been proposed and investigated by many scholars.

Passive solutions in the context of PV modules mostly focus on surface engineering, including ice-phobic coatings that retard ice formation [118], hydrophobic and superhydrophobic treatments [119], micro- and nano-textured surfaces [120,121]. For these coatings to be effective, they must not only resist snow and ice accumulation but also maintain high transparency, offer self-cleaning capabilities, reduce reflection, and possess strong mechanical durability. Indeed, while ice-phobic coatings can effectively reduce winter snow losses [122], they have been found to decrease the effective plane-of-array irradiance during the summer, facilitating soiling/pollen deposition. In some regions one may only add 1–3% to the annual production [123], while more snow rich regions, be it due to altitude or latitude, may yield >15% more energy produced per year [124].

Such challenges prevent the broad applicability of passive solutions in the PV industry. In addition to surface engineering, PV systems can be designed to passively mitigate snow accumulation. As mentioned above, wind erosion, though a secondary factor, can reduce snow coverage by dispersing snow particles. More notably, gravitational forces promote snow shedding when PV modules are installed at steeper tilt angles, allowing accumulated snow to slide off the surface. However, increasing the module tilt to enhance snow shedding can negatively influence the overall solar energy potential, as steeper angles may reduce irradiance under certain conditions. Installing wind



shields, such as snow fences, can effectively control snow drift patterns and minimize snow deposition on PV modules, but their proximity to the modules poses a risk of casting shadows, which worsen the energy yield. These passive strategies, while beneficial for snow management, must be optimized to balance snow removal and energy production for maximum system efficiency [125].

Active mitigation strategies primarily involve mechanical systems and surface heating [126,127]. One approach uses transparent resistive wires [128] or applied reverse current to melt the snow layer on the PV module [129], allowing it to slide off due to gravity [130]. Alternatively, mechanical snow removal is another option [131], though it tends to be more expensive and requires machinery capable of operating under particularly adverse conditions such as extremely cold environments. Moreover, mechanical systems risk damaging modules and are not effective dealing with icing situations. Chemical treatments have been proposed as active solutions for accelerating snow melting but they can be harmful to the environment and increase the degradation rate of PV modules [132,133].



**Table 4: Advantages and disadvantages of active and passive solutions for snow mitigation. Modified from [126]**

Solution Types	Technology/Method	Pros	Cons	Stage of implementation
Passive solutions	Surface engineering	<ol style="list-style-type: none"> <li>1. Less expensive;</li> <li>2. Energy efficient;</li> <li>3. Environment friendly;</li> </ol>	<ol style="list-style-type: none"> <li>1. Effective formulations may not be transparent;</li> <li>2. Must be integrated into module production lines or applied during installation;</li> <li>3. Lack of testing methods to validate effectiveness and durability.</li> </ol>	Production stage
	System layout		<ol style="list-style-type: none"> <li>1. Optimal configurations for snow may conflict with optimizing energy output.</li> </ol>	Design stage
Active solutions	Chemical treatment	<ol style="list-style-type: none"> <li>1. Less expensive;</li> <li>2. Higher TRL</li> </ol>	<ol style="list-style-type: none"> <li>1. Environmental risks;</li> <li>2. Manual application methods;</li> <li>3. Difficult to apply in all environments;</li> </ol>	Operational stage
	Mechanical systems	<ol style="list-style-type: none"> <li>1. Proven to work;</li> </ol>	<ol style="list-style-type: none"> <li>1. Expensive;</li> <li>2. Could damage the module coating;</li> <li>3. Ineffective on ice;</li> <li>4. Requires external power;</li> </ol>	Operational stage
	Surface heating	<ol style="list-style-type: none"> <li>1. High snow removal efficiency;</li> <li>2. Able to resolve the coverage of mixed snow and ice;</li> <li>3. Acceptable running cost;</li> </ol>	<ol style="list-style-type: none"> <li>1. Expensive (installing thin-film heaters or laminating resistive wires);</li> <li>2. Laminating resistive wires may reduce module efficiency;</li> <li>3. Requires external power;</li> <li>4. Uncertain control strategies;</li> </ol>	Operational stage



## 7 INTEGRATION

---

As an intermittent and weather-dependent electricity source, PV requires either supporting power generation from other sources or energy storage to satisfy the balance between production and consumption and minimize challenges from a high share of PV generation [134,135]. Furthermore, in Arctic regions, power system characteristics can vary widely. For example, in Nordic countries, the national power grids extend into many parts of the far north, whereas in North America, high-latitude regions are sparsely populated, and isolated communities commonly have their own isolated microgrids, leading to different challenges.

Large utility-scale PV power plants are currently becoming economically feasible even in high-latitude locations. The addition of significant PV generation to the power system can also significantly impact market-based electricity pricing [136,137]. The cannibalization effect (also known as the duck curve), i.e., the reduction of electricity prices during PV peak production hours due to extensive PV over-production, can undermine the profitability of the planned systems. Another aspect to consider with utility-scale installations is their location: large PV parks use a large land area. A loss of valuable nature or recreation land for PV installations can raise public resistance. Dual use of land, such as integrating PV with agricultural land (agrivoltaics) [138], covering parking lots with PV carports [139], or building PV on wasteland may be more acceptable.

Residential and rooftop PV installations take advantage of collocating PV and residential loads. When PV is consumed on site (self-consumption), the producer avoids any transfer cost and electricity taxes, which can increase profitability in some markets [140,141]. Moreover, self-consumption reduces the need for grid interaction, which helps local low-voltage grids to host more PV [142] and minimizes the need for battery storage for isolated locations. In some markets, such as larger utilities in Alaska, monthly net metering can remove the incentive for self-consumption. Financial incentive structures and market policy greatly affect the design and operational strategy of PV systems.

A variety of different strategies to increase PV generation and support its integration into Arctic power systems are listed in Table 5.

**Table 5: Strategies to integrate PV, their strengths and weaknesses.**

Strategy	Definition	Considerations	Arctic experience
Hybrid (PV + wind) power plant	Adding PV and wind production (with possibly electricity storage) to one entity	<ul style="list-style-type: none"> <li>+ Negative correlation between wind and PV generation in some locations [143,144]</li> <li>+ Potential to use grid upgrades already done for wind power [145]</li> <li>+ Green hydrogen applications [146]</li> <li>- Land use impacts if PV is added to existing wind power parks</li> <li>- Requires location with high solar and wind resource</li> </ul>	<p>Seasonal variation of PV and wind resource</p> <p>Combining variable renewable energy (VRE) production with hydro power</p>
PV generation shifting [56]	Using unconventional installations to shift the production peak from noon toward morning and/or evening	<ul style="list-style-type: none"> <li>+ Increases self-consumption in residential installations [140,147]</li> <li>+ Increases production during peak price hours, reduces cannibalization [140]</li> <li>- Decreases total annual production per module with conventional installations</li> <li>- Increased land-use costs</li> </ul>	<p>Long daylight time during summer -&gt; higher temporal shifting possible</p> <p>Solar elevation during peak production lower -&gt; vulnerable to shading</p>
Energy communities	A community that can share produced VRE energy between individuals	<ul style="list-style-type: none"> <li>+ Sharing electricity between small producers increases the self-consumption [148–150]</li> <li>+ Economically feasible for residents</li> <li>- Legislative barriers</li> <li>- How to account for the electricity transfer within a community?</li> </ul>	<p>Isolated communities in North America</p> <p>Balanced VRE generation when multiple sources and locations are used</p>
Load shifting [151,152]	Shifting electricity consumption to hours of high VRE generation	<ul style="list-style-type: none"> <li>+ Increases self-consumption in residential installations</li> <li>- May decrease comfort for residents</li> </ul>	<p>High heat demand, peaking in winter</p> <p>Electric vehicle (EV) loads are higher in winter [152]</p>



Virtual power plants	Adding multiple power plants, potentially in different locations, to one seller entity	+ Combining different distributed energy resources, smoother and more predictable power output from combined distributed generation, shaping loads in response to generation possible - Electricity transfer from production site to final user, practically requires connection to main grid.	Suitable for the Nordic countries to balance aggregated PV + wind + hydro power output
Balancing power generation	A dispatchable reserve to counter the varying PV generation	+ Dispatchable production counters the variation in VRE production + Technologies widely available - GHG emissions (if hydro not available) - Fuel cost	Hydro power in the Nordic countries Fossil fuels in North America uses Transmission capacity within each region varies
Energy storage	Storing energy for later use	+ Counters the temporal mismatch between production and load - Costs, batteries are expensive - Requires rare earth metals, limited resources globally	Storing energy as heat improves self-consumption [140] High annual variation in PV and load -> need for seasonal storage

Different policies to support PV installations are applied widely. The net-metering aggregation period has a significant effect on profitability. Shorter net metering periods decrease the value of self-consumption, whereas a daily and monthly net metering period makes PV more profitable for a consumer by moving the challenges related to diurnal cycling of PV generation from consumer to power system operator.

Another approach to increase the self-consumption of PV is to enable energy sharing within an energy community. If the PV electricity produced within a community can be used by any member without transferring it through the power grid, the value per produced kWh increases. Advanced metering can be used to account for production and consumption.

Financial support for PV installations, including both direct support and tax credits, encourage actors to invest in PV. Different policies that have been implemented are listed in Table 6. In general, policies that provide upfront investment tax credits tend to incentivize the building of PV plants yet may not directly favor investment in component quality and long-term performance and operations and maintenance. Policies that



provide feed-in tariffs for produced energy tend to support more attention to long-term reliability and optimizing performance. EU’s Renewable Energy Financing Mechanism (RENEWFM) [153] and tax credit of household expenses in Finland [154], as well as the investment tax credit (ITC) in U.S. (ending in 2025) are examples of financial support for PV installations on both ends of this spectrum.

Finally, providing support for disposing and recycling the used PV modules relieve the risk of additional decommissioning costs for the system owner. For example, in Finland, the waste stations accept used PV modules without additional costs.

**Table 6: Different policies to encourage PV investments, their pros and cons.**

Policy	Definition	Considerations	Arctic experience
Aggregated net metering	Period during which the net metering of electricity consumption is done is extended, allowing prosumers to use grid as electricity storage	<ul style="list-style-type: none"> <li>+ Makes PV more profitable for a prosumer</li> <li>- Challenge of supply / demand balance outsourced to other power system players</li> <li>- Costs for the power system - who should pay?</li> </ul>	Seasonal variation in PV generation Finland: net metering on hourly basis, can change to 15 min periods Alaska: larger utilities have monthly net metering, smaller utilities do not.
Investment support	Financial support for PV investments, including direct financial support and tax credits	<ul style="list-style-type: none"> <li>+ Reduces the economic risk for the PV system owners</li> <li>+ Makes PV more bankable</li> <li>+ Incentivizes building PV plants</li> <li>- May create incentives to install unrealistically large PV systems</li> <li>- High quality and O&amp;M are not incentivized</li> </ul>	EU’s RENEWFM for 10-80 MWp ground-mounted PV in Finland [153] Investment tax credit (ITC) in U.S. Tax credit for household expenses (Finland) [154]
Production support	Financial support based on PV generation, including direct support (feed-in tariff, subsidy upon market price, market premium) and tax credits	<ul style="list-style-type: none"> <li>+ Reduces the economic risk for the PV system owners</li> <li>+ Incentivizes high quality and O&amp;M to maximize availability.</li> <li>-Only valuable for long-term ownership models.</li> </ul>	Production tax credit (PTC) in U.S. Finland had renewable energy premium auction in 2018 - all approved bids were wind power [155]



		- Opportunity costs are higher since rewards come over the project lifetime.	
Disposing used modules	A guarantee that disposing of used PV modules does not cause additional costs to system owner	<ul style="list-style-type: none"> <li>+ Reduces the economic risk for the PV system owners</li> <li>+ Makes PV more bankable and the revenue more predictable</li> <li>+ Creates incentive for the public sector to advance PV recycling</li> <li>- Uncertain costs for the state</li> <li>- Removes the incentive to advance PV recycling for the system owners</li> </ul>	Finland: solar modules classified as electronic waste, municipal waste stations accept residential solar modules without cost



## 8 ARCTIC COUNTRY SUMMARIES AND PROJECTIONS

---

The integration of PV systems into high-latitude power grids presents distinct challenges depending on the geographic and political context. In the mainland Nordic high-latitude countries (Norway, Finland, and Sweden), the comparatively high population density and well-established national power grids facilitate the integration of distributed PV systems. Conversely, high-latitude regions in the USA (Alaska), Canada, Greenland, and Russia are characterized by vast area and sparse populations, resulting in a prevalence of fossil-fuel based isolated microgrids. Hydropower and fossil fuels dominate as electricity sources in the Arctic region, with hydropower servicing larger and grid-connected communities across the Arctic. In the Nordic countries, wind and nuclear power also contribute significantly to the electricity mix due to historic incentives, grid-connectivity, and high population densities. Across high-latitude regions, solar PV accounts for less than 1% of the electricity mix. However, regional PV capacity reports are often reported with a several year lag, and the installed capacity has been showing high growth in recent years across the region.

Table 7 outlines the population density and electricity consumption  $>60^{\circ}\text{N}$  in Arctic countries/territories of Alaska, Canada, Greenland, the Faroe Islands, Iceland, Norway, Sweden, Finland, and Russia. Country statistics are presented only for regions around and above  $60^{\circ}\text{N}$ . The precise definition of each of these regions is described for each country in Section 8.2. In Alaska, Canada, Greenland, and Russia, the population density is  $<0.6$  people/ $\text{km}^2$  above  $60^{\circ}\text{N}$ . The Nordic countries report the highest electricity consumption of Arctic regions, with consumption per capita from 24-52 MWh/year. This is likely related to the comparatively low cost of electricity in these areas that has shaped infrastructure and population habits, such as a large share of electrical domestic heating and a developed industry, typically powered by hydropower that has been available for many decades.



**Table 7: Population and electricity demand statistics for regions above 60°N in each country.**

Region North of 60°	Population	Land area (km <sup>2</sup> )	Population density (km <sup>-2</sup> )	Electricity demand per capita (MWh/year)
Alaska (entire state) [156–158]	740 133	1 723 227	0.43	8.2
Canada [159]	118 000	3 716 000	0.03	12.2
Greenland [160]	56 699	2 166 086	0.03	6.6
Faroe Islands [161,162]	54 149	1 399	38.7	8.5
Iceland [163]	383 726	103 000	3.7	52.4
Norway [164–166]	2 271 811	316 509	7.2	31.3
Sweden [133, 134]	1 474 824	268 500	5.5	23.6
Finland [167]	5,603,851	338 485	16.6	14.3
Russia* [168]	2 500 000	4 800 000	0.56	

\*Values are reported only for the Arctic region of Russia as defined by the Arctic Council, as >60°N regional data is difficult to obtain. Note that the website referenced is not accessible in all countries, including the United States.

## 8.1 Electricity Sources in High-Latitude Regions

An overview of the sources of electricity generation in high-latitude countries is presented in Figure 33. Generation is highest in the Nordic countries, related to population density in Table 7. Hydropower is a major contributor across high-latitude regions, especially in Iceland, Norway and Sweden. Together with Finland, Sweden and Norway are the three largest electricity producers and have a common electricity market. This is due to the prevalence of energy intensive industries in these countries. Fossil-fuel



based electricity forms most of North American electricity generation, particularly in off-grid communities, while fossil-fuels play a minor role in grid-tied Nordic countries. Wind power is the dominating intermittent renewable energy source, especially prevalent in Sweden, Finland, and the Faroe Islands. Some nuclear power is also present in the high-latitude countries but is only reported above 60°N in Finland. All Swedish nuclear reactors are located outside the selected high-latitude region in this study. Iceland appears to be an exception as the power demand per capita is substantially higher than the other selected regions, and electricity generation is almost completely based on abundant hydropower and geothermal energy. Variable renewable power has just recently begun to be employed in Iceland, still with very low capacity.

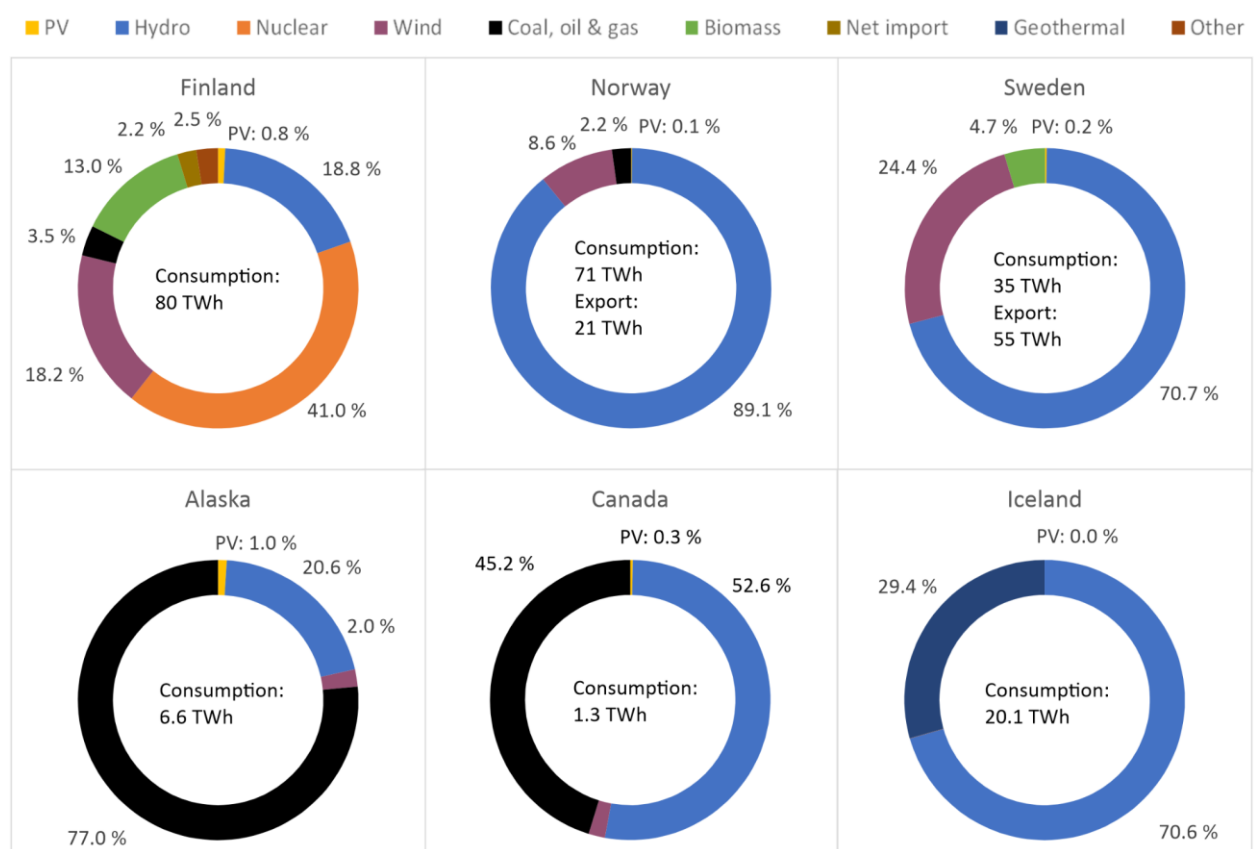


Figure 33: The annual electricity consumption and sources for Finland [169], Norway [165], Sweden [170], Alaska [171], Canada [172], and Iceland [173], including only the regions in these countries above 60°N. Export is explicitly stated for net exporters, net import is expressed as an electricity source.

## 8.2 Regional Summaries

### 8.2.1 Alaska, United States

Alaska is the largest state in the United States with a population of 736,081 according to the 2020 census, making it the 3rd least populated state in the United States and the least densely populated state. Because of its separation from the 48 Contiguous



States, the electric grid in Alaska is not connected to the continental grids of the United States or Canada. The primary electric grid in Alaska is referred to as the Railbelt and runs almost 1000 km from the community of Homer (59 °N) in the south to Fairbanks (65 °N) on the northern end. In the middle lies Anchorage, Alaska's most populous city with about 300,000 people. The Railbelt Grid serves more than 75% of Alaska's population [174] and the peak winter loads generally reach about 750 MW with total annual generation reaching 4649 GWh, based on 2020 data [175]. Nearly 73 percent of the Railbelt's electricity comes from natural gas [176] with hydro making up 18% of generation. The remaining generation is based on coal and naphtha, along with small amounts of wind and solar [175]. The largest solar facility currently in operation is 8.5 MWp and went into commercial operation in September 2023. Recently plans were announced for a 45 MWp array, which will be built in the southern portion of the Railbelt grid and is expected to be operational in 2027 [177].

Outside of the Railbelt region of Alaska there are more than 150 islanded, stand-alone electrical grids serving rural villages, which are generally not accessible by road [176]. These grids generally rely on diesel generators to provide electricity. In recent years, wind and solar have been integrated into many of these community grids and some advanced systems can meet 100% of the community load with renewables during periods when the solar and wind resources are sufficient. Due to significant government investment, the number of islanded communities with "diesel off"-capabilities is expected to increase significantly in the coming years. Currently, funding is committed to build community scale solar plus storage along with integration technology in dozens of remote communities.

At the end of 2023 total PV capacity was about 30 MWp in Alaska, with 16 MWp coming from rooftop net metered systems and the remaining from community and utility scale installations, which are generally ground mounted [178].

Alaska does not have official goals for future installed solar capacity, but independent power producers have indicated that they have hundreds of MWp in their installation pipeline for the rail belt [179].

## 8.2.2 Canada

Canada is the second largest country in the world, with >27% of its land mass lies north of the tree line [180]. Canada's internal borders subdivide the country into 10 southern provinces and 3 Arctic territories with their southern borders at 60°N. For the purposes of this study, we summarize statistics from the Arctic territories of the Yukon, Northwest Territories, and Nunavut, though some land mass >60°N also exists in Quebec and Newfoundland. The territories are referred to together as 'Canada's North'.

Nearly 50% of Canada's land mass is above 60°N; however, only 0.5% of the country's population lives year-round in this region [181]. The region is nonetheless rich in history, culture, natural resources, and wildlife. Canada's North is home to over 150 communities, the majority of which are connected to remote, islanded microgrids. A few short transmission lines exist close to large communities in each territory. In the Yukon and Northwest Territories, electricity is provided primarily by hydroelectric dams



alongside oil and gas. Nunavut, on the other hand, has historically relied on fossil fuel resources for electricity. Multiple diesel generators, including backup generators, are used to provide year-round power to microgrid communities. As of 2021, 53% of the electricity mix in Canada's North came from hydro resources, 45% from coal, oil, and gas, and the remaining from a mix of wind and solar.

Given the lowering cost of PV modules, aging grid infrastructure, high local electricity costs, and desire to reduce emissions, there have been a growing number of solar energy deployments in Canada's North in recent years. In a 2025 report by the Canadian Renewable Energy Association, the total capacity of solar installations in Canada's northern territories was reported to be >35 MWp [182], significantly exceeding the region's 2030 projected solar capacity of 9.1 MWp, predicted in 2016 by the Canada Energy Regulator [140].

Though solar capacity is growing, it is not without its challenges. Integration of solar energy into existing grid infrastructure is an on-going challenge for maintaining reliable and secure energy in a region where power shortages can have severe consequences. Utility operators are hesitant to accept new risks that are introduced by new solar technologies, and concerns over significant seasonal fluctuations have been raised [183]. Nonetheless, efforts to decarbonize northern Canada are underway, but must also address community and utility energy priorities.

### 8.2.3 Greenland

Greenland is the world's largest island, stretching from 59.8°N to 83.6°N, thus the entire region is considered high-latitude. With an area of 2.2 million square kilometers and a population of 57,000, the island is the least densely populated territory in the world. The population lives in 17 towns and 54 settlements located along the coast, with more than 60% of the population living in the five largest towns.

Due to the large geographical distances, inter-connecting electrical grids is infeasible, hence towns and settlements are connected to small independent microgrids. Electricity is mainly generated from hydropower and diesel-based units which are operated by the national utility, Nukissiorfiit. In 2022, the existing five hydropower plants supplied 82.7% of the electricity generation. In some of the towns with hydropower, electricity is also used to cover part of the heating load.

Solar energy also exists in Greenland. Although it is still a small source of generation, it is a growing industry. As of October 2024, there were 162 registered PV systems in Greenland with a combined capacity of 2 MWp. Of these systems, 146 were privately owned and located in the towns, the majority of which are roof-top systems with a capacity between 4-12 kWp. The remaining 16 systems (620 kWp) were owned by Nukissiorfiit, including both roof-top and ground-mounted systems.

Greenland has a uniform pricing scheme for electricity, water, and heating, meaning all settlements pay the same electricity price regardless of the actual generation costs. This means that locations dependent on costly diesel-based generation have electricity prices below the actual generation costs. Since the re-introduction of country-wide



uniform electricity pricing in 2012 and a 40% reduction in the feed-in tariff (only for diesel-based locations), private investments in PV have declined. The current investment in PV is thus driven by the national utility, who by the end of 2024 plans to have an additional 180 kWp solar PV installed.

#### 8.2.4 Iceland

Iceland covers about 100,000 km<sup>2</sup> in the northern Atlantic and includes one major island and some surrounding smaller islands. It stretches from 63°N to 68°N. Most of the approximately 400,000 inhabitants live in the capital Reykjavík region. From a geological point of view, Iceland is young and formed through recent volcanic activity. This is reflected in the electricity production which is entirely based on renewables: hydropower, geothermal energy and some wind power comprise 99.98% [173]. The electric distribution grid is well developed, but some islands, such as Grimsey, are isolated. Solar PV is still rare and the official energy regulatory body Orkostofnun only lists a PV capacity of 36 kWp and a production of 6 MWh, which reflects the grid-connected commercial PV systems in Iceland [173]. Private residential and non-grid tied installations are not listed but in total the PV contributions to the electricity production in Iceland is very small. The largest installation as of October 2024 is likely a 26 kWp plant at a car dealer in Brimborg. However, many summer houses and huts have solar modules connected to a 12 V DC system. The Government Council of Iceland foresees that solar PV will become more economically viable in Iceland in three to five years from 2024, following changes in the electricity market and demand [184]. They suggest that the PV electricity production in the year 2040 could be 400 GWh, or 2% of the electricity production, distributed across different kinds of systems.

#### 8.2.5 Faroe Islands

The Faroe Islands are located in the North Atlantic at 62°N and consist of 18 major islands, 17 of which are inhabited. The majority of the electricity is supplied by the national utility SEV. Electricity generation is derived from three primary sources [185]: fossil fuel thermal generation units (50%), wind power (27%), and hydropower (22%). As of 2023, there were only a few solar PV systems in the country, with a combined annual electricity generation of 180 MWh.

The country has set a target of achieving 100% carbon neutral by 2030, and feasibility studies have shown that solar PV has the potential to play an important role in the future energy systems. While the capacity factor of solar PV is low (around 7%), the seasonal production profile with high production during summer is favorable as this coincides with periods of low hydropower and wind power availability. This allows solar PV to directly displace fossil fuel-based generation. Simulations of the future energy systems indicate that the optimal capacity of solar PV is 40-60 MW, whereas the currently installed capacity is less than 2 MW.

#### 8.2.6 Norway

Norway stretches from 58°N to 71°N, with 40% of the population located above 60°N. Of mainland Norway's 15 counties, 7 have the majority of their population located



above 60°N. This includes Finnmark, Troms, Nordland, Trøndelag, Møre og Romsdal, Vestland, and Innlandet. Unless otherwise stated, all reported numbers for Norway correspond to these seven counties and Svalbard. We assume that this will result in a slight underestimation in PV metrics, electricity consumption/production and population numbers, but a larger underestimation in area.

The Norwegian energy system is characterized by hydropower and high electricity consumption per capita. The high consumption is due to both high household consumption from electric heating and energy-intensive industry. The electricity production is especially high above 60N. In 2023, the counties above 60N covered approximately 60% of the country's electricity production, around 90% of this from hydropower. As shown in Figure 33, the region had an electricity production surplus of 21 TWh in 2023. Table 8 shows a total installed PV capacity in 2023 above 60N at 173 MWp. This is around 30% of the total installed capacity in Norway. The estimated PV electricity production shown in the table, including self-consumption, is at 99 GWh, or 0.1% of total electricity production in the region.

PV has mainly been installed on rooftops in Norway, including residential systems and large-scale systems on flat roofs. In 2023, 75% of the PV capacity above 60N was covered by systems smaller than 100 kWp. In 2024, the first ground mounted utility scale system was completed, with an installed capacity of 7 MWp. The system was built at 61N, and several other ground mounted systems are also planned at higher latitude. With a goal of 8 TWh of Solar PV generation by 2030, a significant increase in PV installations is expected above 60N in Norway.

### 8.2.7 Sweden

Sweden stretches from 55°N to 69°N with substantial land area in the Arctic. It is divided into 21 counties of which six (Norrbotten, Västerbotten, Jämtland, Västernorrland, Dalarna, Gävleborg) are located north of 60°. Unless otherwise stated, the herein reported numbers concerning Sweden correspond to the sum of these six counties, which is a reasonable approximation to the 60°N latitude (less than 1° deviation) with accessible statistics. Close to two thirds of the Swedish land area is north of 60°N, but only 14% of the population (1.5 million) lives there, primarily along the coast of the Baltic Sea.

Strikingly, 49% of the produced electricity in Sweden is produced in the Arctic, but half of it (35 TWh) is exported to Southern Sweden, Norway, and Finland. Nevertheless, the average annual electricity consumption in the Swedish Arctic is 24 MWh per person (2018–2022), which is a result of the existing power intensive industries in the region, such as pulp mills, saw mills, data centers, battery factories, mining related industries and metal refineries, which to some extent have been and are being established based on the abundance of low carbon (hydroelectric) electricity, and closeness to natural resources. Additionally, battery factories, steel plants and ammonia production facilities are being built or planned, related to production of green H<sub>2</sub>. This will likely increase the regional power demand several times over in the coming decade, highlighting the imminent need for added power production [186]. While all major watersheds already have been extensively exploited for hydropower generation (except a few protected



rivers), wind power generation is increasing. Solar PV generated 1% of the electricity in all of Sweden in 2022 but only 0.2% in the Arctic.

At the end of 2023, the PV capacity in Arctic Sweden (350 MWp) is still lagging behind the southern part of the Country (3.6 GWp), but the growth is exponential showing a five-year mean of 58% per year, on par with the rest of Sweden. Virtually all PV systems in Sweden are grid tied, with residential and commercial building applied configurations dominating. However, utility scale ground mounted PV parks are gaining shares [187], and during the year 2023 nine PV parks (approximately 46 MWp) were permitted in the Arctic counties, and 19 PV parks (approximately 1.4 GWp) were waiting for a permit [188]. The largest planned PV parks to date in Arctic Sweden has a capacity of 550 MWp and is to be located on forest land.

The vast area and low population density suggest that there is ample room for additional power generation facilities in the form of land-based wind and utility scale PV in the Arctic Sweden. However, for most of the land there are conflicting interests with indigenous people, public recreation, defense, nature reserves and similar, which is also reflected in the permitting.

There are no official goals for PV development in Sweden or its Arctic counties but given the strong transmission grid and the low correlation with wind power that has already been built, there should – from an electrical grid point-of-view – be plenty of space for a continued and accelerating growth of PV. The Swedish Solar Energy Association is aiming for a national PV capacity of 30 GWp in Sweden in the year 2030. Rescaled based on population, land area and electricity production, this goal should correspond to 4.2, 19.8, and 14.7 GWp in Arctic Sweden, respectively.

### 8.2.8 Finland

Finland is located between 60°N and 70°N (excluding a few islands and the continent cities of Hanko and Raasepori, which are located just below 60°N and have about 36,000 inhabitants altogether), and therefore the whole country is here considered as a high-latitude location. Finland has high electricity consumption per capita, 14 MWh (Table 7), due to high demand of electricity for heating purposes during winter and the energy-intensive industry. Finland has ambitious climate targets, aiming for a 60 % reduction in greenhouse gas emissions (compared to the year 1990 level) by 2030 and reaching carbon neutrality by 2035 [189,190].

Currently, the backbone of the Finnish electricity system consists of nuclear (41.0% of the year 2023 demand), hydro (18.8%) and wind (18.2%) power [169]. Solar PV still has a minor role, 0.8% of the total electricity consumption in 2023 [169]. However, the share of PV is rising rapidly: during 2023, the approximate total capacity of the Finnish PV systems increased from 606 to 1018 MWp [191]. The rise is expected to continue, especially due to the ongoing development of utility-scale PV systems (>1 MWp). In addition to the 250 MWp in operation and 300 MWp under construction in June 2025, Finland has over 26 GWp of utility-scale PV in permitting or pre-planning stage [192]. Assuming that all these projects will be completed is unrealistic, however a major increase in utility-scale PV is expected. According to Fingrid, the national transmission



system operator of Finland, the PV capacity in Finland can reach 9.1 GWp by 2030 [193].

A major increase in PV generation raises concerns about how increased production can be managed in the electricity system. Finland has two major advantages supporting the integration of PV. The dominating variable renewable energy source, wind power, has a negative correlation with PV generation. Since the most suitable areas for PV generation already host a significant amount of wind power, the grid upgrades already done to enable wind power production can be used to host PV generation as well. Moreover, since the annual maintenance of the Finnish nuclear reactors are scheduled for spring and summer, and the combined heat and power (CHP) power plants are only operated during the heating season, the Finnish energy system has room for additional generation during the summer.

### 8.2.9 The Russian Federation

Russia, being the largest country in the world with substantial land mass above the Arctic circle (4.8 million km<sup>2</sup>), is home to around half of the total Arctic population worldwide [194]. Russia is an energy-independent country, consisting of centralized electricity infrastructure (“the Unified Energy System of Russia”) and a large number of islanded energy systems servicing remote communities. These remote communities in Russia are mainly located in northern regions and rely primarily on diesel for electricity. For example, in the Russian Far East, the Russian government reported that 70% of all electricity generation comes from fossil fuels [195]. For the country as a whole, Russia’s electricity mix consists primarily of coal, oil and gas (62%), nuclear energy (19%), and hydropower (17%) [196]. Region-specific data is difficult to come by which specifically encompasses only the high-latitude (>60°N) regions of Russia.

The development of renewable energy technology had a slower start in Russia, with the first regulatory framework supporting renewable energy beginning in 2015. In this framework, the need to supply electricity to remote communities far from centralized power grids, such as for communities in the Extreme North, Far East, and Arctic regions, was identified. In 2013, the first subsidies for developing new PV plants connected to the centralized grid were created. As of 2021, nearly 1 GW of solar capacity has been deployed across the country, primarily in southern regions [197]. Some policy mechanisms have been announced to incentivize adding wind and solar resources into existing remote diesel microgrid infrastructure [195].

The Russian government has set a target to achieve 4.5% of its electricity production from renewable energy resources by 2030 [198]. However, questions remain as to whether this national target will apply to remote, high-latitude communities [195].

## 8.3 Photovoltaic Installation Status

The installed capacity of PV technologies in high-latitude regions is presented in Table 8. For the most part, PV capacity totals in each region are still in the early stages, with total installed capacity typically on the megawatt scale (except Finland, which has



reached one gigawatt), amounting to <1% of the total electricity generation mix above 60°N. The total installed PV capacity >60°N is estimated to be ~1400 MWp as of 2023, assuming that the total installed PV capacity in Russia is primarily concentrated in southern regions. Few high-latitude PV installations exceed >1 MWp to date, although smaller community-scale installations on the order of hundreds of kWp are increasingly emerging in remote microgrids communities in Alaska and Canada. The fraction of installed capacity in this segment is, however, approximately ten times larger in Alaska and Canada compared to the Nordic countries of Finland and Sweden, which shows how the electricity infrastructure in the regions affect the development and type of PV installations.

Despite the relatively young PV industry in the Arctic, a number of factors in recent years are leading to significant PV up-take in these regions, including rising fossil-fuel costs and supply volatility [199], dropping costs of PV modules [200], increasing electricity demands [201], and renewable-integration incentives [202]. In regions with historic PV capacity data availability, PV capacity above 60°N is growing (mean of 2019-2023) by 46-145%rel. per year. The capacity growth is also visualized in Figure 34 for regions >60°N. The growth rates reported in Table 8 are the average relative year-on-year growth rates from 2019-2023, given exponential PV growth trends in these regions.



**Table 8: Installed PV statistics for high-latitude countries (as of 2023).**

Region North of 60°	In-stalled capacity (MWp)	5-yr Average capacity increase (%/y)	PV generation in 2023 (GWh)	Share of utility (> 1 MWp) scale PV (%)	PV fraction of electricity generation (%)
Alaska	29.6	46	~5	45	<1%
Canada	9.3 [203]			80% [172]	0.3%
Greenland	2	NA	NA	0%	NA
Faroe islands	<1	NA	NA	0%	NA
Iceland [173]	0.036	NA	0.006	0%	0%
Norway [204,205]	173	145	99	NA	<1%
Sweden	350	58	273 [170,206]	7% [207]	0.3%
Finland	1020 [191]	54 [191]	800 [191]	4.9% [191]	0.8 [169]
Russia*	1000 [197]		2600 [196]	?	0.2% [196]

\* Only showing data available from public sources, values are for the whole country and not region-divided for above 60°N.

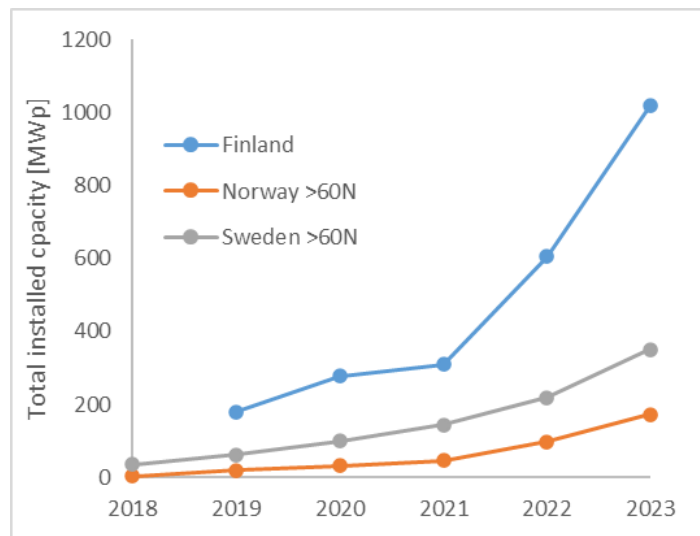


**Figure 34: Historic installed capacity [208] in regions above 60°N for Finland [209], Sweden [207], Norway [204].**



## 9 CONCLUSIONS

---

In conclusion, the greater Arctic region stands at a pivotal crossroads in its energy transition, where the integration of solar photovoltaics (PV) offers a promising pathway toward enhanced energy security and sustainability. The unique environmental and social characteristics of the Arctic, including its unique solar resource, distinct climate, supply chains and grid infrastructure present both opportunities and challenges for the adoption of solar energy technologies.

While the region's long summer days provide ample solar radiation for energy harvesting, the harsh winter conditions and logistical hurdles pose significant obstacles to the widespread implementation of PV systems. Nevertheless, the potential for higher efficiency and longevity of solar modules in colder climates, coupled with the decreasing costs of solar installations, positions solar PV as a viable alternative to traditional fossil fuel sources.

As Arctic communities increasingly seek to reduce their reliance on imported fossil fuels, the need for accurate solar irradiance data and innovative energy storage solutions becomes paramount. These challenges can be met through research and development, stakeholder engagement, and knowledge sharing.

Ultimately, this report underscores the importance of collaboration among researchers, investors, and local communities to harness the benefits of solar PV technology in the greater Arctic regions. By embracing innovative applications and practices, Arctic communities can enhance their energy independence and security. The journey toward a renewable energy future in the Arctic is fraught with challenges, yet it is also rich with opportunities.



## REFERENCES

- [1] Kummu, M., and Varis, O., 2011, “The World by Latitudes: A Global Analysis of Human Population, Development Level and Environment across the North–South Axis over the Past Half Century,” *Appl. Geogr.*, **31**(2), pp. 495–507. <https://doi.org/10.1016/j.apgeog.2010.10.009>.
- [2] Sengupta, M., Xie, Y., Lopez, A., Habte, A., Maclaurin, G., and Shelby, J., 2018, “The National Solar Radiation Data Base (NSRDB),” *Renew. Sustain. Energy Rev.*, **89**, pp. 51–60. <https://doi.org/10.1016/j.rser.2018.03.003>.
- [3] NEO, 2025, “NASA Earth Observations (NEO),” NASA Earth Obs. NEO. [Online]. Available: <https://neo.gsfc.nasa.gov/>. [Accessed: 02-Sept-2025].
- [4] Anderson, K. S., Hansen, C. W., Holmgren, W. F., Jensen, A. R., Mikofski, M. A., and Driesse, A., 2023, “Pvlib Python: 2023 Project Update,” *J. Open Source Softw.*, **8**(92), p. 5994. <https://doi.org/10.21105/joss.05994>.
- [5] Jensen, A. R., Anderson, K. S., Holmgren, W. F., Mikofski, M. A., Hansen, C. W., Boeman, L. J., and Loonen, R., 2023, “Pvlib Iotools—Open-Source Python Functions for Seamless Access to Solar Irradiance Data,” *Sol. Energy*, **266**, p. 112092. <https://doi.org/10.1016/j.solener.2023.112092>.
- [6] Marion, B., 2020, “Albedo Data Sets for Bifacial PV Systems,” *2020 47th IEEE Photovoltaic Specialists Conference (PVSC)*, pp. 0485–0489. <https://doi.org/10.1109/PVSC45281.2020.9300470>.
- [7] Pike, C., Riley, D., Toal, H., and Burnham, L., 2024, “Presenting a Model to Predict Changing Snow Albedo for Improving Photovoltaic Performance Simulation,” *Solar*, **4**(3), pp. 422–439. <https://doi.org/10.3390/solar4030019>.
- [8] Dumitrascu, L., and Beausoleil-Morrison, I., 2020, “A Model for Predicting the Solar Reflectivity of the Ground That Considers the Effects of Accumulating and Melting Snow,” *J. Build. Perform. Simul.*, **13**(3), pp. 334–346. <https://doi.org/10.1080/19401493.2020.1728383>.
- [9] Muñoz Sabater, J., “ERA5-Land Hourly Data from 1950 to Present,” Copernic. Clim. Change Serv. C3S Clim. Data Store CDS. [Online]. Available: <https://cds.climate.copernicus.eu/datasets/reanalysis-era5-land?tab=overview>. [Accessed: 18-Sept-2024].
- [10] National Snow and Ice Data Center, “Frozen Ground & Permafrost.” [Online]. Available: <https://nsidc.org/learn/parts-cryosphere/frozen-ground-permafrost>. [Accessed: 02-Sept-2025].
- [11] Heginbottom, J., Brown, J., Ferrians, O., and Melnikov, E. S., 2002, “Circum-Arctic Map of Permafrost and Ground-Ice Conditions, Version 2.” <https://doi.org/10.7265/SKBG-KF16>.
- [12] Babar, B., Luppino, L. T., Boström, T., and Anfinson, S. N., 2020, “Random Forest Regression for Improved Mapping of Solar Irradiance at High Latitudes,” *Sol. Energy*, **198**, pp. 81–92. <https://doi.org/10.1016/j.solener.2020.01.034>.
- [13] Gueymard, C. A., Lara-Fanego, V., Sengupta, M., and Xie, Y., 2019, “Surface Albedo and Reflectance: Review of Definitions, Angular and Spectral Effects, and Intercomparison of Major Data Sources in Support of Advanced Solar Irradiance Modeling over the Americas,” *Sol. Energy*, **182**, pp. 194–212. <https://doi.org/10.1016/j.solener.2019.02.040>.
- [14] Stoffel, T., Renné, D., Myers, D., Wilcox, S., Sengupta, M., George, R., and Turchi, C., 2010, *Concentrating Solar Power: Best Practices Handbook for the Collection and Use of Solar Resource Data*, NREL/TP-550-47465, National Renewable Energy Laboratory, Golden, CO. [Online]. Available: <https://docs.nrel.gov/docs/fy10osti/47465.pdf>.
- [15] Karlsson, K.-G., Anttila, K., Trentmann, J., Stengel, M., Fokke Meirink, J., Devasthale, A., Hanschmann, T., Kothe, S., Jääskeläinen, E., Sedlar, J., Benas, N., van Zadelhoff, G.-J., Schlundt, C., Stein, D., Finkensieper, S., Håkansson, N., and Hollmann, R., 2017, “CLARA-A2: The Second Edition of the CM SAF Cloud and Radiation Data Record from 34 Years of Global AVHRR Data,” *Atmospheric Chem. Phys.*, **17**(9), pp. 5809–5828. [https://doi.org/https://doi.org/10.5676/EUM\\_SAF\\_CM/CLARA\\_AVHRR/V002\\_01](https://doi.org/https://doi.org/10.5676/EUM_SAF_CM/CLARA_AVHRR/V002_01).
- [16] Babar, B., Graversen, R., and Boström, T., 2018, “Evaluating CM-SAF Solar Radiation CLARA-A1 and CLARA-A2 Datasets in Scandinavia,” *Sol. Energy*, **170**, pp. 76–85. <https://doi.org/10.1016/j.solener.2018.05.009>.
- [17] Urraca, R., Gracia-Amillo, A. M., Koubli, E., Huld, T., Trentmann, J., Riihelä, A., Lindfors, A. V., Palmer, D., Gottschalg, R., and Antonanzas-Torres, F., 2017, “Extensive Validation of CM SAF Surface Radiation Products over Europe,” *Remote Sens. Environ.*, **199**, pp. 171–186. <https://doi.org/10.1016/j.rse.2017.07.013>.



- [18] Babar, B., Graversen, R., and Boström, T., 2019, “Solar Radiation Estimation at High Latitudes: Assessment of the CMSAF Databases, ASR and ERA5,” *Sol. Energy*, **182**, pp. 397–411. <https://doi.org/10.1016/j.solener.2019.02.058>.
- [19] Polo, J., Wilbert, S., Ruiz-Arias, J. A., Meyer, R., Gueymard, C., Sári, M., Martín, L., Mieslinger, T., Blanc, P., Grant, I., Boland, J., Ineichen, P., Remund, J., Escobar, R., Troccoli, A., Sengupta, M., Nielsen, K. P., Renne, D., Geuder, N., and Cebecauer, T., 2016, “Preliminary Survey on Site-Adaptation Techniques for Satellite-Derived and Reanalysis Solar Radiation Datasets,” *Sol. Energy*, **132**, pp. 25–37. <https://doi.org/10.1016/j.solener.2016.03.001>.
- [20] Matsui, N., Long, C. N., Augustine, J., Halliwell, D., Uttal, T., Longenecker, D., Niebergall, O., Wendell, J., and Albee, R., 2012, “Evaluation of Arctic Broadband Surface Radiation Measurements,” *Atmospheric Meas. Tech.*, **5**(2), pp. 429–438. <https://doi.org/10.5194/amt-5-429-2012>.
- [21] Lanconelli, C., Busetto, M., Dutton, E. G., König-Langlo, G., Maturilli, M., Sieger, R., Vitale, V., and Yamamouchi, T., 2011, “Polar Baseline Surface Radiation Measurements during the International Polar Year 2007–2009,” *Earth Syst. Sci. Data*, **3**(1), pp. 1–8. <https://doi.org/10.5194/essd-3-1-2011>.
- [22] Jensen, A. R., Sifnaios, I., Anderson, K. S., and Gueymard, C. A., 2025, “SolarStations.Org—A Global Catalog of Solar Irradiance Monitoring Stations,” *Sol. Energy*, **295**, p. 113457. <https://doi.org/10.1016/j.solener.2025.113457>.
- [23] National Center for Atmospheric Research/University Corporation for Atmospheric Research, and University, P. M. G. P. and C. R. C. O. S., 2017, “Arctic System Reanalysis Version 2.” <https://doi.org/10.5065/D6X9291B>.
- [24] Lanconelli, C., Riihimäki, L., Driemel, A., Augustine, J., Badosa, J., Baika, S., Bonifaz, R., Carstea, E., Colle, S., Cox, C. J., Cuevas-Agulló, E., da Silva, A. K., Denn, F. M., Duck, B., Duprat, T., Fabbri, B., Fekete, D., Hodgetts, G., Ijima, O., Kallis, A., Knap, W., Kustov, V., Lin, K.-W., Lupi, A., Maturilli, M., Morel, B., Ntsangwane, L., Ohtake, J., Olano, X., Olefs, M., Omori, M., Ogawa, Y., PETERS, A., Ramanathan, K., Schmidthusen, H., Suarez, L., Tully, M., Vogt, R., Vuilleumier, L., Wacker, S., and Xia, X., 2023, “Baseline Surface Radiation Data Snapshot 2023-03-31.” <https://doi.org/10.1594/PANGAEA.957398>.
- [25] “CAMS Radiation Service,” SoDa. [Online]. Available: <https://www.soda-pro.com/web-services/radiation/cams-radiation-service>. [Accessed: 09-Feb-2026].
- [26] Doelling, D., 2017, “CERES Level 3 SYN1deg-1Hour Terra-Aqua-MODIS HDF4 File - Edition 4A.” [https://doi.org/10.5067/TERRA+AQUA/CERES/SYN1DEG-1HOUR\\_L3.004A](https://doi.org/10.5067/TERRA+AQUA/CERES/SYN1DEG-1HOUR_L3.004A).
- [27] Karlsson, K.-G., Anttila, K., Trentmann, J., Stengel, M., Solodovnik, I., Meirink, J. F., Devasthale, A., Kothe, S., Jääskeläinen, E., Sedlar, J., Benas, N., van Zadelhoff, G.-J., Stein, D., Finkensieper, S., Håkansson, N., Hollmann, R., Kaiser, J., and Werscheck, M., 2020, “CLARA-A2.1: CM SAF cLOUD, Albedo and Surface RADIATION Dataset from AVHRR Data - Edition 2.1.” [https://doi.org/10.5676/EUM\\_SAF\\_CM/CLARA\\_AVHRR/V002\\_01](https://doi.org/10.5676/EUM_SAF_CM/CLARA_AVHRR/V002_01).
- [28] Environment and Climate Change Canada, 2026, “Climate Data Extraction Tool.” [Online]. Available: <https://climate-change.canada.ca/climate-data/>.
- [29] C3S, 2018, “ERA5 Hourly Data on Single Levels from 1940 to Present.” <https://doi.org/10.24381/CDS.ADBB2D47>.
- [30] FMI, “FMI Download Observations,” Finn. Meteorol. Inst. [Online]. Available: <https://en.ilmatieseenlaitos.fi/download-observations>. [Accessed: 12-Feb-2026].
- [31] “Data Portal | ICOS.” [Online]. Available: <https://data.icos-cp.eu/portal/#%7B%22filterCategories%22:%7B%22project%22:%5B%22icos%22%5D,%22level%22:%5B1,2%5D,%22station-class%22:%5B%22ICOS%22%5D%7D%7D>. [Accessed: 09-Feb-2026].
- [32] “LandbruksMeteorologisk Tjeneste.” [Online]. Available: <https://imt.nibio.no/>. [Accessed: 09-Feb-2026].
- [33] Wang, D., 2024, “MODIS/Terra+Aqua Surface Radiation Daily/3-Hour L3 Global 1km SIN Grid V062.” <https://doi.org/10.5067/MODIS/MCD18A1.062>.
- [34] Wang, D., 2024, “MODIS/Terra+Aqua Downward Shortwave Radiation Daily/3-Hour L3 Global 0.05Deg CMG V062.” <https://doi.org/10.5067/MODIS/MCD18C1.062>.
- [35] Schaaf, C., 2019, “MODIS/Terra+Aqua BRDF/Albedo Gap-Filled Snow-Free Daily L3 Global 30ArcSec CMG V006.” <https://doi.org/10.5067/MODIS/MCD43GF.006>.
- [36] Schaaf, C., and Wang, Z., 2021, “MODIS/Terra+Aqua BRDF/Albedo Daily L3 Global - 500m V061.” <https://doi.org/10.5067/MODIS/MCD43A3.061>.



- [37] Schaaf, C., and Wang, Z., 2021, “MODIS/Terra+Aqua BRDF/Albedo Albedo Daily L3 Global 0.05Deg CMG V061.” <https://doi.org/10.5067/MODIS/MCD43C3.061>.
- [38] Schaaf, C., and Wang, Z., 2021, “MODIS/Terra+Aqua BRDF/Albedo Parameter1 Band1 Daily L3 Global 30ArcSec CMG V061.” <https://doi.org/10.5067/MODIS/MCD43D01.061>.
- [39] Gelaro, R., McCarty, W., Suárez, M. J., Todling, R., Molod, A., Takacs, L., Randles, C. A., Darmenov, A., Bosilovich, M. G., Reichle, R., Wargan, K., Coy, L., Cullather, R., Draper, C., Akella, S., Buchard, V., Conaty, A., Da Silva, A. M., Gu, W., Kim, G.-K., Koster, R., Lucchesi, R., Merkova, D., Nielsen, J. E., Par-tyka, G., Pawson, S., Putman, W., Rienecker, M., Schubert, S. D., Sienkiewicz, M., and Zhao, B., 2017, “The Modern-Era Retrospective Analysis for Research and Applications, Version 2 (MERRA-2),” *J. Clim.*, **30**(14), pp. 5419–5454. <https://doi.org/10.1175/JCLI-D-16-0758.1>.
- [40] “Meteonorm.” [Online]. Available: <https://meteonorm.com/>. [Accessed: 09-Feb-2026].
- [41] “NASA POWER Homepage,” Predict. Worldw. Energy Resour. POWER. [Online]. Available: <https://power.larc.nasa.gov/>. [Accessed: 09-Feb-2026].
- [42] Pfeifroth, U., Kothe, S., Müller, R., Trentmann, J., Hollmann, R., Fuchs, P., and Werscheck, M., 2017, “Sur- face Radiation Data Set - Heliosat (SARAH) - Edition 2.” [https://doi.org/10.5676/EUM\\_SAF\\_CM/SA- RAH/V002](https://doi.org/10.5676/EUM_SAF_CM/SA- RAH/V002).
- [43] “Norsk Klimaservicesenter.” [Online]. Available: <https://seklima.met.no/>. [Accessed: 09-Feb-2026].
- [44] “SMHI Open Data Portal.” [Online]. Available: <https://opendata.smhi.se/>. [Accessed: 09-Feb-2026].
- [45] “SolarAnywhere - Trusted Global Solar Data & Intelligence Services,” SolarAnywhere. [Online]. Available: <https://www.solaranywhere.com/>. [Accessed: 09-Feb-2026].
- [46] “SolarAnywhere - High Latitude Data,” SolarAnywhere. [Online]. Available: <https://www.solar- anywhere.com/support/geographic-coverage/high-latitude/>. [Accessed: 09-Feb-2026].
- [47] “Data, Software and Services for Solar Projects | Solargis.” [Online]. Available: <https://solargis.com/>. [Ac- cessed: 09-Feb-2026].
- [48] “Solar, Wind and Weather Data Power Built for Renewables | Solcast™.” [Online]. Available: <https://sol- cast.com>. [Accessed: 09-Feb-2026].
- [49] “STRÅNG Data Extraction.” [Online]. Available: <https://strang.smhi.se/extraction/index.php>. [Accessed: 09- Feb-2026].
- [50] Friesen, G., Micheli, L., Eder, G. C., Müller, T., Ali, J. M. Y., Rivera, M., Vásquez, J. A., Oreski, G., Burn- ham, L., Baldus-Jeursen, C., Granlund, A., Urrejola, E., Rodríguez-Gallegos, C. D., and Goriawala, S., 2025, *Optimisation of Photovoltaic Systems for Different Climates*, IEA PVPS. [Online]. Available: <https://iea-pvps.org/key-topics/t13-optimisation-pv-systems-different-climates-2025/>. [Accessed: 19-Nov- 2025].
- [51] “RTF Solar PV,” CCHRC Sens. Data. [Online]. Available: <http://cchrc.rcs.alaska.edu/pro- ject.php?name=FglONjYo>. [Accessed: 16-Oct-2025].
- [52] Poissant, Y., Thevenard, D., and Turcotte, D., 2004, *Performance Monitoring of the Nunavut Arctic College PV System: Nine Years of Reliable Electricity Generation*, CANMET Energy Technology Centre. [Online]. Available: [https://www.nri.nu.ca/sites/default/files/documents/nac\\_pv\\_system\\_performance.pdf](https://www.nri.nu.ca/sites/default/files/documents/nac_pv_system_performance.pdf).
- [53] Tonita, E. M., Russell, A. C. J., Valdivia, C. E., and Hinzer, K., 2023, “Optimal Ground Coverage Ratios for Tracked, Fixed-Tilt, and Vertical Photovoltaic Systems for Latitudes up to 75°N,” *Sol. Energy*, **258**, pp. 8– 15. <https://doi.org/10.1016/j.solener.2023.04.038>.
- [54] Rodríguez-Gallegos, C. D., Liu, H., Gandhi, O., Singh, J. P., Krishnamurthy, V., Kumar, A., Stein, J. S., Wang, S., Li, L., Reindl, T., and Peters, I. M., 2020, “Global Techno-Economic Performance of Bifacial and Tracking Photovoltaic Systems,” *Joule*, **4**(7), pp. 1514–1541. <https://doi.org/10.1016/j.joule.2020.05.005>.
- [55] Rodríguez-Gallegos, C. D., Bieri, M., Gandhi, O., Singh, J. P., Reindl, T., and Panda, S. K., 2018, “Monofa- cial vs Bifacial Si-Based PV Modules: Which One Is More Cost-Effective?,” *Sol. Energy*, **176**, pp. 412–438. <https://doi.org/10.1016/j.solener.2018.10.012>.
- [56] Pike, C., Whitney, E., Wilber, M., and Stein, J. S., 2021, “Field Performance of South-Facing and East-West Facing Bifacial Modules in the Arctic,” *Energies*, **14**(4), p. 1210. <https://doi.org/10.3390/en14041210>.
- [57] Jouttijärvi, S., Lobaccaro, G., Kamppinen, A., and Miettunen, K., 2022, “Benefits of Bifacial Solar Cells Combined with Low Voltage Power Grids at High Latitudes,” *Renew. Sustain. Energy Rev.*, **161**, p. 112354. <https://doi.org/10.1016/j.rser.2022.112354>.
- [58] Khan, M. R., Hanna, A., Sun, X., and Alam, M. A., 2017, “Vertical Bifacial Solar Farms: Physics, Design, and Global Optimization,” *Appl. Energy*, **206**, pp. 240–248. <https://doi.org/10.1016/j.apenergy.2017.08.042>.



- [59] Bhaduri, S., and Kottantharayil, A., 2019, “Mitigation of Soiling by Vertical Mounting of Bifacial Modules,” *IEEE J. Photovolt.*, **9**(1), pp. 240–244. <https://doi.org/10.1109/JPHOTOV.2018.2872555>.
- [60] Kahana, L., 2025, “Vertical Rooftop PV Performs Better than Conventional Rooftop Solar under the Snow,” *PV Mag*. [Online]. Available: <https://www.pv-magazine.com/2025/01/08/vertical-rooftop-pv-performs-better-than-conventional-rooftop-solar-under-the-snow/>. [Accessed: 16-Oct-2025].
- [61] NREL, 2022, “System Advisor Model Version 2022.11.21,” *Natl. Renew. Energy Lab*. [Online]. Available: <https://sam.nrel.gov/>. [Accessed: 02-Sept-2025].
- [62] Tonita, E., Ovaitt, S., Toal, H., Hinzer, K., Pike, C., and Deline, C., 2025, “Vertical Bifacial Photovoltaic System Model Validation: Study With Field Data, Various Orientations, and Latitudes,” *IEEE J. Photovolt.*, **15**(4), pp. 600–609. <https://doi.org/10.1109/JPHOTOV.2025.3561395>.
- [63] Tonita, E. M., Valdivia, C. E., Russell, A. C. J., Martinez-Szewczyk, M., Bertoni, M. I., and Hinzer, K., 2024, “Quantifying Spectral Albedo Effects on Bifacial Photovoltaic Module Measurements and System Model Predictions,” *Prog. Photovolt. Res. Appl.*, **32**(7), pp. 468–480. <https://doi.org/10.1002/pip.3789>.
- [64] Riedel-Lyngskær, N., Berrian, D., Alvarez Mira, D., Aguilar Protti, A., Poulsen, P. B., Libal, J., and Vedde, J., 2020, “Validation of Bifacial Photovoltaic Simulation Software against Monitoring Data from Large-Scale Single-Axis Trackers and Fixed Tilt Systems in Denmark,” *Appl. Sci.*, **10**(23), p. 8487. <https://doi.org/10.3390/app10238487>.
- [65] Theristis, M., Riedel-Lyngskær, N., Stein, J. S., Deville, L., Micheli, L., Driesse, A., Hobbs, W. B., Ovaitt, S., Daxini, R., Barrie, D., Campanelli, M., Hodges, H., Ledesma, J. R., Lokhat, I., McCormick, B., Meng, B., Miller, B., Motta, R., Noirault, E., Parker, M., Polo, J., Powell, D., Moretón, R., Prilliman, M., Ransome, S., Schneider, M., Schnierer, B., Tian, B., Warner, F., Williams, R., Wittmer, B., and Zhao, C., 2023, “Blind Photovoltaic Modeling Intercomparison: A Multidimensional Data Analysis and Lessons Learned,” *Prog. Photovolt. Res. Appl.*, **31**(11), pp. 1144–1157. <https://doi.org/10.1002/pip.3729>.
- [66] Russell, A. C. J., Valdivia, C. E., Bohémier, C., Haysom, J. E., and Hinzer, K., 2022, “DUET: A Novel Energy Yield Model With 3-D Shading for Bifacial Photovoltaic Systems,” *IEEE J. Photovolt.*, **12**(6), pp. 1576–1585. <https://doi.org/10.1109/JPHOTOV.2022.3185546>.
- [67] Stein, J., Reise, C., Bonilla Castro, J., Friesen, G., Maugeri, G., Urrejola, E., and Ranta, S., 2021, *Bifacial Photovoltaic Modules and Systems: Experience and Results From International Research and Pilot Applications*, IEA-PVPS T13-14:2021, International Energy Agency Photovoltaic Power Systems Programme, Paris, France. [Online]. Available: <https://www.osti.gov/servlets/purl/1779379/>.
- [68] de Simón-Martín, M., Alonso-Tristán, C., and Díez-Mediavilla, M., 2017, “Diffuse Solar Irradiance Estimation on Building’s Façades: Review, Classification and Benchmarking of 30 Models under All Sky Conditions,” *Renew. Sustain. Energy Rev.*, **77**, pp. 783–802. <https://doi.org/10.1016/j.rser.2017.04.034>.
- [69] Le, A. H. T., Srinivasa, A., Bowden, S. G., Hameiri, Z., and Augusto, A., 2023, “Temperature and Illumination Dependence of Silicon Heterojunction Solar Cells with a Wide Range of Wafer Resistivities,” *Prog. Photovolt. Res. Appl.*, **31**(5), pp. 536–545. <https://doi.org/10.1002/pip.3657>.
- [70] Li, B., “IV Curve Correction Tool Version 0.0.7,” *Lawrence Berkeley Natl. Lab*. [Online]. Available: <https://pvtools.lbl.gov/iv-curve-correction-tool/>. [Accessed: 02-Sept-2025].
- [71] Zhang, S. M. F., Seif, J. P., Abbott, M. D., Le, A. H. T., Allen, T. G., Perez-Wurfl, I., and Hameiri, Z., 2022, “Illumination-Dependent Temperature Coefficients of the Electrical Parameters of Modern Silicon Solar Cell Architectures,” *Nano Energy*, **98**, p. 107221. <https://doi.org/10.1016/j.nanoen.2022.107221>.
- [72] Haschke, J., Seif, J. P., Riesen, Y., Tomasi, A., Cattin, J., Tous, L., Choulat, P., Aleman, M., Cornagliotti, E., Uruena, A., Russell, R., Duerinckx, F., Champlaud, J., Levrat, J., Abdallah, A. A., Aïssa, B., Tabet, N., Wyrsh, N., Despeisse, M., Szlufcik, J., Wolf, S. D., and Ballif, C., 2017, “The Impact of Silicon Solar Cell Architecture and Cell Interconnection on Energy Yield in Hot & Sunny Climates,” *Energy Environ. Sci.*, **10**(5), pp. 1196–1206. <https://doi.org/10.1039/C7EE00286F>.
- [73] Looney, E. E., Liu, Z., Classen, A., Liu, H., Riedel, N., Braga, M., Balaji, P., Augusto, A., Buonassisi, T., and Marius Peters, I., 2021, “Representative Identification of Spectra and Environments (RISE) Using k-Means,” *Prog. Photovolt. Res. Appl.*, **29**(2), pp. 200–211. <https://doi.org/10.1002/pip.3358>.
- [74] Paudyal, B. R., and Imenes, A. G., 2021, “Investigation of Temperature Coefficients of PV Modules through Field Measured Data,” *Sol. Energy*, **224**, pp. 425–439. <https://doi.org/10.1016/j.solener.2021.06.013>.
- [75] Le, A. H. T., Balaji, P., Augusto, A., and Hameiri, Z., 2023, “Temperature-Dependent Performance of Ultra-Thin Silicon Heterojunction Solar Cells for Space Applications,” *2023 IEEE 50th Photovoltaic Specialists Conference (PVSC)*, pp. 1–1. <https://doi.org/10.1109/PVSC48320.2023.10359936>.



- [76] Kibriya, T., 2018, “A Review of Geotechnical Problems Facing Solar Based Renewable Energy Facilities in Frost Affected Regions of North America,” *Int. J. Appl. Eng. Res.*, **13**(10), pp. 7309–7316.
- [77] Hao, D., Shi, Y., Chen, R., Lu, Z., Ji, Y., Lv, Z., and Liu, L., 2025, “Response of Thermo-Hydro-Mechanical Fields to Pile Material in Pile–Soil System Under Freezing Based on Numerical Analysis,” *Buildings*, **15**(4), p. 534. <https://doi.org/10.3390/buildings15040534>.
- [78] Hinkel, K. M., and Hurd Jr., J. K., 2006, “Permafrost Destabilization and Thermokarst Following Snow Fence Installation, Barrow, Alaska, U.S.A.,” *Arct. Antarct. Alp. Res.*, **38**(4), pp. 530–539. [https://doi.org/10.1657/1523-0430\(2006\)38%5B530:PDATFS%5D2.0.CO;2](https://doi.org/10.1657/1523-0430(2006)38%5B530:PDATFS%5D2.0.CO;2).
- [79] O’Neill, H. B., and Burn, C. R., 2015, “Permafrost Degradation Adjacent to Snow Fences along the Dempster Highway, Peel Plateau, NWT,” *7th Canadian Permafrost Conference: Proceedings of a Conference Held*, pp. 20–23. [Online]. Available: <https://members.cgs.ca/documents/conference2015/GeoQuebec/papers/219.pdf>.
- [80] Andenæs, E., Jelle, B. P., Ramlo, K., Kolås, T., Selj, J., and Foss, S. E., 2018, “The Influence of Snow and Ice Coverage on the Energy Generation from Photovoltaic Solar Cells,” *Sol. Energy*, **159**, pp. 318–328. <https://doi.org/10.1016/j.solener.2017.10.078>.
- [81] Herrmann, W., and Bogdanski, N., 2011, “Outdoor Weathering of PV Modules — Effects of Various Climates and Comparison with Accelerated Laboratory Testing,” *2011 37th IEEE Photovoltaic Specialists Conference*, pp. 002305–002311. <https://doi.org/10.1109/PVSC.2011.6186415>.
- [82] Blieske, U., and Stollwerck, G., 2013, “Chapter Four - Glass and Other Encapsulation Materials,” *Semiconductors and Semimetals*, G.P. Willeke, and E.R. Weber, eds., Elsevier, pp. 199–258. <https://doi.org/10.1016/B978-0-12-381343-5.00004-5>.
- [83] Tonita, E. M., Jordan, D. C., Ovaitt, S., Toal, H., Hinzer, K., Pike, C., and Deline, C., “Long-Term Photovoltaic System Performance in Cold, Snowy Climates,” *Prog. Photovolt. Res. Appl.*, **n/a**(n/a). <https://doi.org/10.1002/pip.70014>.
- [84] Jordan, D. C., Anderson, K., Perry, K., Muller, M., Deceglie, M., White, R., and Deline, C., 2022, “Photovoltaic Fleet Degradation Insights,” *Prog. Photovolt. Res. Appl.*, **30**(10), pp. 1166–1175. <https://doi.org/10.1002/pip.3566>.
- [85] Schill, C., Anderson, A., Baldus-Jeursen, C., Burnham, L., Micheli, L., Parlevliet, D., Pilat, E., Stridh, B., and Urrejola, E., 2022, *Soiling Losses – Impact on the Performance of Photovoltaic Power Plants*, 978-3-907281-09-3, International Energy Agency Photovoltaic Power Systems Programme, Paris, France. [Online]. Available: <https://iea-pvps.org/wp-content/uploads/2023/01/IEA-PVPS-T13-21-2022-REPORT-Soiling-Losses-PV-Plants.pdf>.
- [86] IEA, 2025, *Guideline for the Optimization of PV System Key Performance Indicators*, IEA PVPS Task 13 Subtask 3.2 Team.
- [87] Frimannslund, I., Thiis, T., Aalberg, A., and Thorud, B., 2021, “Polar Solar Power Plants – Investigating the Potential and the Design Challenges,” *Sol. Energy*, **224**, pp. 35–42. <https://doi.org/10.1016/j.solener.2021.05.069>.
- [88] Libbrecht, K. G., 2005, “The Physics of Snow Crystals,” *Rep. Prog. Phys.*, **68**(4). [Online]. Available: <https://doi.org/10.1088/0034-4885/68/4/R03>.
- [89] Jelle, B. P., 2013, “The Challenge of Removing Snow Downfall on Photovoltaic Solar Cell Roofs in Order to Maximize Solar Energy Efficiency—Research Opportunities for the Future,” *Energy Build.*, **67**, pp. 334–351. <https://doi.org/10.1016/j.enbuild.2013.08.010>.
- [90] Eidevåg, T., Thomson, E. S., Kallin, D., Casselgren, J., and Rasmuson, A., 2022, “Angle of Repose of Snow: An Experimental Study on Cohesive Properties,” *Cold Reg. Sci. Technol.*, **194**, p. 103470. <https://doi.org/10.1016/j.coldregions.2021.103470>.
- [91] Sommer, C. G., Lehning, M., and Fierz, C., 2018, “Wind Tunnel Experiments: Influence of Erosion and Deposition on Wind-Packing of New Snow,” *Front. Earth Sci.*, **6**. <https://doi.org/10.3389/feart.2018.00004>.
- [92] Granlund, A., Narvesjö, J., and Petersson, A. M., 2019, “The Influence of Module Tilt on Snow Shadowing of Frameless Bifacial Modules,” *WIP*, pp. 1646–1650. <https://doi.org/10.4229/EUPVSEC20192019-5CV.4.36>.
- [93] Hosseini, S., Taheri, S., Pouresmaeil, E., and Taheri, H., 2020, “Analysis of Electrical Behaviour of PV Arrays Covered with Non-Uniform Snow,” *Electron. Lett.*, **56**(4), pp. 192–194. <https://doi.org/10.1049/el.2019.3221>.



- [94] Pawluk, R. E., Chen, Y., and She, Y., 2019, "Photovoltaic Electricity Generation Loss Due to Snow – A Literature Review on Influence Factors, Estimation, and Mitigation," *Renew. Sustain. Energy Rev.*, **107**, pp. 171–182. <https://doi.org/10.1016/j.rser.2018.12.031>.
- [95] Townsend, T., and Powers, L., 2011, "Photovoltaics and Snow: An Update from Two Winters of Measurements in the SIERRA," *2011 37th IEEE Photovoltaic Specialists Conference*, pp. 003231–003236. <https://doi.org/10.1109/PVSC.2011.6186627>.
- [96] Marion, B., Schaefer, R., Caine, H., and Sanchez, G., 2013, "Measured and Modeled Photovoltaic System Energy Losses from Snow for Colorado and Wisconsin Locations," *Sol. Energy*, **97**, pp. 112–121. <https://doi.org/10.1016/j.solener.2013.07.029>.
- [97] Baldus-Jeursen, C., Petsiuk, A. L., Rheault, S.-A., Pelland, S., Côté, A., Poissant, Y., and Pearce, J. M., 2023, "Snow Losses for Photovoltaic Systems: Validating the Marion and Townsend Models," *IEEE J. Photovolt.*, **13**(4), pp. 610–620. <https://doi.org/10.1109/JPHOTOV.2023.3264644>.
- [98] Ma, J., Khoury, A., and Rodgers, M., 2023, "Evaluation of PV Snow Loss Models in the East Coast of Canada Using AI Computer Vision," *2023 IEEE 50th Photovoltaic Specialists Conference (PVSC)*, pp. 1–5. <https://doi.org/10.1109/PVSC48320.2023.10360003>.
- [99] Hashemi, B., Taheri, S., and Cretu, A.-M., 2022, "Systematic Analysis and Computational Intelligence Based Modeling of Photovoltaic Power Generation in Snow Conditions," *IEEE J. Photovolt.*, **12**(1), pp. 406–420. <https://doi.org/10.1109/JPHOTOV.2021.3123198>.
- [100] Øgaard, M. B., Frimannslund, I., Riise, H. N., and Selj, J., 2022, "Snow Loss Modeling for Roof Mounted Photovoltaic Systems: Improving the Marion Snow Loss Model," *IEEE J. Photovolt.*, **12**(4), pp. 1005–1013. <https://doi.org/10.1109/JPHOTOV.2022.3166909>.
- [101] Riley, D., Burnham, L., Dice, P., and Braid, J., 2023, "An Enhanced Snow-Shedding Model: The Module Frame as a Key Variable," *2023 IEEE 50th Photovoltaic Specialists Conference (PVSC)*, pp. 1–3. <https://doi.org/10.1109/PVSC48320.2023.10359767>.
- [102] Weiß, K.-A., Klimm, E., and Kaaya, I., 2022, "Accelerated Aging Tests vs Field Performance of PV Modules," *Prog. Energy*, **4**(4), p. 042009. <https://doi.org/10.1088/2516-1083/ac890a>.
- [103] Segbefia, O. K., Akhtar, N., and Sætre, T. O., 2023, "Moisture Induced Degradation in Field-Aged Multicrystalline Silicon Photovoltaic Modules," *Sol. Energy Mater. Sol. Cells*, **258**, p. 112407. <https://doi.org/10.1016/j.solmat.2023.112407>.
- [104] IEC, 2021, "IEC 61215-2:2021: Terrestrial Photovoltaic (PV) Modules - Design Qualification and Type Approval." [Online]. Available: <https://webstore.iec.ch/en/publication/61350>. [Accessed: 02-Sept-2025].
- [105] IEC, 2020, "IEC 62938:2020: Photovoltaic (PV) Modules - Non-Uniform Snow Load Testing." [Online]. Available: <https://webstore.iec.ch/en/publication/33027>. [Accessed: 02-Sept-2025].
- [106] Köntges, M., Kurtz, S., Jahn, U., Berger, K. A., Kato, K., Friesen, T., Liu, H., and Van Iseghem, M., 2014, *Review of Failures of Photovoltaic Modules*, IEA-PVPS T13-01:2014, International Energy Agency Photovoltaic Power Systems Programme, Paris, France. [Online]. Available: [https://iea-pvps.org/wp-content/uploads/2020/01/IEA-PVPS\\_T13-01\\_2014\\_Review\\_of\\_Failures\\_of\\_Photovoltaic\\_Modules\\_Final.pdf](https://iea-pvps.org/wp-content/uploads/2020/01/IEA-PVPS_T13-01_2014_Review_of_Failures_of_Photovoltaic_Modules_Final.pdf).
- [107] Mathiak, G., Sommer, J., Herrmann, W., Bogdanski, N., Althaus, J., and Reil, F., 2016, "PV Module Damages Caused by Hail Impact and Non-Uniform Snow Load," *32nd Eur. Photovolt. Sol. Energy Conf. Exhib.* 1692-1696, pp. 1692–1696. <https://doi.org/10.4229/EUPVSEC20162016-5DO.10.4>.
- [108] Jahn, U., Herteleer, B., Tjengdrawira, C., Tsanakas, I., Richter, M., Dickeson, G., Astigarraga, A., Tanahashi, T., Valencia, F., Green, M., Anderson, A., Stridh, B., Lagunas Alonso, A. R., and Sangpong-sanont, Y., 2022, *Guidelines for Operation and Maintenance of Photovoltaic Power Plants in Different Climates*, IEA-PVPS T13-25:2022, International Energy Agency Photovoltaic Power Systems Programme, Paris, France. [Online]. Available: <https://iea-pvps.org/wp-content/uploads/2022/11/IEA-PVPS-Report-T13-25-2022-OandM-Guidelines.pdf>.
- [109] Bogenrieder, J., Camus, C., Hüttner, M., Offermann, P., Hauch, J., and Brabec, C. J., 2018, "Technology-Dependent Analysis of the Snow Melting and Sliding Behavior on Photovoltaic Modules," *J. Renew. Sustain. Energy*, **10**(2), p. 021005. <https://doi.org/10.1063/1.5001556>.
- [110] Lindh, M., Granlund, A., Sundström, J., Axelson, M., and Petersson, A. M., 2024, *Effekter Och Hantering Av Snölaster Vid Takmonterade Solelanläggningar*, P2018-016202, Swedish Energy Agency, Eskilstuna, Sweden. [Online]. Available: [https://www.ri.se/sites/default/files/2024-02/Effekter-och-hantering-av-solelanl%C3%A4ggnings-vid-takmonterade-solelanl%C3%A4ggnings\\_slutrapport.pdf](https://www.ri.se/sites/default/files/2024-02/Effekter-och-hantering-av-solelanl%C3%A4ggnings-vid-takmonterade-solelanl%C3%A4ggnings_slutrapport.pdf).



- [111] Romer, P., Pethani, K. B., and Beinert, A. J., 2024, “Effect of Inhomogeneous Loads on the Mechanics of PV Modules,” *Prog. Photovolt. Res. Appl.*, **32**(2), pp. 84–101. <https://doi.org/10.1002/pip.3738>.
- [112] Schneller, E. J., Seigneur, H., Lincoln, J., and Gabor, A. M., 2019, “The Impact of Cold Temperature Exposure in Mechanical Durability Testing of PV Modules,” *2019 IEEE 46th Photovoltaic Specialists Conference (PVSC)*, pp. 1521–1524. <https://doi.org/10.1109/PVSC40753.2019.8980533>.
- [113] Granlund, A., Lindh, M., Vikberg, T., and Petersson, A. M., 2022, “Evaluation of Snow Removal Methods for Rooftop Photovoltaics,” *8th World Conference on Photovoltaic Energy Conversion; 1122-1128*, WIP, Milan, Italy, p. 7 pages, 5364 kb. <https://doi.org/10.4229/WCPEC-82022-4DO.4.6>.
- [114] Sander, M., Dietrich, S., Pander, M., Ebert, M., Karrass, M., Lippmann, R., Broddack, M., and Wald, D., 2013, “Influence of Manufacturing Processes and Subsequent Weathering on the Occurrence of Cell Cracks in PV Modules,” *28th European Photovoltaic Solar Energy Conference and Exhibition; 3275-3279*, WIP, Paris, France, pp. 3275–3279. <https://doi.org/10.4229/28THEUPVSEC2013-4AV.5.30>.
- [115] Rowell, M. W., Daroczi, S. G., Harwood, D. W. J., and Gabor, A. M., 2018, “The Effect of Laminate Construction and Temperature Cycling on the Fracture Strength and Performance of Encapsulated Solar Cells,” *2018 IEEE 7th World Conference on Photovoltaic Energy Conversion (WCPEC) (A Joint Conference of 45th IEEE PVSC, 28th PVSEC & 34th EU PVSEC)*, pp. 3927–3931. <https://doi.org/10.1109/PVSC.2018.8547978>.
- [116] Kempe, M. D., Jorgensen, G. J., Terwilliger, K. M., McMahon, T. J., Kennedy, C. E., and Borek, T. T., 2007, “Acetic Acid Production and Glass Transition Concerns with Ethylene-Vinyl Acetate Used in Photovoltaic Devices,” *Sol. Energy Mater. Sol. Cells*, **91**(4), pp. 315–329. <https://doi.org/10.1016/j.solmat.2006.10.009>.
- [117] Lee, K., Kim, D., Kim, S. H., Park, G., Kim, B. K., and Kim, J., 2025, “Improving the Physical Properties of Polyolefin Elastomer Encapsulants by Radical Initiators for Reliable Photovoltaic Modules,” *Polym. Test.*, **151**, p. 108954. <https://doi.org/10.1016/j.polymertesting.2025.108954>.
- [118] Hejazi, V., Sobolev, K., and Nosonovsky, M., 2013, “From Superhydrophobicity to Icephobicity: Forces and Interaction Analysis,” *Sci. Rep.*, **3**(1), p. 2194. <https://doi.org/10.1038/srep02194>.
- [119] Sojoudi, H., Wang, M., Boscher, N. D., McKinley, G. H., and Gleason, K. K., 2016, “Durable and Scalable Icephobic Surfaces: Similarities and Distinctions from Superhydrophobic Surfaces,” *Soft Matter*, **12**(7), pp. 1938–1963. <https://doi.org/10.1039/C5SM02295A>.
- [120] Jung, S., Dorrestijn, M., Raps, D., Das, A., Megaridis, C. M., and Poulikakos, D., 2011, “Are Superhydrophobic Surfaces Best for Icephobicity?,” *Langmuir*, **27**(6), pp. 3059–3066. <https://doi.org/10.1021/la104762g>.
- [121] Eberle, P., Tiwari, M. K., Maitra, T., and Poulikakos, D., 2014, “Rational Nanostructuring of Surfaces for Extraordinary Icephobicity,” *Nanoscale*, **6**(9), pp. 4874–4881. <https://doi.org/10.1039/C3NR06644D>.
- [122] Manni, M., Failla, M. C., Nocente, A., Lobaccaro, G., and Jelle, B. P., 2022, “The Influence of Icephobic Nanomaterial Coatings on Solar Cell Panels at High Latitudes,” *Sol. Energy*, **248**, pp. 76–87. <https://doi.org/10.1016/j.solener.2022.11.005>.
- [123] Andrews, R. W., Pollard, A., and Pearce, J. M., 2013, “The Effects of Snowfall on Solar Photovoltaic Performance,” *Sol. Energy*, **92**, pp. 84–97. <https://doi.org/10.1016/j.solener.2013.02.014>.
- [124] Powers, L., Newmiller, J., and Townsend, T., 2010, “Measuring and Modeling the Effect of Snow on Photovoltaic System Performance,” *2010 35th IEEE Photovoltaic Specialists Conference*, pp. 000973–000978. <https://doi.org/10.1109/PVSC.2010.5614572>.
- [125] Frimannslund, I., Thiis, T., Ferreira, A. D., and Thorud, B., 2022, “Impact of Solar Power Plant Design Parameters on Snowdrift Accumulation and Energy Yield,” *Cold Reg. Sci. Technol.*, **201**, p. 103613. <https://doi.org/10.1016/j.coldregions.2022.103613>.
- [126] Zheng, J., Liu, W., Cui, T., Wang, H., Chen, F., Gao, Y., Fan, L., Ali Abaker Omer, A., Ingenhoff, J., Zhang, X., and Liu, W., 2023, “A Novel Domino-like Snow Removal System for Roof PV Arrays: Feasibility, Performance, and Economic Benefits,” *Appl. Energy*, **333**, p. 120554. <https://doi.org/10.1016/j.apenergy.2022.120554>.
- [127] Tanahashi, T., Chiba, T., Adachi, S., Tsuno, Y., Ikeda, K., and Oozeki, T., 2023, “Mitigation of Heavy Snow Load on PV Modules Installed in a Snowy Region,” *2023 PV Reliability Workshop*, National Renewable Energy Laboratory, p. 76. [Online]. Available: <https://docs.nrel.gov/docs/fy24osti/87918.pdf>.
- [128] Anadol, M. A., 2020, “Snow Melting on Photovoltaic Module Surface Heated with Transparent Resistive Wires Embedded in Polyvinyl Butyral Interlayer,” *Sol. Energy*, **212**, pp. 101–112. <https://doi.org/10.1016/j.solener.2020.10.073>.



- [129] Rahmatmand, A., Harrison, S. J., and Oosthuizen, P. H., 2018, “An Experimental Investigation of Snow Removal from Photovoltaic Solar Panels by Electrical Heating,” *Sol. Energy*, **171**, pp. 811–826. <https://doi.org/10.1016/j.solener.2018.07.015>.
- [130] Yan, C., Qu, M., Chen, Y., and Feng, M., 2020, “Snow Removal Method for Self-Heating of Photovoltaic Panels and Its Feasibility Study,” *Sol. Energy*, **206**, pp. 374–380. <https://doi.org/10.1016/j.solener.2020.04.064>.
- [131] Borrebæk, P.-O. A., Jelle, B. P., and Zhang, Z., 2020, “Avoiding Snow and Ice Accretion on Building Integrated Photovoltaics – Challenges, Strategies, and Opportunities,” *Sol. Energy Mater. Sol. Cells*, **206**, p. 110306. <https://doi.org/10.1016/j.solmat.2019.110306>.
- [132] Fay, L., and Shi, X., 2012, “Environmental Impacts of Chemicals for Snow and Ice Control: State of the Knowledge,” *Water. Air. Soil Pollut.*, **223**(5), pp. 2751–2770. <https://doi.org/10.1007/s11270-011-1064-6>.
- [133] Omazic, A., Oreski, G., Halwachs, M., Eder, G. C., Hirschl, C., Neumaier, L., Pinter, G., and Erceg, M., 2019, “Relation between Degradation of Polymeric Components in Crystalline Silicon PV Module and Climatic Conditions: A Literature Review,” *Sol. Energy Mater. Sol. Cells*, **192**, pp. 123–133. <https://doi.org/10.1016/j.solmat.2018.12.027>.
- [134] Gandhi, O., Kumar, D. S., Rodríguez-Gallegos, C. D., and Srinivasan, D., 2020, “Review of Power System Impacts at High PV Penetration Part I: Factors Limiting PV Penetration,” *Sol. Energy*, **210**, pp. 181–201. <https://doi.org/10.1016/j.solener.2020.06.097>.
- [135] Sampath Kumar, D., Gandhi, O., Rodríguez-Gallegos, C. D., and Srinivasan, D., 2020, “Review of Power System Impacts at High PV Penetration Part II: Potential Solutions and the Way Forward,” *Sol. Energy*, **210**, pp. 202–221. <https://doi.org/10.1016/j.solener.2020.08.047>.
- [136] Shimomura, M., Keeley, A. R., Matsumoto, K., Tanaka, K., and Managi, S., 2024, “Beyond the Merit Order Effect: Impact of the Rapid Expansion of Renewable Energy on Electricity Market Price,” *Renew. Sustain. Energy Rev.*, **189**, p. 114037. <https://doi.org/10.1016/j.rser.2023.114037>.
- [137] Stringer, T., Joanis, M., and Abdoli, S., 2024, “Power Generation Mix and Electricity Price,” *Renew. Energy*, **221**, p. 119761. <https://doi.org/10.1016/j.renene.2023.119761>.
- [138] International Energy Agency Photovoltaic Power Systems Programme (IEA PVPS) Task 13, 2025, *Dual Land Use for Agriculture and Solar Power Production: Overview and Performance of Agrivoltaic Systems*, IEA-PVPS T13-29:2025, International Energy Agency Photovoltaic Power Systems Programme, OECD/IEA, Paris, France. [Online]. Available: <https://iea-pvps.org/wp-content/uploads/2025/03/IEA-PVPS-T13-29-2025-REPORT-Dual-Land-Use.pdf>.
- [139] Ranta, S., Akulenko, E., Huerta, H., Wang, S., Jouttijärvi, S., and Miettunen, K., 2024, “Feasibility and Greenhouse Gas Emissions of Timber Structures in Solar Photovoltaic Carport Construction,” *Front. Built Environ.*, **10**. <https://doi.org/10.3389/fbuil.2024.1379956>.
- [140] Jouttijärvi, S., Karttunen, L., Ranta, S., and Miettunen, K., 2024, “Techno-Economic Analysis on Optimizing the Value of Photovoltaic Electricity in a High-Latitude Location,” *Appl. Energy*, **361**, p. 122924. <https://doi.org/10.1016/j.apenergy.2024.122924>.
- [141] Cai, Q., Qing, J., Xu, Q., Shi, G., and Liang, Q.-M., 2024, “Techno-Economic Impact of Electricity Price Mechanism and Demand Response on Residential Rooftop Photovoltaic Integration,” *Renew. Sustain. Energy Rev.*, **189**, p. 113964. <https://doi.org/10.1016/j.rser.2023.113964>.
- [142] Jouttijärvi, S., Thorning, J., Manni, M., Huerta, H., Ranta, S., Di Sabatino, M., Lobaccaro, G., and Miettunen, K., 2023, “A Comprehensive Methodological Workflow to Maximize Solar Energy in Low-Voltage Grids: A Case Study of Vertical Bifacial Panels in Nordic Conditions,” *Sol. Energy*, **262**, p. 111819. <https://doi.org/10.1016/j.solener.2023.111819>.
- [143] Lindberg, O., Lingfors, D., Arnqvist, J., van der Meer, D., and Munkhammar, J., 2023, “Day-Ahead Probabilistic Forecasting at a Co-Located Wind and Solar Power Park in Sweden: Trading and Forecast Verification,” *Adv. Appl. Energy*, **9**, p. 100120. <https://doi.org/10.1016/j.adapen.2022.100120>.
- [144] Martinez, A., and Iglesias, G., 2024, “Hybrid Wind-Solar Energy Resources Mapping in the European Atlantic,” *Sci. Total Environ.*, **928**, p. 172501. <https://doi.org/10.1016/j.scitotenv.2024.172501>.
- [145] Ludwig, D., Breyer, C., Solomon, A. A., Seguin, R., Ludwig, D., Breyer, C., Solomon, A. A., and Seguin, R., 2020, “Evaluation of an Onsite Integrated Hybrid PV-Wind Power Plant,” *AIMS Energy*, **8**(5), pp. 988–1006. <https://doi.org/10.3934/energy.2020.5.988>.
- [146] Ibáñez-Rioja, A., Järvinen, L., Puranen, P., Kosonen, A., Ruuskanen, V., Hynynen, K., Ahola, J., and Kau-ranen, P., 2023, “Off-Grid Solar PV–Wind Power–Battery–Water Electrolyzer Plant: Simultaneous



- Optimization of Component Capacities and System Control,” *Appl. Energy*, **345**, p. 121277. <https://doi.org/10.1016/j.apenergy.2023.121277>.
- [147] Ranta, S., Stein, J. S., Huerta, H., Heinonen, A., and Whitney, E., 2019, “Self-Consumption Rate Achieved by the Bifacial East-West Vertical PV System Compared to the Conventional South Facing System in Nordic Conditions,” *WIP*, p. 4 pages, 7381 kb. <https://doi.org/10.4229/EUPVSEC20192019-6CO.15.5>.
- [148] Huang, P., Han, M., Zhang, X., Hussain, S. A., Jayprakash Bhagat, R., and Hogarehalli Kumar, D., 2022, “Characterization and Optimization of Energy Sharing Performances in Energy-Sharing Communities in Sweden, Canada and Germany,” *Appl. Energy*, **326**, p. 120044. <https://doi.org/10.1016/j.apenergy.2022.120044>.
- [149] Sørensen, Å. L., Sartori, I., Lindberg, K. B., and Andresen, I., 2019, “Analysing Electricity Demand in Neighbourhoods with Electricity Generation from Solar Power Systems: A Case Study of a Large Housing Cooperative in Norway,” *IOP Conf. Ser. Earth Environ. Sci.*, **352**(1), p. 012008. <https://doi.org/10.1088/1755-1315/352/1/012008>.
- [150] Huang, P., Lovati, M., Zhang, X., Bales, C., Hallbeck, S., Becker, A., Bergqvist, H., Hedberg, J., and Maturi, L., 2019, “Transforming a Residential Building Cluster into Electricity Prosumers in Sweden: Optimal Design of a Coupled PV-Heat Pump-Thermal Storage-Electric Vehicle System,” *Appl. Energy*, **255**, p. 113864. <https://doi.org/10.1016/j.apenergy.2019.113864>.
- [151] Bolt, G., Wilber, M., Huang, D., Sambor, D. J., Aggarwal, S., and Whitney, E., 2022, “Modeling and Evaluating Beneficial Matches between Excess Renewable Power Generation and Non-Electric Heat Loads in Remote Alaska Microgrids,” *Sustainability*, **14**(7), p. 3884. <https://doi.org/10.3390/su14073884>.
- [152] Wilber, M., Whitney, E., and Hauptert, C., 2022, “A Global Daily Solar Photovoltaic Load Coverage Factor Map for Passenger Electric Vehicles,” *2022 IEEE PES/IAS PowerAfrica*, pp. 1–4. <https://doi.org/10.1109/PowerAfrica53997.2022.9905364>.
- [153] European Climate, Infrastructure and Environment Executive Agency, 2025, “RENEWFM: €52 Million to 9 Renewable Energy Projects in Finland and Estonia - European Climate, Infrastructure and Environment Executive Agency,” *Eur. Clim. Infrastruct. Environ. Exec. Agency*. [Online]. Available: [https://cinea.ec.europa.eu/news-events/news/renewfm-eu52-million-9-renewable-energy-projects-finland-and-estonia-2025-04-30\\_en](https://cinea.ec.europa.eu/news-events/news/renewfm-eu52-million-9-renewable-energy-projects-finland-and-estonia-2025-04-30_en). [Accessed: 16-Oct-2025].
- [154] Vero Skatt, 2024, “Tax Credit Amount and the Credit Threshold,” *Vero Skatt*. [Online]. Available: <https://www.vero.fi/en/individuals/deductions/Tax-credit-for-household-expenses/tax-credit-amount/>. [Accessed: 05-Sept-2025].
- [155] Energy Authority, “Energy Authority,” *Energiavirasto*. [Online]. Available: <https://energiavirasto.fi/en/frontpage>. [Accessed: 14-Nov-2024].
- [156] U.S. Census Bureau, 2024, “QuickFacts: Alaska.” [Online]. Available: <https://www.census.gov/quickfacts/fact/table/AK/PST045224>.
- [157] Encyclopædia Britannica, Inc., “What’s the Largest U.S. State by Area?” [Online]. Available: <https://www.britannica.com/topic/largest-U-S-state-by-area>.
- [158] U.S. Energy Information Administration, 2026, “Alaska Electricity — State Energy Information Data.” [Online]. Available: <https://www.eia.gov/states/AK/data/dashboard/electricity>.
- [159] Statistics Canada, 2021, “Census of Population: 2021 Census Data.” [Online]. Available: <https://www12.statcan.gc.ca/census-recensement/index-eng.cfm>. [Accessed: 05-Sept-2025].
- [160] Statistics Greenland, 2024, *Greenland in Figures 2024*, 21st edition, Statistics Greenland, Nuuk, Greenland. [Online]. Available: <https://stat.gl/publ/en/GF/2024/pdf/Greenland%20in%20Figures%202024.pdf>.
- [161] Faroe Islands, “Faroe Islands - Facts and Figures,” *Faroe Isl.* [Online]. Available: <https://www.faroeislands.fo/the-big-picture/facts-and-figures>. [Accessed: 05-Sept-2025].
- [162] Statistics Faroe Islands, “Electricity Sales of SEV.” [Online]. Available: <https://hagstova.fo/en/environment/energy/electricity-sales-sev>. [Accessed: 05-Sept-2025].
- [163] Statistics Iceland, “Statistics Iceland.” [Online]. Available: <https://statice.is>. [Accessed: 16-Oct-2024].
- [164] Statbank Norway, “01222: Population and Changes during the Quarter (M) 1997K4 - 2025K2.” [Online]. Available: <https://www.ssb.no/en/system/>. [Accessed: 05-Sept-2025].
- [165] Statbank Norway, “08308: Production of Electricity, by Type of Power (GWh) (C) 2006 - 2024.” [Online]. Available: <https://www.ssb.no/en/system/>. [Accessed: 05-Sept-2025].
- [166] Statbank Norway, “10314: Net Consumption of Electricity, by Consumer Group (GWh) (M) (Closed Series) 2010 - 2023.” [Online]. Available: <https://www.ssb.no/en/system/>. [Accessed: 05-Sept-2025].



- [167] Statistics Finland, “Environment and Nature.” [Online]. Available: [https://stat.fi/tup/suoluk/suoluk\\_alue\\_en.html](https://stat.fi/tup/suoluk/suoluk_alue_en.html). [Accessed: 14-June-2024].
- [168] Arctic Council, Russian’s Chairmanship, n.d., “Arctic Regions of Russia.” [Online]. Available: <https://as.arctic-russia.ru/en/useful/#:~:text=Russia’s%20Arctic%20zone%20includes%20nine,%25%20of%20the%20country’s%20territory>.
- [169] Finnish Energy, “Statistics on Electricity: Electricity Year 2023,” Finn. Energy. [Online]. Available: <https://energia.fi/en/statistics/statistics-on-electricity/>. [Accessed: 22-Jan-2024].
- [170] Official Statistics of Sweden, “Elproduktion Och Bränsleanvändning (MWh) Efter Region, Produktionsätt, Bränsletyp Och År,” Stat. Database. [Online]. Available: [https://www.statistikdatabasen.scb.se:443/pxweb/en/ssd/START\\_\\_BE\\_\\_BE0101\\_\\_BE0101A/BefolkManad/](https://www.statistikdatabasen.scb.se:443/pxweb/en/ssd/START__BE__BE0101__BE0101A/BefolkManad/). [Accessed: 12-June-2024].
- [171] Alaska Center for Energy and Power, 2024, *Alaska’s Railbelt Electric System: Decarbonization Scenarios For 2050*, University of Alaska Fairbanks, Fairbanks, Alaska. [Online]. Available: <https://www.uaf.edu/acep/files/media/ACEP-Railbelt-Decarb-one-pager-v3.1.pdf>.
- [172] Canada Energy Regulator, 2016, “Canada’s Energy Future Data Appendices.” <https://doi.org/10.35002/ZJR8-8X75>.
- [173] National Electricity Regulatory Authority, “Electricity: Appendix OS-2023-T002-01,” Orkustofnun. [Online]. Available: [https://orkustofnun.is/information/numerical\\_data/electricity](https://orkustofnun.is/information/numerical_data/electricity). [Accessed: 16-Oct-2024].
- [174] Holdmann, G. P., Wies, R. W., and Vandermeer, J. B., 2019, “Renewable Energy Integration in Alaska’s Remote Islanded Microgrids: Economic Drivers, Technical Strategies, Technological Niche Development, and Policy Implications,” *Proc. IEEE*, **107**(9), pp. 1820–1837. <https://doi.org/10.1109/JPROC.2019.2932755>.
- [175] Denholm, P., Schwarz, M., DeGeorge, E., Stout, S., and Wiltse, N., 2022, *Renewable Portfolio Standard Assessment for Alaska’s Railbelt*, NREL/TP-5700-81698, National Renewable Energy Laboratory, Golden, CO. <https://doi.org/10.2172/1844210>.
- [176] REAP, “Alaska’s Energy Infrastructure.” [Online]. Available: <https://alaskarenewableenergy.org/ppf/alaskas-energy-infrastructure/>. [Accessed: 29-Aug-2024].
- [177] DeMarban, A., 2024, “Homer Electric Deal Sets Stage for a Dramatic Jump in Solar Power Production in Alaska,” Anchorage Dly. News. [Online]. Available: <https://www.adn.com/business-economy/energy/2024/08/18/homer-electric-deal-sets-stage-for-a-dramatic-jump-in-solar-power-production-in-alaska/>. [Accessed: 29-Aug-2024].
- [178] Pike, C., 2024, “High Latitude Solar Workshop Country Report: United States.” [Online]. Available: [https://www.sandia.gov/app/uploads/sites/243/dlm\\_uploads/2024/03/3.5-PikeChris-UnitedStates-20240314.pdf](https://www.sandia.gov/app/uploads/sites/243/dlm_uploads/2024/03/3.5-PikeChris-UnitedStates-20240314.pdf).
- [179] “Solar in Alaska? Understanding Growing Opportunity.” [Online]. Available: <https://cleancapital.com/resources/experts-only-episode-130-130-solar-in-alaska-understanding-growing-opportunity/>.
- [180] Statistics Canada, “Geography,” Stat. Can. [Online]. Available: <https://www150.statcan.gc.ca/n1/pub/11-402-x/2011000/chap/geo/geo-eng.htm>. [Accessed: 02-Sept-2025].
- [181] Arctic Council, “Canada,” Arct. Counc. [Online]. Available: <https://arctic-council.org/about/states/canada/>. [Accessed: 02-Sept-2025].
- [182] Canadian Renewable Energy Association, 2025, *CanREA’s 2025 Annual Data Release*, Canadian Renewable Energy Association. [Online]. Available: <https://www.renewablesassociation.ca>.
- [183] Yukon Energy, 2023, “The Impact of Solar on the Yukon Grid,” Yukon Energy. [Online]. Available: <https://yukonenergy.ca/about-us/news-events/the-impact-of-solar-on-the-yukon-grid/>. [Accessed: 02-Sept-2025].
- [184] Government of Iceland, 2024, *Bætt Orkunýtni Og Ný Tækifæri Til Orkuöflunar: Skýrsla Starfshóps Umhverfis-, Orku- Og Loftslagsráðherra*, Government of Iceland Ministry of the Environment, Energy and Climate. [Online]. Available: [https://www.stjornarradid.is/library/02-Rit--skyrslur-og-skrar/URN/URN\\_Skyrsla\\_Baett\\_Orkunytnei\\_Vefur.pdf](https://www.stjornarradid.is/library/02-Rit--skyrslur-og-skrar/URN/URN_Skyrsla_Baett_Orkunytnei_Vefur.pdf).
- [185] Statbank, “UO03020 Electricity Production of SEV by Hydro, Wind and Thermal in MWh (1990-2024).” [Online]. Available: [https://statbank.hagstova.fo:443/pxweb/en/H2/H2\\_\\_UO\\_\\_UO03/ork\\_elgerd.px/](https://statbank.hagstova.fo:443/pxweb/en/H2/H2__UO__UO03/ork_elgerd.px/). [Accessed: 05-Sept-2025].
- [186] SKGS, 2024, *The Swedish Industry’s Demand for Electricity up to 2035*. [Online]. Available: <https://skgs.org/app/uploads/sites/2/2024/09/Swedish-Industries-Electricity-Demand-SKGS-2024.pdf>.



- [187] Westerberg, A. O., and Lindahl, J., 2023, *National Survey Report of PV Power Applications in Sweden*, IEA, Paris, France. [Online]. Available: <https://iea-pvps.org/wp-content/uploads/2024/09/National-Survey-Report-of-PV-Power-Applications-in-Sweden-2023.pdf>.
- [188] Nätverket för solparker, 2024, *Kartläggning Av Solparker – Helår 2023*, Nätverket för solparker. [Online]. Available: [https://www.solparker.com/\\_files/ugd/94f4eb\\_0dbe79f835ef4fe7a2c89d173d59be93.pdf](https://www.solparker.com/_files/ugd/94f4eb_0dbe79f835ef4fe7a2c89d173d59be93.pdf).
- [189] Finnish Ministry of the Environment, “Finland’s National Climate Policy,” Finn. Minist. Environ. [Online]. Available: <https://ym.fi/en/finland-s-national-climate-change-policy>. [Accessed: 07-Aug-2024].
- [190] IEA, 2023, *Finland 2023: Energy Policy Review*, IEA, Paris, France. [Online]. Available: <https://iea.blob.core.windows.net/assets/07c88e41-c17b-4ea1-b35d-85dff665de4/Finland2023-EnergyPolicyReview.pdf>. [Accessed: 05-Sept-2025].
- [191] Fingrid, “Fingrid,” Fingrid. [Online]. Available: <https://www.fingrid.fi/en/>. [Accessed: 04-Jan-2024].
- [192] Renewables Finland, “Solar Power Projects in Finland,” Renew. Finl. [Online]. Available: <https://suomenuusiutuivat.fi/en/solar-power/solar-power-projects-in-finland/>. [Accessed: 12-Nov-2025].
- [193] Fingrid, 2024, “Prospects for Future Electricity Production and Consumption Q1 2024,” Fingrid. [Online]. Available: <https://www.fingrid.fi/en/grid/development/prospects-for-future-electricity-production-and-consumption-q3-2024/prospects-for-future-electricity-production-and-consumption-q1-2024/>. [Accessed: 07-Aug-2024].
- [194] Arctic Council, Russian’s Chairmanship, “Arctic Regions of Russia,” Arct. Council.
- [195] Boute, A., 2016, “Off-Grid Renewable Energy in Remote Arctic Areas: An Analysis of the Russian Far East,” *Renew. Sustain. Energy Rev.*, **59**, pp. 1029–1037. <https://doi.org/10.1016/j.rser.2016.01.034>.
- [196] IEA, “Russia,” IEA. [Online]. Available: <https://www.iea.org/countries/russia/electricity>. [Accessed: 02-Sept-2025].
- [197] Popel’, O. S., and Tarasenko, A. B., 2021, “Modern Development Trends in Photovoltaics (Review),” *Therm. Eng.*, **68**(11), pp. 807–825. <https://doi.org/10.1134/S0040601521100037>.
- [198] Agyekum, E. B., Mehmood, U., Kamel, S., Shouran, M., Elgamli, E., and Adebayo, T. S., 2022, “Technical Performance Prediction and Employment Potential of Solar PV Systems in Cold Countries,” *Sustainability*, **14**(6), p. 3546. <https://doi.org/10.3390/su14063546>.
- [199] Energy Institute, 2025, “Statistical Review of World Energy: Coal Price Index.” [Online]. Available: <https://www.energyinst.org/statistical-review>.
- [200] Ayres, D., and Zamora, L., 2024, *Renewable Power Generation Costs in 2023*, 978-92-9260-621-3, IRENA, Masdar City, United Arab Emirates. [Online]. Available: [https://www.irena.org/-/media/Files/IRENA/Agency/Publication/2024/Sep/IRENA\\_Renewable\\_power\\_generation\\_costs\\_in\\_2023.pdf](https://www.irena.org/-/media/Files/IRENA/Agency/Publication/2024/Sep/IRENA_Renewable_power_generation_costs_in_2023.pdf).
- [201] Svenska Kraftnät, Energinet, Fingrid, Statnett, 2023, *Nordic Grid Development Perspective 2023*. [Online]. Available: [https://www.svk.se/siteassets/om-oss/rapporter/2023/svk\\_ngpd2023.pdf](https://www.svk.se/siteassets/om-oss/rapporter/2023/svk_ngpd2023.pdf).
- [202] de Witt, M., Stefánsson, H., and Valfells, Á., 2019, *Energy Security in the Arctic: Policies and Technologies for Integration of Renewable Energy*. [Online]. Available: [https://arcticyearbook.com/images/yearbook/2019/Briefing-Notes/6\\_AY2019\\_BN\\_De\\_Witt.pdf](https://arcticyearbook.com/images/yearbook/2019/Briefing-Notes/6_AY2019_BN_De_Witt.pdf).
- [203] Canadian Renewable Energy Association, 2024, “News Release: New 2023 Data Shows 11.2% Growth for Wind, Solar & Energy Storage,” Can. Renew. Energy Assoc. [Online]. Available: <https://renewablesassociation.ca/news-release-new-2023-data-shows-11-2-growth-for-wind-solar-energy-storage/>.
- [204] NVE, n.d., “Installed capacity and PV production.” [Online]. Available: <https://www.nve.no/energi/energisystem/solkraft/oversikt-over-solkraftanlegg-i-norge/>. [Accessed: 16-Oct-2025].
- [205] Norwegian Water Resources and Energy Directorate, 2023, *Oppdrag Om Solkraft Og Annen Lokal Energiproduksjon*, Norwegian Water Resources and Energy Directorate. [Online]. Available: <https://www.nve.no/media/16143/oppdrag-om-solkraft-og-annen-lokal-energiproduksjon.pdf>.
- [206] Official Statistics of Sweden, “Electricity Production by Type of Production. Monthly 2017M01 - 2025M06,” Stat. Database. [Online]. Available: [https://www.statistikdatabasen.scb.se:443/pxweb/en/ssd/START\\_\\_BE\\_\\_BE0101\\_\\_BE0101A/BefolkManad/](https://www.statistikdatabasen.scb.se:443/pxweb/en/ssd/START__BE__BE0101__BE0101A/BefolkManad/). [Accessed: 12-June-2024].
- [207] Swedish Energy Agency, “Nätanslutna solcellsanläggningar,” Swed. Energy Agency. [Online]. Available: <https://www.energimyndigheten.se/statistik/officiell-energistatistik/tillforsel-och-anvandning/natanslutna-solcellsanlaggningar/>. [Accessed: 05-Sept-2025].



- [208] Baldus-Jeursen, C., Poissant, Y., Gall, N., and McKay, P., 2021, *National Survey Report of PV Power Applications in Canada*, IEA, Paris, France. [Online]. Available: <https://iea-pvps.org/wp-content/uploads/2022/11/NSR-Canada-2021.pdf>.
- [209] Fingrid, "Fingrid Open Data." [Online]. Available: <https://data.fingrid.fi/en>. [Accessed: 05-Sept-2025].

